(12) INTERNATIONAL APPLICATION PUBLISHED UNDER THE PATENT COOPERATION TREATY (PCT)

(19) World Intellectual Property Organization
International Bureau

(43) International Publication Date
19 November 2015 (19.11.2015)

WIPO | PCT

(10) International Publication Number
WO 2015/175846 A2

(51) International Patent Classification:
C12Q 1/68 (2006.01) *G01N 33/574* (2006.01)

(21) International Application Number:
PCT/US2015/030908

(22) International Filing Date:
14 May 2015 (14.05.2015)

(25) Filing Language: English

(26) Publication Language: English

(30) Priority Data:
61/994,689 16 May 2014 (16.05.2014) US
62/032,117 1 August 2014 (01.08.2014) US

(71) Applicant: **UNIVERSITY OF MASSACHUSETTS** [US/US]; 225 Franklin Street, 33rd Floor, Boston, Massachusetts 02110 (US).

(72) Inventors: **GREEN, Michael R.**; 368 Green Street, Boylston, Massachusetts 01505 (US). **MA, Leyuan**; 21 Sumac Circle, Holden, Massachusetts 01520 (US).

(74) Agent: **DEYOUNG, Janice Kugler**; Fish & Richardson P.C., P.O. Box 1022, Minneapolis, Minnesota 55440-1022 (US).

(81) Designated States *(unless otherwise indicated, for every kind of national protection available)*: AE, AG, AL, AM, AO, AT, AU, AZ, BA, BB, BG, BH, BN, BR, BW, BY, BZ, CA, CH, CL, CN, CO, CR, CU, CZ, DE, DK, DM, DO, DZ, EC, EE, EG, ES, FI, GB, GD, GE, GH, GM, GT, HN, HR, HU, ID, IL, IN, IR, IS, JP, KE, KG, KN, KP, KR, KZ, LA, LC, LK, LR, LS, LU, LY, MA, MD, ME, MG, MK, MN, MW, MX, MY, MZ, NA, NG, NI, NO, NZ, OM, PA, PE, PG, PH, PL, PT, QA, RO, RS, RU, RW, SA, SC, SD, SE, SG, SK, SL, SM, ST, SV, SY, TH, TJ, TM, TN, TR, TT, TZ, UA, UG, US, UZ, VC, VN, ZA, ZM, ZW.

(84) Designated States *(unless otherwise indicated, for every kind of regional protection available)*: ARIPO (BW, GH, GM, KE, LR, LS, MW, MZ, NA, RW, SD, SL, ST, SZ, TZ, UG, ZM, ZW), Eurasian (AM, AZ, BY, KG, KZ, RU, TJ, TM), European (AL, AT, BE, BG, CH, CY, CZ, DE, DK, EE, ES, FI, FR, GB, GR, HR, HU, IE, IS, IT, LT, LU, LV, MC, MK, MT, NL, NO, PL, PT, RO, RS, SE, SI, SK, SM, TR), OAPI (BF, BJ, CF, CG, CI, CM, GA, GN, GQ, GW, KM, ML, MR, NE, SN, TD, TG).

Declarations under Rule 4.17:

— *as to applicant's entitlement to apply for and be granted a patent (Rule 4.17(ii))*

— *as to the applicant's entitlement to claim the priority of the earlier application (Rule 4.17(iii))*

Published:

— *without international search report and to be republished upon receipt of that report (Rule 48.2(g))*

(54) Title: TREATING CHRONIC MYELOGENOUS LEUKEMIA (CML)

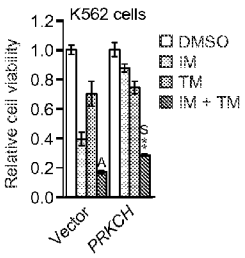


Fig 4A

(57) Abstract: Methods for treating chronic myeloid leukemia (CML), e.g., BCR-ABL inhibitor imatinib mesylate (IM)-resistant CML, using combination treatments, e.g., combined treatment with a BCR-ABL inhibitor, e.g., IM, and a MEK inhibitor, e.g., trametinib.

WO 2015/175846 A2

Treating Chronic Myelogenous Leukemia (CML)

CLAIM OF PRIORITY

This application claims the benefit of U.S. Provisional Patent Application Serial Nos. 61/994,689, filed on May 16, 2014, and 62/032,117, filed on August 1, 2014. The entire contents of the foregoing are hereby incorporated by reference.

FEDERALLY SPONSORED RESEARCH OR DEVELOPMENT

This invention was made with Government support under Grant No. R01 CA163926 awarded by the National Institutes of Health. The Government has certain rights in the invention.

TECHNICAL FIELD

The present invention relates to methods for treating chronic myeloid leukemia (CML), e.g., BCR-ABL inhibitor imatinib mesylate (IM)-resistant CML, using combination treatments, e.g., combined treatment with a BCR-ABL inhibitor, e.g., IM, and a MEK inhibitor, e.g., trametinib.

BACKGROUND

Chronic myeloid leukemia (CML) is a hematopoietic malignancy characterized by an increase and unregulated growth of predominantly myeloid cells in the bone marrow, and their accumulation in the blood (*1*). A hallmark of CML is the Philadelphia chromosome resulting from a reciprocal translocation between the long arms of chromosomes 9 and 22 (*2, 3*). This chromosomal translocation leads to expression of BCR-ABL, an oncogenic fusion-protein with a constitutively activated ABL tyrosine kinase. BCR-ABL can transform myeloid progenitor cells and drives the development of 95% of CML cases. BCR-ABL promotes leukemogenesis by activating downstream signaling proteins that increase cell survival and proliferation (*4*). These pathways include, but are not limited to, the RAS/mitogen-activated protein kinase (RAF/MEK/ERK), phosphatidylinositol 3-kinase/AKT (PI3K/AKT), and JAK/STAT signaling cascades (*5*).

The first-line treatment for CML is imatinib mesylate (IM), which binds to the ABL kinase domain and inhibits phosphorylation of substrates (*6*). Although IM dramatically improves patient survival when used to treat early-stage disease, the drug

is not curative. Resistance to IM can develop, especially in advanced-stage disease, leading to disease relapse and progression (*7*). Resistance to IM can result from multiple mechanisms that can be broadly classified as either BCR-ABL-dependent or BCR-ABL-independent (*8*). BCR-ABL-dependent resistance is most commonly due to the acquisition of point mutations in the ABL kinase domain that interfere with IM binding and subsequent kinase inhibition (*9-11*). However, in 50% or more of IM-resistant CML patients there is no mutation in BCR-ABL (*12, 13*) and the basis of such BCR-ABL-independent IM resistance is not understood.

SUMMARY

Previous studies have shown that a human BCR-ABL+ CML cell line, K562R, is resistant to IM due to over-expression of the Src family kinase LYN (Donato et al., Blood 101, 690-698 (2003)), however the clinical relevance of this finding is not well established. Our results reveal a previously-unknown survival pathway that promotes BCR-ABL-independent IM resistance and also contributes to the intrinsic IM resistance of CML stem cells. The mechanism described herein is therapeutically targetable and clinically relevant, which was confirmed by showing the efficacy of combined treatment with IM and trametinib both in cell culture and in IM-resistant CML mouse models.

Combined treatment with IM and trametinib represents a promising new therapeutic approach for treating CML patients with BCR-ABL-independent IM resistance. Furthermore, combined treatment with IM and trametinib synergistically kills CML stem cells with negligible effect on normal hematopoietic cells; currently, the intrinsic IM-resistance of CML stem cells is a major obstacle in long-term treatment of CML and essentially prevents a cure for the disease. Thus, the methods described herein have the potential to cure CML as opposed to the current treatment, which is effective only for the long-term management of CML.

Thus, in a first aspect, the invention provides methods for treating chronic myeloid leukemia (CML) in a mammalian subject that include administering a combination of a BCR-ABL inhibitor and a MEK inhibitor. Also provided herein is the use of a BCR-ABL inhibitor and a MEK inhibitor in the treatment of chronic myeloid leukemia (CML) in a mammalian subject.

In some embodiments, the CML is BCR-ABL inhibitor imatinib mesylate (IM)-resistant CML, e.g., BCR-ABL independent IM-resistant CML, wherein the BCR-ABL is wild-type or lacks a mutation that confers IM-resistance.

In some embodiments, the BCR-ABL inhibitor is imatinib, Nilotinib (AMN107); Dasatinib (BMS-345825); Bosutinib (SKI-606); Ponatinib (AP24534); Bafetinib (INNO-406); thiazol or a thiazol derivatives, e.g., 1,3,4 thiadiazole derivatives.

In some embodiments, the BCR-ABL inhibitor is imatinib.

In some embodiments, the MEK inhibitor is Trametinib (GSK1120212), Selumetinib, MEK162, PD-325901, cobimetinib (XL518; [3,4-Difluoro-2-(2-fluoro-4-iodoanilino)phenyl]{3-hydroxy-3-[(2S)-piperidin-2-yl]azetidin-1-yl} methanone), CL-1040, or PD035901.

In some embodiments, the MEK inhibitor is trametinib.

In some embodiments, the subject is human.

In another aspect, the invention provides methods for selecting a subject with chronic myeloid leukemia (CML) for treatment with a BCR-ABL inhibitor and a MEK inhibitor. The methods include detecting a level of PRKCH mRNA or PKCeta protein in a sample comprising leukemic cells, e.g., leukemic stem cells, from the subject; comparing the level of PRKCH mRNA or PKCeta protein in the sample to a reference level; selecting a subject who has a level of PRKCH mRNA or PKCeta protein above the reference level for treatment with a BCR-ABL inhibitor and a MEK inhibitor; and optionally administering the treatment to the selected subject.

In some embodiments, the CML is BCR-ABL inhibitor imatinib mesylate (IM)-resistant CML, e.g., BCR-ABL independent IM-resistant CML, wherein the BCR-ABL is wild-type or lacks a mutation that confers IM-resistance. In some embodiments, the methods include determining that the subject has BCR-ABL independent IM-resistant CML, e.g., determining that the BCR-ABL is wild-type or lacks a mutation that confers IM-resistance.

In some embodiments,the CML is BCR-ABL inhibitor imatinib mesylate (IM)-resistant CML.

In some embodiments,the BCR-ABL inhibitor is imatinib, Nilotinib (AMN107); Dasatinib (BMS-345825); Bosutinib (SKI-606); Ponatinib (AP24534); Bafetinib (INNO-406); thiazol or a thiazol derivatives, e.g., 1,3,4 thiadiazole derivatives.

In some embodiments,the BCR-ABL inhibitor is imatinib.

In some embodiments,the MEK inhibitor is Trametinib (GSK1120212), Selumetinib, MEK162, PD-325901, cobimetinib (XL518; [3,4-Difluoro-2-(2-fluoro-4-iodoanilino)phenyl]{3-hydroxy-3-[(2S)-piperidin-2-yl]azetidin-1-yl} methanone), CL-1040, or PD035901.

In some embodiments, the MEK inhibitor is trametinib.

In some embodiments, the level of PRKCH mRNA is determined using RNA in situ hybridization, Southern or Northern analyses, polymerase chain reaction analyses and probe arrays.

In some embodiments, the level of PKCeta protein is determined using an immunoassay.

In some embodiments, determining that the BCR-ABL is wild-type or lacks a mutation that confers IM-resistance comprises sequencing the BCR-ABL gene or a kinase domain thereof in leukemic cells of the subject, e.g., a mutation known in the art or described herein. Methods known in the art can be used to determine whether a new mutation confers IM-resistance.

Unless otherwise defined, all technical and scientific terms used herein have the same meaning as commonly understood by one of ordinary skill in the art to which this invention belongs. Methods and materials are described herein for use in the present invention; other, suitable methods and materials known in the art can also be used. The materials, methods, and examples are illustrative only and not intended to be limiting. All publications, patent applications, patents, sequences, database entries, and other references mentioned herein are incorporated by reference in their entirety. In case of conflict, the present specification, including definitions, will control.

Other features and advantages of the invention will be apparent from the following detailed description and Figures, and from the claims.

DESCRIPTION OF DRAWINGS

Figs. 1A-F. A large-scale shRNA screen identifies IMSGs. (A) Schematic summary of the screen. (B) Relative viability of IMSG KD K562 cells in the presence of IM, as measured by MTT assay (n=4). The results were normalized to that obtained with DMSO-treated cells, which was set to 1. IMSG shRNAs that conferred >2-fold increase in cell survival (indicated by the red line) relative to the NS control shRNA

were considered positive. (C) Relative viability of IMSG KD KYO-1 cells in the presence of IM, as measured by MTT assay (n=4). The results were normalized and positives determined as described in (B). (D) Colony formation assay monitoring survival of BCR-ABL+ mouse primary bone marrow cells expressing an IMSG shRNA in the presence of IM (n=3). IMSG shRNAs that conferred >2-fold increase in colony number (indicated by the red line) relative to the NS control shRNA were considered positive. (E) Relative $IC50^{IM}$ of IMSG KD K562 cells (n=4). (F) Cell viability, as measured by MTT assay, of IMSG KD K562 cells treated with 500 nM dasatinib or 10 μM IM for 3 days (n=4). K562 cells expressing an NS shRNA (K562/NS) and IM-resistant K562 cells (K562R) were analyzed as controls. Data are represented as mean ± SD. *$P \leq 0.05$, **$P \leq 0.01$. Statistical tests and exact *P* values are provided in table 4.

Fig. 2. Knockdown of IMSGs in BCR-ABL+ cells results in sustained RAF/MEK/ERK signaling after IM treatment. Immunoblot analysis monitoring the activity of BCR-ABL (as measured by phosphorylated (p) and total (t) BCR-ABL and CRKL), SFKs (p-SFK and t-LYN), JAK/STAT (p- and t-STAT5), PI3K/AKT (p- and t-AKT), MEK/ERK (p- and t-ERK1/2), and PKC (p- and t-MARCKS) pathways in IMSG KD K562 cells treated in the presence or absence of IM. β-actin (ACTB) was monitored as a loading control.

Figs. 3A-H. IMSG knockdown increases RAF/MEK/ERK signaling through upregulation of PKCη, an activator of CRAF. (A) qRT-PCR analysis monitoring expression of different *PKC* isotypes in IMSG KD K562 cells. Each colored dot represents an individual IMSG KD K562 cell line. Error bars indicate median with interquartile range. The results were normalized to that obtained with the NS control shRNA, which was set to 1. The dashed lines indicate >2-fold change in gene expression relative to that obtained with the NS shRNA. (B) Relative $IC50^{IM}$ in K562 cells expressing empty vector and in two independently derived K562 clonal cell lines ectopically expressing *PRKCH* (n=4). Data are represented as mean ± SD. (C) qRT-PCR analysis monitoring expression of *PRKCH* in BCR-ABL wild-type IM-sensitive patient samples (n=11), and BCR-ABL mutant (n=11) or BCR-ABL wild-type (n=11) IM-resistant CML patient samples. Error bars indicate median with interquartile range. (D) qRT-PCR analysis monitoring expression of three IMSGs in BCR-ABL mutant (n=11) or BCR-ABL wild-type (n=11) IM-resistant CML patient samples. For

ELF5, BCR-ABL mutant (n=9). Error bars indicate median with interquartile range. (E) Relative viability, as measured by trypan blue cell counting, of primary leukemic cells from BCR-ABL independent IM-resistant CML patient samples (n=5) expressing a NS or *PRKCH* shRNA and treated with DMSO or IM. The results were normalized to that obtained with DMSO-treated cells expressing a NS shRNA, which was set to 1. Data are represented as mean ± SEM. *$P \leq 0.05$, **$P \leq 0.01$. Statistical tests and exact *P* values are provided in table 4. (F) Immunoblot analysis monitoring RAF/MEK/ERK activity (as measured by p- and t-MEK and p- and t-ERK1/2) in *PRKCH* KD K562 cells (left) and in K562/*PRKCH-1* cells in the absence or presence of IM (right). (G) Immunoblot analysis monitoring p- and t-ERK1/2 levels in K562/*PRKCH-1* cells expressing an *ARAF*, *BRAF* or *CRAF* shRNA, treated with DMSO or IM for 1 h. (H) (Top) Schematic of CRAF showing the kinase domain bearing a potential PKC phosphorylation site at S497/S499. (Bottom) *In vitro* phosphorylation assay. Wild-type (WT) or kinase-dead mutant (Mut; K384R) PKCη was used in an *in vitro* phosphorylation reaction containing either GST or a GST-CRAF(aa491-505) fusion-protein. The phosphorylated product was visualized by autoradiography. The Coomassie-stained gel shows the abundance of each protein.

Figs. 4A-H. Combined treatment with IM and a MEK inhibitor has beneficial effects. (A and B) Cell viability, as measured by MTT assay, of K562/*PRKCH-1* (A; n=4) or IMSG KD K562 cells (B; n=3 or 4) treated with 0.1 μM IM, 1.5 nM trametinib (TM) or a combination of the two drugs, as indicated. The results were normalized to that observed with DMSO, which was set to 1. Data are represented as mean ± SD. Asterisks indicate comparisons between the combined drug treatment and single drug treatments. Combined drug treatment was synergistic (S), additive (A) or antagonistic (G). (C) Colony formation assay monitoring survival of BCR-ABL+ mouse primary bone marrow cells ectopically expressing *Prkch* and treated with IM, TM or a combination, as described in (A) (n=3). Data are represented as mean ± SD. (D) Relative viability, as measured by trypan blue cell counting, of primary leukemic cells isolated from IM-sensitive (IM-S) CML patients and treated with 5 μM IM (n=3), or isolated from BCR-ABL-independent IM-resistant (IM-R) CML patients and treated with 5 μM IM, 5 μM TM or a combination (n=6). The results were normalized to those obtained by DMSO treatment of the same samples (IM-S or IM-R [IM-SR]), which was set to 1. Error bars indicate median with interquartile range.

Matched samples from the same patient are indicated by dots of the same color. (E and F) White blood cell (WBC) count of leukemic mice derived by transplantation of BCR-ABL+ mouse primary bone marrow cells ectopically expressing *Prkch* (E) or knocked down for an IMSG (F), and treated at day 7 with either IM, TM or a combination of the two drugs as indicated (n=4 or 5 mice per group). Data are represented as mean ± SEM. The same NS control is used in the two graphs shown in (F), which were derived from a single experiment. (G and H) Kaplan-Meier survival curves of leukemic mice derived as described in (E and F). The indicated cohorts of mice (n=5 for *Prkch* overexpression and n=6 for IMSG knockdown) were treated with either vehicle, IM (100 mg/kg twice a day), TM (2 mg/kg once a day), or both IM and TM by oral gavage starting at day 7 (indicated by the arrow). The same NS control is used in the curves shown in (H), which were derived from a single experiment. $*P \leq 0.05$, $**P \leq 0.01$. Statistical tests and exact *P* values are provided in table 4.

Figs. 5A-G. *PRKCH* modulates proliferation of BCR-ABL+ cells, disease progression, and IM-sensitivity. (A) Immunoblot analysis monitoring p- and t-ERK1/2 levels in BCR-ABL+ mouse primary bone marrow cells expressing an NS shRNA or one of two *Prkch* shRNAs. (B) Colony formation assay after knockdown of *Prkch* in BCR-ABL+ mouse primary bone marrow cells (n=3). Data are represented as mean ± SD. (C) Colony formation assay monitoring survival of BCR-ABL+ mouse primary bone marrow cells expressing a NS or one of two *Prkch* shRNAs and treated with 0.1 μM IM. Data are represented as mean ± SD. (D) WBC count of leukemic mice derived by transplantation of *Prkch* KD BCR-ABL+ mouse primary bone marrow cells (n=4 or 5). Data are represented as mean ± SEM. (E) (Top) Representative spleen and lung images of leukemic mice derived as described in (D). Mice were sacrificed at day 17. (Bottom) Spleen weight of mice (n=4). Data are represented as mean ± SEM. (F) Hematoxylin and eosin (H&E) staining of spleen and lung sections from leukemic mice derived as described in (D). Scale bars, 50 μm. (G) Kaplan-Meier survival curve of untreated leukemic mice (n=6) or leukemic mice treated with IM at day 14 (indicated by the arrow) (n=5), derived as described in (D). $*P \leq 0.05$, $**P \leq 0.01$. Statistical tests and exact *P* values are provided in table 4.

Figs. 6A-C. IM-resistant murine and human CML stem cells contain high levels of *PRKCH*. (A) qRT-PCR analysis monitoring *Prkch* expression in BCR-ABL+ murine CML stem cells (Lin-Sca1+Kit+), progenitor cells (Lin-) and mature cells (Lin+Gr1+) (n=3). Data are represented as mean ± SD. (B) qRT-PCR analysis

monitoring *PRKCH* expression in human CML stem cells (CD34+CD38-) and progenitor cells (CD34+CD38+) isolated from CML patient samples (n=5). Data are from three technical replicates and are means ± SD. (C) *PRKCH* expression in CD34+CD38- and CD34+CD38+ cells, mined from a previous expression profiling study (50). Matched samples from the same patient are indicated by dots of the same color. Error bars indicate median with interquartile range. *$P \leq 0.05$, **$P \leq 0.01$. Statistical tests and exact *P* values are provided in table 4.

Figs. 7A-G. High *Prkch* levels contribute to the IM resistance of CML stem cells. (A) Intracellular phosphorylated ERK1/2 levels in Lin- and Lin-Sca1+Kit+ BCR-ABL+ *Prkch* KD or control bone marrow cells. As a negative control, cells were incubated with a conjugated IgG isotype antibody. (B) Intracellular phosphorylated ERK1/2 levels in Lin- and Lin-Sca1+Kit+ BCR-ABL+ bone marrow cells treated with DMSO, IM or trametinib. (C) Colony formation assay monitoring survival of BCR-ABL+ murine stem cells expressing a NS or one of two *Prkch* shRNAs and treated with 0.1 μM IM (n=3). Data are represented as mean ± SD. (D) FACS determination of the number of BCR-ABL+ Lin-Sca1+Kit+ bone marrow cells expressing a NS or *Prkch* shRNA after IM treatment of mice (n=4 or 5). Data are represented as mean ± SEM. (E) FACS determination of the number of BCR-ABL+ Lin-Sca1+Kit+ bone marrow cells after treatment of mice with vehicle (n=10), IM (n=12), TM (n=10) or both IM and TM (n=12). Data are represented as mean ± SEM. Asterisks indicate comparisons between the combined drug treatment and single drug treatments. Combined drug treatment was synergistic (S). (F) Relative viability, as measured by trypan blue cell counting, of BCR-ABL+ human CML stem cells (CD34+CD38-) expressing a NS or *Prkch* shRNA and treated with DMSO or IM (n=3). Data are represented as mean ± SEM. (G) Relative viability of BCR-ABL+ human CML stem cells treated with DMSO, IM, TM or a combination of drugs (n=3). Data are represented as mean ± SEM. *$P \leq 0.05$, **$P \leq 0.01$. Statistical tests and exact *P* values are provided in table 4.

Fig. 8. Elevated PKCη levels lead to IM resistance in CML and CML stem cells. Relative contributions of BCR-ABL and PKCη to RAF/MEK/ERK signaling are indicated by arrow size and shading.

Fig. 9. IM sensitivity of non-validating candidates isolated from the primary shRNA screen. MTT assay showing relative viability of IMSG KD K562 cells in the

presence of IM. The results were normalized to that obtained with DMSO-treated cells, which was set to 1. The red line indicates a 2-fold increase in cell survival relative to that of the non-silencing (NS) control shRNA; none of the shRNAs shown here were considered positive. The NS control is the same as that used in Fig. 1B. Data are represented as mean ± SD (n=4). *P≤0.05, **P≤0.01. Statistical tests and exact P values are provided in table 4.

Figs. 10A-D. Confirmation of validating candidates using a second shRNA. (A) MTT assay showing relative viability of IM-treated K562 cells expressing a second IMSG shRNA unrelated to that isolated in the primary screen and used in Fig. 1B (n=4). The results were normalized as described in Fig. 1B. IMSG shRNAs that conferred >2-fold increase in cell survival (indicated by the red line) relative to that of the NS control shRNA were considered positive. (B) MTT assay showing relative viability of IM-sensitive K562 cells, experimentally-derived IM-resistant K562R cells, and IM-resistant patient-derived SUPB15 cells treated with 10 μM IM (n=4). The results were normalized to that obtained with DMSO-treated cells, which was set to 1. (C and D) qRT-PCR analysis monitoring knockdown efficiencies, in K562 cells, of IMSG shRNAs isolated from the primary screen (B; n=3) or a second, unrelated IMSG shRNA (C; n=3). Data are represented as mean ± SD. *P≤0.05, **P≤0.01. Statistical tests and exact P values are provided in table 4.

Figs. 11A-C. IM sensitivity following candidate IMSG knockdown in mouse primary bone marrow cells. (A) qRT-PCR analysis monitoring knockdown efficiencies of mouse IMSG shRNAs in mouse primary bone marrow cells (n=3). (B) Colony formation assay monitoring survival of BCR-ABL+ mouse primary bone marrow cells expressing an IMSG shRNA in the presence of IM (n=3). IMSG shRNAs that conferred >2-fold increase in colony formation relative to that of the NS control shRNA (indicated by the red line) were considered positive. (C) qRT-PCR analysis monitoring knockdown efficiencies, in mouse primary bone marrow cells, of a second set of mouse IMSG shRNAs unrelated to those used in (A) but the same as those used in (B) (n=3). Data are represented as mean ± SD. *P≤0.05, **P≤0.01. Statistical tests and exact P values are provided in table 4.

Fig. 12. Relative IC50IM of candidate IMSG KD K562 cells. The NS control used here is the same as that used in Fig. 1E, which was derived from the same experiment. Data are represented as mean ± SD (n=4).

Figs. 13A-B. Confirmation that IMSG knockdown in K562 cells increases PRKCH and PKCη levels. (A) qRT-PCR analysis monitoring expression of PRKCH in K562 cells expressing a second shRNA targeting each IMSG, unrelated to that used in Fig. 3A. The results were normalized to that obtained with the NS control shRNA, which was set to 1. The scatter dot plot shows the median line with interquartile range. Statistical tests and exact P values are provided in table 4. (B) Immunoblot analysis showing the level of PKCη in IMSG KD K562 cells. beta-actin (ACTB) was monitored as a loading control.

Figs. 14A-C. Demonstration that ELF5 is a direct transcriptional repressor of PRKCH. (**A**) Chromatin immunoprecipitation assay monitoring binding of ELF5 to the *PRKCH* promoter at the transcription start site (TSS) and at 500 and 1000 bp upstream of the TSS (n=3). The results were normalized to that obtained with an IgG control antibody, which was set to 1. (**B and C**) Expression of a luciferase reporter driven by the *PRKCH* promoter in K562 cells expressing a NS shRNA or one of two unrelated *ELF5* shRNAs (B; n=3) or in K562 cells ectopically expressing *ELF5* or, as a control, empty vector (C; n=3). Shown are firefly luciferase activities normalized to that of *Renilla* luciferase. Data are represented as mean ± SD. **P*≤0.05, ***P*≤0.01. Statistical tests and exact *P* values are provided in table 4.

Figs. 15A-B. Confirmation of elevated PKCη levels in K562/PRKCH cells, and role of PRKCH in IM resistance. (**A**) Immunoblot analysis showing the levels of PKCη and phosphorylated and total ERK1/2 (p-ERK1/2 and t-ERK1/2, respectively) in K562 cells expressing empty vector and in two independently derived K562 clonal cell lines ectopically expressing *PRKCH*. **(B)** MTT assay measuring relative viability of representative IMSG KD K562 cell lines expressing a NS or *PRKCH* shRNA, and treated in the presence or absence of IM. Data are represented as mean ± SD (n=4). Asterisks indicate comparisons between the two IM-treated samples. **P*≤0.05, ***P*≤0.01. Statistical tests and exact *P* values are provided in table 4.

Figs. 16A-B. Confirmation that PKCη functions through CRAF to increase RAF/MEK/ERK signaling. (**A**) Immunoblot analysis showing RAF/MEK/ERK activity (as measured by p- and t-MEK and p- and t-ERK1/2) in K562 cells expressing a second *PRKCH* shRNA unrelated to that used in Fig. 3F. The level of PKCη was monitored as a control. β-actin (ACTB) was monitored as a loading control. (**B**) Immunoblot analysis showing p- and t-ERK1/2 levels in K562/*PRKCH-1*

cells, treated in the absence or presence of IM, expressing a second *ARAF*, *BRAF* or *CRAF* shRNA unrelated to that used in Fig. 3G. The levels of total (t-) ARAF, BRAF and CRAF, and PKCη were monitored as controls. ACTB was monitored as a loading control.

Figs. 17A-B. Comparison of combined treatment with IM and trametinib to IM and a JAK-STAT or PI3K inhibitor. (**A**) Cell viability, as measured by trypan blue cell counting, of primary leukemic cells from BCR-ABL-independent IM-resistant CML patients (n=6) treated with DMSO. 5 μM IM, 5 μM TM or a combination of the two drugs. The results were normalized to that observed with DMSO, which was set to 1. Data are represented as mean ± SD. The data are the same as those shown in Fig. 4D, but plotted to show the results for each individual patient sample. Asterisks indicate comparisons between the combined drug treatment and single drug treatments. Combined drug treatment was synergistic (S) or additive (A). (**B**) Relative viability, as measured by trypan blue cell counting, of primary leukemic cells isolated from IM-sensitive CML patients and treated with 5 μM IM (n=3), or isolated from BCR-ABL-independent IM-resistant CML patients and treated with 5 μM IM, 5 μM TM or a combination (n=6), or treated with 0.5 μM TG101348 (TG, a JAK-STAT inhibitor) or 10 nM rapamycin (Rapa, a PI3K inhibitor) alone or in combination with 5 μM IM (n=4). The results were normalized to those obtained by DMSO treatment of the same samples, which was set to 1. Error bars indicate median with interquartile range. Matched samples from the same patient are indicated by dots of the same color. Samples IM-SR/DMSO, IM-S/IM, IM-R/IM and IM-R/IM + TM are the same as those in Fig. 4D and are shown to facilitate comparison. The results presented here and in Fig. 4D were derived from a single experiment. For statistical significance, only comparisons between double treatments and IM alone were made. Statistical tests and exact *P* values are provided in table 4.

Figs. 18A-D. Effectiveness of retroviruses co-expressing BCR-ABL and either PRKCH or an Elf5 or Clec5a shRNA. (**A**) Immunoblot analysis monitoring levels of PKCη and BCR-ABL in NIH 3T3 cells transduced with a retrovirus expressing BCR-ABL or one co-expressing BCR-ABL and murine *Prkch*. The percentage of GFP+ cells obtained was similar using both retroviruses, demonstrating equivalent virus titers. The same virus titers were used for transduction of primary mouse bone marrow cells. (**B**) qRT-PCR analysis monitoring knockdown efficiencies in

32D/BCR-ABL cells of one of two unrelated *Elf5* (left) or *Clec5a* (right) shRNAs. Data are represented as mean ± SD (n=3). *$P \leq 0.05$, **$P \leq 0.01$. (**C**) Immunoblot analysis monitoring levels of PKCη and phosphorylated and total ERK1/2 (p-ERK1/2 and t-ERK1/2, respectively) in 32D/BCR-ABL cells expressing an NS, *Elf5* or *Clec5a* shRNA. (**D**) qRT-PCR analysis monitoring knockdown efficiencies of *Elf5* (left) and *Clec5a* (right) in mouse primary bone marrow cells transduced with a retrovirus co-expressing BCR-ABL and either an *Elf5* or *Clec5a* shRNA. The most effective *Elf5* shRNA (*Elf5-1*) and *Clec5a* shRNA (*Clec5a-1*), as determined by the results in (B), were used here and in Fig. 4 F and H. Data are represented as mean ± SD (n=3). *$P \leq 0.05$, **$P \leq 0.01$. Statistical tests and exact *P* values are provided in table 4.

Figs. 19A-B. Knockdown of PRKCH in BCR-ABL+ cells decreases colony formation. (**A**) qRT-PCR analysis monitoring knockdown efficiency of *Prkch* in mouse primary bone marrow cells expressing one of two unrelated *Prkch* shRNAs. The results were normalized to that obtained with a NS control, which was set to 1. Data are represented as mean ± SD (n=3). *$P \leq 0.05$, **$P \leq 0.01$. Statistical tests and exact *P* values are provided in table 4. (**B**) Micrograph showing typical colonies of BCR-ABL+ mouse primary bone marrow cells expressing a NS shRNA or one of two unrelated *Prkch* shRNAs. Scale bar, 100 μm.

Fig. 20. Confirmation of IM sensitivity of murine CML progenitor cells. Colony formation assay monitoring survival of BCR-ABL+ murine progenitor cells (Lin-Sca1+Kit+-depleted Lin- cells) expressing a NS shRNA and treated with DMSO or 0.1 μM IM (n=3). Data are represented as mean ± SD. As a comparison, see Fig. 7C, which shows the results of a similar analysis of IM-resistant murine CML stem cells. *$P \leq 0.05$, **$P \leq 0.01$. Statistical tests and exact *P* values are provided in table 4.

Figs. 21A-B. Analysis of phosphorylated-ERK1/2 levels in CML progenitor and stem cells. (**A**) Intracellular phosphorylated ERK1/2 levels in Lin- and Lin-Sca1+Kit+ BCR-ABL+ *Prkch* KD or control bone marrow cells (n=3). The results were background corrected and then normalized to that obtained with the NS control shRNA, which was set to 1. Data are represented as mean ± SEM. (**B**) Intracellular phosphorylated-ERK1/2 levels in Lin- and Lin-Sca1+Kit+ BCR-ABL+ bone marrow cells treated with DMSO, IM or trametinib. (n=4). The results were background corrected and then normalized to that obtained with DMSO, which was set to 1. Data are represented as mean ± SEM. *$P \leq 0.05$, **$P \leq 0.01$. Statistical tests and exact *P*

values are provided in table 4. These results accompany the representative experiment shown in Fig. 7, A and B.

Figs. 22A-D. Synergistic induction of apoptosis in murine CML stem cells by IM and trametinib. (**A**) Apoptosis assay. CML mice (n=5) were orally gavaged with vehicle or IM. BCR-ABL+ bone marrow cells were stained with a Lin/Sca1/Kit antibody cocktail, then with Annexin V and 7-AAD followed by FACS. Data are represented as mean ± SEM. (**B**) FACS analysis showing representative Annexin V/7-AAD staining of murine CML stem cells expressing a NS shRNA or one of two unrelated *Prkch* shRNAs isolated from mice treated with vehicle or IM. These data provided the basis for the bar graph in (A). (**C**) Apoptosis assay. Mice were orally gavaged with vehicle (n=6), IM (n=6), TM (n=5) or both (n=5). BCR-ABL+ bone marrow cells were stained as described in (A). Data are represented as mean ± SEM. (**D**) FACS analysis showing representative Annexin V/7-AAD staining of murine CML stem cells isolated from mice treated with vehicle, IM, TM or a combination of IM and TM. These data provided the basis for the bar graph in (C). $*P \leq 0.05$, $**P \leq 0.01$. Statistical tests and exact *P* values are provided in table 4.

Figs. 23A-B. Effect of IM and trametinib on normal hematopoietic stem cells. (**A**) FACS determination of the percentage of normal (BCR-ABL-) murine Lin-Sca1+Kit+ bone marrow cells after treatment with vehicle (n=21), IM (n=21), TM (n=9) or both IM and TM (n=9). Data are represented as mean ± SEM. (**B**) Relative viability, as measured by trypan blue cell counting, of normal human hematopoietic CD34+ cells and hematopoietic stem cells (CD34+CD38-) treated with DMSO, IM, TM or a combination of drugs (n=4). The results were normalized to that obtained in cells treated with DMSO, which was set to 1. Data are represented as mean ± SD. $*P \leq 0.05$, $**P \leq 0.01$. Statistical tests and exact *P* values are provided in table 4.

DETAILED DESCRIPTION

CML, like several other malignancies, is propagated by a small population of stem cells, elimination of which is likely required to achieve long-term remission and cure (*14, 15*). An important limitation of IM treatment is that although IM inhibits BCR-ABL activity in CML stem cells, these cells do not depend on BCR-ABL activity for survival and are thus not eliminated (*16, 17*). These findings imply that CML stem cells use survival signals other than BCR-ABL to maintain viability in the presence of IM. Understanding the mechanism by which CML stem cells are

intrinsically resistant to IM is essential for devising strategies to eradicate residual leukemia. To gain insight into how IM resistance can occur in the absence of BCR-ABL mutations, an RNA interference (RNAi) screen was performed to identify genes that regulate IM responsiveness. Our results reveal a survival pathway that promotes BCR-ABL-independent IM resistance and also contributes to the IM resistance of CML stem cells.

Without wishing to be bound by theory, the present inventors have identified a molecular pathway whose increased activity promotes BCR-ABL-independent IM resistance and also contributes to the IM resistance of CML stem cells. See, e.g., the schematic model in Figure 8 and below. In typical IM-sensitive CML cells, BCR-ABL is the major contributor to RAF/MEK/ERK signaling. Thus, treatment with IM substantially reduces RAF/MEK/ERK signaling, leading to inhibition of proliferation and induction of apoptosis. In BCR-ABL-independent, IM resistant CML cells, elevated levels of Protein Kinase C *eta* (PKCη), due to decreased expression of one or more IM-sensitizing genes (IMSGs), results in phosphorylation and activation of CRAF, thereby augmenting RAF/MEK/ERK signaling. Following treatment with IM, RAF/MEK/ERK signaling is sustained, resulting in drug resistance.

A previous study analyzing IM resistance resulting from mutations in BCR-ABL found that IM treatment "paradoxically" increased RAF/MEF/ERK signaling through a RAS-directed pathway (Konuma et al. Exp Hematol 39, 697-709 e695 (2011)). Although the IM-resistance mechanism we describe, like that in Packer et al. (Cancer Cell 20, 715-727 (2011)), involves increased RAF/MEK/ERK signaling, there are several important differences. For example, in the experiments described herein the increased RAF/MEK/ERK signaling was not dependent upon RAS but rather initiated by PKCη, was constitutive and not induced by IM, and, as discussed below, was also relevant to the intrinsic IM resistance of CML stem cells. In addition, several reports have described experimentally derived BCR-ABL-independent IM-resistant CML cell lines in which RAF/MEK/ERK signaling is increased by a mechanism that was not determined (Aceves-Luquero et al., PLoS One 4, e6124 (2009); Hentschel et al., Int J Oncol 39, 585-591 (2011); Nambu et al., Cancer Sci 101, 137-142 (2010).) or have provided other evidence that RAF/MEK/ERK signaling can contribute to IM resistance (Chang et al., Blood 110, 994-1003 (2007); Chu et al., Blood 103, 3167-3174 (2004); Mizuchi et al., Biochem

Biophys Res Commun 326, 645-651 (2005); Pellicano et al., Leukemia 25, 1159-1167 (2011)).

The mechanistic basis by which IMSGs regulate *PRKCH* expression is largely unknown. One of the IMSGs identified, *ELF5*, is directly bound at the transcription start-site of *PRKCH,* and can decrease *PRKCH* expression. Thus, ELF5 is a direct transcriptional repressor of *PRKCH*, explaining why decreased ELF5 levels result in increased *PRKCH* expression. Whether other IMSGs function directly or indirectly to regulate PRKCH expression remained to be determined.

It is possible that the RNAi screen described herein, like other large-scale RNAi screens (Mullenders and Bernards, Oncogene 28, 4409-4420 (2009)), was not saturating and thus there may be other IMSGs, and regulators of *PRKCH* expression, that remain to be identified. The present results suggest that a variety of diverse perturbations can increase *PRKCH* expression. A previous expression profiling study revealed that the level of *PRKCH* in CML cells increased following one week of IM treatment (Bruennert et al., Leukemia 23, 983-985 (2009)), perhaps due to selection of and enrichment for cells with high *PRKCH* expression. This finding may also be explained by induction of PRKCH expression by IM treatment, although we found in IMSG KD K562 cell lines and CML stem cells that PRKCH is highly expressed in the absence of IM. In addition to its role in IM resistance, elevated *Prkch* expression also accelerates disease progression in a mouse model of CML. Consistent with this idea, in a previous expression profiling study, *PRKCH* levels were found to increase during disease progression in CML patients. In the same study, the expression levels of seven of nine IMSGs analyzed decreased during disease progression (Radich et al., Proc Nat Acad Sci USA 103, 2794-2799 (2006)).

The IM-resistance mechanism described herein is therapeutically targetable, which was demonstrated by the showing that combined treatment with IM and the FDA-approved MEK inhibitor trametinib synergistically kills BCR-ABL+ IMSG KD cells and prolongs survival in several mouse models of BCR-ABL-independent IM-resistant CML. These results are also relevant to another current challenge of CML treatment: the intrinsic resistance of CML stem cells to IM. Both human and murine CML stem cells contain high levels of *PRKCH* and provide evidence that this is responsible, at least in part, for their IM resistance. The high *PRKCH* levels in CML stem cells promotes RAF/MEK/ERK signaling, which helps explain why CML stem cells are not dependent upon BCR-ABL for survival (*16, 17*). Collectively, these results provide a rationale for our finding that CML stem cells, but not normal hematopoietic stem cells, are efficiently

killed by combined treatment with IM and trametinib, and suggest a therapeutic strategy for their eradication.

Chronic Myelogenous Leukemia (CML)

CML is a clonal stem cell disorder that is typically associated with the presence in more than 95% of patients of leukemic cells that have the Philadelphia chromosome (Ph1) (see, e.g., Kurzrock et al., Ann Intern Med 138 (10): 819-30, 2003; Goldman and Melo, N Engl J Med 349 (15): 1451-64, 2003), a reciprocal translocation between chromosomes 9 and 22. The Ph1 translocation results in the transfer of the Abelson (ABL) oncogene from chromosome 9 to the breakpoint cluster region (BCR) of chromosome 22, creating a fused BCR/ABL gene that codes for an abnormal, constitutively active tyrosine kinase that is essential to the growth and survival of leukemic cells. The Ph1 can be detected in bone marrow aspirate or peripheral blood samples using known methods, including cytogenetic studies, Southern blot analysis, Fluorescent in situ hybridization, or RT-PCR. See also the National Cancer Institute: PDQ® Chronic Myelogenous Leukemia Treatment. Bethesda, MD: National Cancer Institute. Date last modified 03/28/2014. Available at: http://www.cancer.gov/cancertopics/pdq/treatment/CML/HealthProfessional. Accessed May 6, 2014.

Bone marrow sampling is often done to assess cellularity, fibrosis, and cytogenetics. CML is typically staged into three phases: chronic, accelerated, and blastic phases based on myoblasts counts. Chronic-phase CML is characterized by less than 10% blasts and promyelocytes in the peripheral blood and bone marrow. Accelerated-phase CML is characterized by 10% to 19% blasts in either the peripheral blood or bone marrow. Blastic-phase CML is characterized by 20% or more blasts in the peripheral blood or bone marrow. When 20% or more blasts are present along with fever, malaise, and progressive splenomegaly, the patient has entered blast crisis (Cortes JE, et al., Cancer 106 (6): 1306-15, 2006).

IM-resistant CML

Although imatinib is successful in treating many patients, development of resistance against imatinib is common (Valenti, Biologics. 1(4): 433–448, 2007). As noted above, resistance may be the result of one or several mechanisms, including molecular resistance caused by mutation of the BCR/ABL gene, or BCR/ABL independent resistance, e.g., associated with stem cell-specific survival factors, e.g.,

associated with increased RAF/MEK/ERK signaling that is not dependent upon RAS but rather initiated by PKCη. Patients with CML are considered to be imatinib-resistant when response is lost or is not seen with a daily dose of >400 mg imatinib (Valenti, 2007; Kantarjian et al., Blood. 101(2):473, 2003; Baccarani et al., Blood. 108(6):1809-20, 2006).

Methods of treating CML

Described herein are methods for treating CML, e.g., treating or reducing the risk of developing IM-resistant CML, that include the use of a combination of at least one BCR/ABL inhibitor and at least one MEK inhibitor.

Subject selection

The methods described herein are useful in the treatment of subjects with CML, e.g., IM-resistant CML, e.g., in which the IM-resistant subject lacks a mutation in BCR-ABL that confers drug-resistance (i.e., BCR-ABL independent IM-resistance).

Any method known in the art can be used to diagnose CML in a subject, including detecting the presence of the Ph1 translocation in leukemic cells of the subject, e.g., as described above. Other methods can also be used.

As described herein, CML stem cells have elevated levels of PRKCH expression and PKCη protein. Thus in some embodiments the methods can include detecting levels of PRKCH mRNA, or PKCη protein or activity, in leukemic cells, e.g., stem cells of the subject. Routine methods can be used to detect expression levels. A nucleic acid sequence of human PRKCH cDNA is in GenBank at accession no. NM_006255.3; the sequence of human PKCη protein is at accession no. NP_006246.2. For example, antibodies (including antibodies that bind specifically to the phosphorylated form) are commercially available from Abcam, Cell Sciences, Life Technologies, MBL International, Novus Biologicals, Bethyl Laboratories, and Santa Cruz Biotechnology, Inc. The presence and/or level of a protein can be evaluated using methods known in the art, e.g., using quantitative immunoassay methods. In some embodiments, high throughput methods, e.g., protein or gene chips as are known in the art (see, e.g., Ch. 12, Genomics, in Griffiths et al., Eds. Modern genetic Analysis, 1999,W. H. Freeman and Company; Ekins and Chu, Trends in Biotechnology, 1999, 17:217-218; MacBeath and Schreiber, Science 2000, 289(5485):1760-1763; Simpson, Proteins and Proteomics: A Laboratory Manual, Cold

Spring Harbor Laboratory Press; 2002; Hardiman, Microarrays Methods and Applications: Nuts & Bolts, DNA Press, 2003), can be used to detect the presence and/or level of PKCη.

The presence and/or level of mRNA in a sample can also be evaluated using methods known in the art, e.g., both by *in situ* and/or by *in vitro* formats. For example, isolated mRNA can be used in hybridization or amplification assays that include, but are not limited to, RNA in situ hybridization (RNA ISH, e.g., a branched DNA assay), Southern or Northern analyses, polymerase chain reaction analyses and probe arrays. One method for the detection of mRNA levels involves contacting the isolated mRNA with a nucleic acid molecule (probe) that can hybridize to the mRNA encoded by the PRKCH gene being detected. The nucleic acid probe can be, for example, a full-length PRKCH nucleic acid, such as the cDNA deposited with ATCC as Accession Number NM_006255.3, or a portion thereof, such as an oligonucleotide of at least 7, 15, 30, 50, 100, 250 or 500 nucleotides in length and sufficient to specifically hybridize under stringent conditions to PRKCH mRNA or genomic DNA. Other suitable probes for use in the assays are described herein. Alternatively, levels or presence of PRKCH mRNA can be detected with nucleic acid amplification, e.g., by rtPCR (Mullis (1987) U.S. Patent No. 4,683,202), ligase chain reaction (Barany (1991) Proc. Natl. Acad. Sci. USA 88:189-193), self-sustained sequence replication (Guatelli et al., (1990) Proc. Natl. Acad. Sci. USA 87:1874-1878), transcriptional amplification system (Kwoh et al., (1989), Proc. Natl. Acad. Sci. USA 86:1173-1177), Q-Beta Replicase (Lizardi et al., (1988) Bio/Technology 6:1197), rolling circle replication (Lizardi et al., U.S. Patent No. 5,854,033) or any other nucleic acid amplification method, followed by the detection of the amplified molecules using techniques known in the art. The level of PRKCH mRNA, or PKCeta protein, can then be compared to a reference level, and a subject who has a level at or above the reference level, or above the reference level, can be selected for treatment using the methods described herein.

Suitable reference values can be determined using methods known in the art, e.g., using standard clinical trial methodology and statistical analysis. The reference values can have any relevant form. In some cases, the reference comprises a predetermined value for a meaningful level of PRKCH, e.g., a control reference level that represents a normal level of PRKCH, e.g., a level in an unaffected subject or a

subject who is not at risk of developing CML, and/or a disease reference that represents a level of the proteins associated with CML.

In some embodiments, the subject has imatinib-resistant CML, and the methods are used to treat the IM-resistant CML in the subject. In some embodiments, the subject has CML but has not yet developed imatinib resistance, and the methods are used to treat CML in the subject or to prevent or reduce the risk of development of IM-resistant CML in the subject. In some embodiments, the subject has BCR-ABL independent IM-resistance, i.e., is IM-resistant but has no mutations in the BCR-ABL kinase domain that would confer drug-resistance (i.e., no mutations in the region of the sequence at GenBank Acc No. NM_005157.4 that encodes amino acids 235 to 497 of GenBank NP_005148.2, shown underlined below, that would confer resistance). More than 90 BCR-ABL point mutations have been identified, including mutations in the P-loop, the C-helix, SH2 domain, substrate binding site, activation loop and C-terminal lobe M237I; M244V; L248V; G250A; G250E; G250V; Q252H; Y253F; Y253H; E255D; E255K; E255R; E255V; E275K; D276G; E281K; E285N; E292K; F311V; T315I; F317C; F317L; F317V; G321E; D325N; S348L; M351T; Y353H; E355A; E355G; E355K; F359C; F359V; E373G; V379I; A380S; L387A; M388H; H396P; H396R; see Bixby and Talpaz, Hematology: 461-476 (2009); Soverini et al., Clin Cancer Res 12: 7374–7379 (2006); also Fig. 1 of Soverini et al., Blood, 118:1208-1215 (2011). Nine of these mutations account for more than 85% of all mutations: M244V, G250E, Y253F/H, E255K/V, T315I, M351T, and F359V. The T315I mutation (shown in bold and upper case below) is the most clinically relevant.

Reference sequence of human bcr/abl gene product; the kinase domain is underlined. From GenBank Acc No. NM_005157.4

```
   1 mleiclklvg ckskkglsss sscyleealq rpvasdfepq glseaarwns
kenllagpse
  61 ndpnlfvaly dfvasgdntl sitkgeklrv lgynhngewc eaqtkngqgw
vpsnyitpvn
 121 slekhswyhg pvsrnaaeyl lssgingsfl vresesspgq rsislryegr
vyhyrintas
 181 dgklyvsses rfntlaelvh hhstvadgli ttlhypapkr nkptvygvsp
nydkwemert
 241 ditmkhklgg gqygevyegv wkkysltvav ktlkedtmev eeflkeaavm
keikhpnlvq
 301 llgvctrepp fyiiTefmty gnlldylrec nrqevnavvl lymatqissa
meylekknfi
 361 hrdlaarncl vgenhlvkva dfglsrlmtg dtytahagak fpikwtapes
laynkfsiks
 421 dvwafgvllw eiatygmspy pgidlsqvye llekdyrmer pegcpekvye
lmracwqwnp
```

```
 481 sdrpsfaeih qafetmfqes sisdevekel gkqgvrgavs tllqapelpt
ktrtsrraae
 541 hrdttdvpem phskgqgesd pldhepavsp llprkergpp egglnederl
lpkdkktnlf
 601 salikkkkkt aptppkrsss fremdgqper rgageeegrd isngalaftp
ldtadpaksp
 661 kpsngagvpn galresggsg frsphlwkks stltssrlat geeegggsss
krflrscsas
 721 cvphgakdte wrsvtlprdl qstgrqfdss tfgghksekp alprkragen
rsdqvtrgtv
 781 tppprlvkkn eeaadevfkd imesspgssp pnltpkplrr qvtvapasgl
phkeeaekgs
 841 algtpaaaep vtptskagsg apggtskgpa eesrvrrhkh ssespgrdkg
klsrlkpapp
 901 pppaasagka ggkpsqspsq eaageavlga ktkatslvda vnsdaakpsq
pgeglkkpvl
 961 patpkpqsak psgtpispap vpstlpsass alagdqpsst afiplistrv
slrktrqppe
1021 riasgaitkg vvldstealc laisrnseqm ashsavleag knlytfcvsy
vdsiqqmrnk
1081 fafreainkl ennlrelqic patagsgpaa tqdfskllss vkeisdivqr
(SEQ ID NO:1)
```

Methods for identifying mutations in subjects with CML are also known in the art, and include direct sequencing, optionally combined with nested PCR and/or denaturing-high performance liquid chromatography (D-HPLC) analysis; allele-specific PCR (e.g., fluorescent allele-specific PCR); pyrosequencing; high resolution melting; double gradient denaturing electrophoresis; MALDT-TOF mass spectrometry; nanofluidic array (Oehler et al., Lekuemia 2008); fluorescence PCR and PNA clamping; fluorescence polarization template-directed dye-terminator incorporation (FP-TDI); and microarray analysis. Other methods of nucleic acid analysis can include direct manual sequencing (Church and Gilbert, *Proc. Natl. Acad. Sci. USA* 81:1991-1995 (1988); Sanger et al., *Proc. Natl. Acad. Sci. USA* 74:5463-5467 (1977); Beavis et al., U.S. Pat. No. 5,288,644); automated fluorescent sequencing; single-stranded conformation polymorphism assays (SSCP) (Schafer et al., *Nat. Biotechnol.* 15:33-39 (1995)); clamped denaturing gel electrophoresis (CDGE); two-dimensional gel electrophoresis (2DGE or TDGE); conformational sensitive gel electrophoresis (CSGE); denaturing gradient gel electrophoresis (DGGE) (Sheffield et al., *Proc. Natl. Acad. Sci. USA* 86:232-236 (1989)); denaturing high performance liquid chromatography (DHPLC, Underhill et al., *Genome Res.* 7:996-1005 (1997)); infrared matrix-assisted laser desorption/ionization (IR-MALDI) mass spectrometry (WO 99/57318); mobility shift analysis (Orita et al., *Proc. Natl. Acad. Sci. USA* 86:2766-2770 (1989)); restriction enzyme analysis (Flavell et al., *Cell* 15:25 (1978); Geever et al., *Proc. Natl. Acad. Sci. USA* 78:5081 (1981)); quantitative real-

time PCR (Raca et al., *Genet Test* 8(4):387-94 (2004)); heteroduplex analysis; chemical mismatch cleavage (CMC) (Cotton et al., *Proc. Natl. Acad. Sci. USA* 85:4397-4401 (1985)); RNase protection assays (Myers et al., *Science* 230:1242 (1985)); use of polypeptides that recognize nucleotide mismatches, e.g., *E. coli* mutS protein; and combinations of such methods. See, e.g., Gerber et al., U.S. Patent Publication No. 2004/0014095 which is incorporated herein by reference in its entirety. Other methods can also be used.

Although the methods described herein refer to treatment of CML, the methods can also be used to treat other IM-resistant BCR-ABL+ leukemia, e.g., Ph+ Acute Lymphoblastic Leukemia (~20% in adult, 5% in children), Ph+ Acute Myelogenous Leukemia (~2%), and potentially KIT+ gastrointestinal stromal tumors (GIST, as Imatinib can also inhibit KIT kinase) as well.

BCR-ABL inhibitors

A number of BCR/ABL inhibitors are known in the art. For example, imatinib (GLEEVEC) has been successfully used in the treatment of CML. Additional BCR/ABL inhibitors include Nilotinib (AMN107); Dasatinib (BMS-345825); Bosutinib (SKI-606); Ponatinib (AP24534); Bafetinib (INNO-406); and thiazol and thiazol derivatives, e.g., 1,3,4 thiadiazole derivatives.

MEK inhibitors

A number of MEK inhibitors (which specifically inhibit mitogen-activated protein kinase kinase enzymes MEK1 and/or MEK2) are known in the art. For example, Trametinib (GSK1120212) has been used for the treatment of certain cancers. Other examples of MEK inhibitors include Selumetinib, MEK162, PD-325901, cobimetinib (XL518; [3,4-Difluoro-2-(2-fluoro-4-iodoanilino)phenyl]{3-hydroxy-3-[(2S)-piperidin-2-yl]azetidin-1-yl} methanone), CL-1040, and PD035901.

Pharmaceutical compositions

The methods described herein include the manufacture and use of pharmaceutical compositions, which include a BCR-ABL inhibitor, e.g., IM, and a MEK inhibitor, e.g., trametinib as active ingredients. Also included are the pharmaceutical compositions themselves.

Pharmaceutical compositions typically include a pharmaceutically acceptable carrier. As used herein the language "pharmaceutically acceptable carrier" includes saline, solvents, dispersion media, coatings, antibacterial and antifungal agents,

isotonic and absorption delaying agents, and the like, compatible with pharmaceutical administration.

Pharmaceutical compositions are typically formulated to be compatible with its intended route of administration. Examples of routes of administration include parenteral, e.g., intravenous, intradermal, subcutaneous, oral (e.g., inhalation), transdermal (topical), transmucosal, and rectal administration.

Methods of formulating suitable pharmaceutical compositions are known in the art, see, e.g., Remington: The Science and Practice of Pharmacy, 21st ed., 2005; and the books in the series Drugs and the Pharmaceutical Sciences: a Series of Textbooks and Monographs (Dekker, NY). For example, solutions or suspensions used for parenteral, intradermal, or subcutaneous application can include the following components: a sterile diluent such as water for injection, saline solution, fixed oils, polyethylene glycols, glycerine, propylene glycol or other synthetic solvents; antibacterial agents such as benzyl alcohol or methyl parabens; antioxidants such as ascorbic acid or sodium bisulfite; chelating agents such as ethylenediaminetetraacetic acid; buffers such as acetates, citrates or phosphates and agents for the adjustment of tonicity such as sodium chloride or dextrose. pH can be adjusted with acids or bases, such as hydrochloric acid or sodium hydroxide. The parenteral preparation can be enclosed in ampoules, disposable syringes or multiple dose vials made of glass or plastic.

Pharmaceutical compositions suitable for injectable use can include sterile aqueous solutions (where water soluble) or dispersions and sterile powders for the extemporaneous preparation of sterile injectable solutions or dispersion. For intravenous administration, suitable carriers include physiological saline, bacteriostatic water, Cremophor EL™ (BASF, Parsippany, NJ) or phosphate buffered saline (PBS). In all cases, the composition must be sterile and should be fluid to the extent that easy syringability exists. It should be stable under the conditions of manufacture and storage and must be preserved against the contaminating action of microorganisms such as bacteria and fungi. The carrier can be a solvent or dispersion medium containing, for example, water, ethanol, polyol (for example, glycerol, propylene glycol, and liquid polyetheylene glycol, and the like), and suitable mixtures thereof. The proper fluidity can be maintained, for example, by the use of a coating such as lecithin, by the maintenance of the required particle size in the case of dispersion and by the use of surfactants. Prevention of the action of microorganisms

can be achieved by various antibacterial and antifungal agents, for example, parabens, chlorobutanol, phenol, ascorbic acid, thimerosal, and the like. In many cases, it will be preferable to include isotonic agents, for example, sugars, polyalcohols such as mannitol, sorbitol, sodium chloride in the composition. Prolonged absorption of the injectable compositions can be brought about by including in the composition an agent that delays absorption, for example, aluminum monostearate and gelatin.

Sterile injectable solutions can be prepared by incorporating the active compound in the required amount in an appropriate solvent with one or a combination of ingredients enumerated above, as required, followed by filtered sterilization. Generally, dispersions are prepared by incorporating the active compound into a sterile vehicle, which contains a basic dispersion medium and the required other ingredients from those enumerated above. In the case of sterile powders for the preparation of sterile injectable solutions, the preferred methods of preparation are vacuum drying and freeze-drying, which yield a powder of the active ingredient plus any additional desired ingredient from a previously sterile-filtered solution thereof.

Oral compositions generally include an inert diluent or an edible carrier. For the purpose of oral therapeutic administration, the active compound can be incorporated with excipients and used in the form of tablets, troches, or capsules, e.g., gelatin capsules. Oral compositions can also be prepared using a fluid carrier for use as a mouthwash. Pharmaceutically compatible binding agents, and/or adjuvant materials can be included as part of the composition. The tablets, pills, capsules, troches and the like can contain any of the following ingredients, or compounds of a similar nature: a binder such as microcrystalline cellulose, gum tragacanth or gelatin; an excipient such as starch or lactose, a disintegrating agent such as alginic acid, Primogel, or corn starch; a lubricant such as magnesium stearate or Sterotes; a glidant such as colloidal silicon dioxide; a sweetening agent such as sucrose or saccharin; or a flavoring agent such as peppermint, methyl salicylate, or orange flavoring.

For administration by inhalation, the compounds can be delivered in the form of an aerosol spray from a pressured container or dispenser that contains a suitable propellant, e.g., a gas such as carbon dioxide, or a nebulizer. Such methods include those described in U.S. Patent No. 6,468,798.

Systemic administration of a therapeutic compound as described herein can also be by transmucosal or transdermal means. For transmucosal or transdermal administration, penetrants appropriate to the barrier to be permeated are used in the

formulation. Such penetrants are generally known in the art, and include, for example, for transmucosal administration, detergents, bile salts, and fusidic acid derivatives. Transmucosal administration can be accomplished through the use of nasal sprays or suppositories. For transdermal administration, the active compounds are formulated into ointments, salves, gels, or creams as generally known in the art.

The pharmaceutical compositions can also be prepared in the form of suppositories (e.g., with conventional suppository bases such as cocoa butter and other glycerides) or retention enemas for rectal delivery.

In one embodiment, the therapeutic compounds are prepared with carriers that will protect the therapeutic compounds against rapid elimination from the body, such as a controlled release formulation, including implants and microencapsulated delivery systems. Biodegradable, biocompatible polymers can be used, such as ethylene vinyl acetate, polyanhydrides, polyglycolic acid, collagen, polyorthoesters, and polylactic acid. Such formulations can be prepared using standard techniques, or obtained commercially, e.g., from Alza Corporation and Nova Pharmaceuticals, Inc. Liposomal suspensions (including liposomes targeted to selected cells with monoclonal antibodies to cellular antigens) can also be used as pharmaceutically acceptable carriers. These can be prepared according to methods known to those skilled in the art, for example, as described in U.S. Patent No. 4,522,811.

The pharmaceutical compositions can be included in a container, pack, or dispenser together with instructions for administration.

Dosing

An "effective amount" is an amount sufficient to effect beneficial or desired results. For example, a therapeutic amount is one that achieves the desired therapeutic effect. This amount can be the same or different from a prophylactically effective amount, which is an amount necessary to prevent onset of disease or disease symptoms. An effective amount can be administered in one or more administrations, applications or dosages. A therapeutically effective amount of a therapeutic compound (i.e., an effective dosage) depends on the therapeutic compounds selected. The compositions can be administered one from one or more times per day to one or more times per week; including once every other day. The skilled artisan will appreciate that certain factors may influence the dosage and timing required to effectively treat a subject, including but not limited to the severity of the disease or disorder, previous treatments, the general health and/or age of the subject, and other

diseases present. Moreover, treatment of a subject with a therapeutically effective amount of the therapeutic compounds described herein can include a single treatment or a series of treatments.

Dosage, toxicity and therapeutic efficacy of the therapeutic compounds can be determined by standard pharmaceutical procedures in cell cultures or experimental animals, e.g., for determining the LD50 (the dose lethal to 50% of the population) and the ED50 (the dose therapeutically effective in 50% of the population). The dose ratio between toxic and therapeutic effects is the therapeutic index and it can be expressed as the ratio LD50/ED50. Compounds which exhibit high therapeutic indices are preferred. While compounds that exhibit toxic side effects may be used, care should be taken to design a delivery system that targets such compounds to the site of affected tissue in order to minimize potential damage to uninfected cells and, thereby, reduce side effects.

The data obtained from cell culture assays and animal studies can be used in formulating a range of dosage for use in humans. The dosage of such compounds lies preferably within a range of circulating concentrations that include the ED50 with little or no toxicity. The dosage may vary within this range depending upon the dosage form employed and the route of administration utilized. For any compound used in the method of the invention, the therapeutically effective dose can be estimated initially from cell culture assays. A dose may be formulated in animal models to achieve a circulating plasma concentration range that includes the IC50 (i.e., the concentration of the test compound which achieves a half-maximal inhibition of symptoms) as determined in cell culture. Such information can be used to more accurately determine useful doses in humans. Levels in plasma may be measured, for example, by high performance liquid chromatography.

Alternatively, doses approved by the FDA can be used, e.g., for trametinib, 1-2 mg orally once a day, and up to a maximum of 800 mg/day of imatinib.

EXAMPLES

The invention is further described in the following examples, which do not limit the scope of the invention described in the claims.

MATERIALS AND METHODS

The following materials and methods were used in the Examples set forth herein.

Study design

The overall study objective was to identify mechanisms underlying BCR-ABL-independent IM-resistance in CML and CML stem cells. The study used cultured human CML cell lines, BCR-ABL+ mouse primary bone marrow cells, mouse models of BCR-ABL-independent IM-resistant CML, and bone marrow or blood samples from CML patients. The study consisted of a series of controlled laboratory experiments and measured multiple parameters including gene expression, cell viability, apoptosis, cell signaling pathway activity, and leukemic progression as described below. For animal experiments, mice were randomly allocated to each group for drug treatment after bone marrow transplantation, and were subsequently analyzed in a non-blinded fashion. Animal sample sizes were selected based on precedent established by previous publications and an understanding that at least n=5 is generally required to achieve statistical significance. Human CML samples were selected on the basis of sample availability and a requirement to achieve statistical significance. For mouse experiments involving shRNAs, the most efficacious shRNA of multiple shRNAs tested and validated in cell culture was used, a criterion that was established prospectively. All quantitative data were collected from experiments performed in at least triplicate.

Clone IDs for individual shRNAs used in this study are listed in table 5 and primer sequences used for qRT-PCR analysis are listed in table 6.

Table 5. List of clone IDs for shRNAs obtained from Open Biosystems/Thermo Scientific.

Human Gene	First shRNA	Second shRNA
ABCB6	TRCN0000060318	
ADARB2	TRCN0000051893	
AIFM3	TRCN0000064545	
AKR1C1	TRCN0000036544	
AKR1C3	TRCN0000026540	
ANO2	TRCN0000138764	
ARAF	TRCN0000000571	TRCN0000000568
ASAH3L	TRCN0000050685	
BAP1	TRCN0000007373	TRCN0000007372
BAZ2A	TRCN0000015571	
BCAP29	TRCN0000060447	TRCN0000060444
BMI1	TRCN0000020158	

Table 5. List of clone IDs for shRNAs obtained from Open Biosystems/Thermo Scientific.		
BMP6	TRCN0000058615	
BRAF	TRCN0000006291	TRCN0000006292
C6orf224	TRCN0000140490	
CCL14	TRCN0000057850	
CD22	TRCN0000057623	TRCN0000057625
CELA1	TRCN0000003679	TRCN0000003681
CHRNA1	TRCN0000060992	
CLEC5A	TRCN0000054035	TRCN0000054034
CMYA5	TRCN0000129695	
CRAF	TRCN0000001067	TRCN0000001068
CUBN	TRCN0000055649	
CYP46A1	TRCN0000063810	
DGKD	TRCN0000000672	
DNASE1L1	TRCN0000049688	TRCN0000049690
DPM1	TRCN0000036188	TRCN0000036186
DUSP13	TRCN0000003064	
EBF1	TRCN0000013828	TRCN0000013830
EFEMP2	TRCN0000053336	
EFNA3	TRCN0000058722	
EHD2	TRCN0000053473	
ELF5	TRCN0000013875	TRCN0000013877
EXOSC7	TRCN0000051072	TRCN0000051070
E2F4	TRCN0000013809	TRCN0000013810
FAHD1	TRCN0000050068	
FAM92A1	TRCN0000136349	
GDAP1L1	TRCN0000136540	
GFRA2	TRCN0000060710	
GHRH	TRCN0000083152	
GRK5	TRCN0000000842	
GTF3C4	TRCN0000013402	
IDH3A	TRCN0000027270	TRCN0000027310
IDS	TRCN0000051546	
IFT140	TRCN0000147721	
IL1A	TRCN0000059211	
ITCH	TRCN0000002087	
KCNC4	TRCN0000044942	
KCNH3	TRCN0000044593	
KIR2DL2	TRCN0000061458	
LEP	TRCN0000058353	
LGALS9	TRCN0000057446	
LILRA3	TRCN0000056945	TRCN0000056946
LMO7	TRCN0000006490	
LRAT	TRCN0000035998	
MED8	TRCN0000052951	
MEGF8	TRCN0000055555	TRCN0000055554
MEP1A	TRCN0000050903	
MMP7	TRCN0000051847	TRCN0000051844

Table 5. List of clone IDs for shRNAs obtained from Open Biosystems/Thermo Scientific.		
MOV10	TRCN0000049978	
NCBP1	TRCN0000059506	
OBFC2A	TRCN0000134695	
OR2D2	TRCN0000060969	
PAG1	TRCN0000123270	
POLR1C	TRCN0000052904	
PRKCH	TRCN0000006296	TRCN0000006295
PRSS1	TRCN0000052119	
PSMD10	TRCN0000058074	
RASL10B	TRCN0000047610	
RCVRN	TRCN0000053264	TRCN0000053263
RFK	TRCN0000037600	
RIN2	TRCN0000062647	
RPP38	TRCN0000049875	TRCN0000049876
RPS6KB1	TRCN0000003162	
SEC23IP	TRCN0000064955	
SGK493	TRCN0000037531	
SH3TC1	TRCN0000062611	
SOX18	TRCN0000017449	
STK11	TRCN0000000408	TRCN0000000409
STYXL1	TRCN0000003054	TRCN0000003052
TCEAL1	TRCN0000013415	TRCN0000013413
TM4SF18	TRCN0000122444	
TMEM140	TRCN0000138719	TRCN0000138320
TRAF4	TRCN0000034239	TRCN0000034241
TRIM24	TRCN0000021262	
UBAP2L	TRCN0000007681	TRCN0000007679
WDR45L	TRCN0000148944	
WDR92	TRCN0000053730	
WNT7B	TRCN0000061877	TRCN0000061875
ZACN	TRCN0000060205	TRCN0000060204
ZFP82	TRCN0000016086	
ZHX1	TRCN0000020354	
ZKSCAN3	TRCN0000017750	
Mouse Gene		
Bap1	TRCN0000030719	TRCN0000030721
Bcap29	TRCN0000099810	TRCN0000099811
Cd22	TRCN0000067945	TRCN0000067946
Cela1	TRCN0000092406	TRCN0000092407
Clec5a	TRCN0000067713	TRCN0000067715
Dnase1l1	TRCN0000108731	TRCN0000108730
Dpm1	TRCN0000111999	TRCN0000111996
Ebf1	TRCN0000086578	TRCN0000086580
Human Gene	**First shRNA**	**Second shRNA**
Elf5	TRCN0000081940	TRCN0000081938
Exosc7	TRCN0000051070	TRCN0000051068
E2f4	TRCN0000085633	TRCN0000085634
Idh3a	TRCN0000041785	TRCN0000041786

Table 5. List of clone IDs for shRNAs obtained from Open Biosystems/Thermo Scientific.		
Megf8	V3LMM_497156	V3LMM_457695
Mmp7	TRCN0000031250	TRCN0000031251
Prkch	TRCN0000022812	TRCN0000022811
Rcvrn	TRCN0000053267	V3LMM_504872
Rpp38	TRCN0000099598	TRCN0000099599
Stk11	TRCN0000024146	TRCN0000024147
Styxl1	TRCN0000071409	TRCN0000071412
Tceal1	TRCN0000108607	TRCN0000108608
Tmem140	TRCN0000177850	TRCN0000178239
Traf4	TRCN0000067747	TRCN0000067743
Ubap2l	TRCN0000007677	TRCN0000007679
Wnt7b	TRCN0000071779	TRCN0000071780

Table 6. List of primer sequences used for quantitative real-time RT-PCR.				
Forward primer sequence (5' → 3')		**#**	**Forward primer sequence (5' → 3')**	**#**
Human Gene				
BAP1	ATCTGGGTCCTGTCATCAGC	1.	GCTGCCTTGGATTGGTCTG	2.
BCAP29	AACTAGTAGAAGACCAGGAG	3.	CGAAAGTCTCTCTGACTGC	4.
CD22	CACCTCAATGACAGTGGTCAG	5.	TGGATCGGATACCCATAGCAG	6.
CELA1	TCCAGCTCCTCCTACTGG	7.	CAGAATACTTGCCATTCACC	8.
CLEC5A	AGGTGGCGTTGGATCAACAA	9.	TTAGGCCAATGGTCGCACAG	10.
DNASE1L1	CTGCACACCACTCCTAAGGC	11.	CAGGCGCTTTTTGGTCAGT	12.
DPM1	ATGGATGCTGATCTCTCACACC	13.	CCATTTCCTTTGTAGCGAGTTCC	14.
EBF1	CCTGGTGTTGTGGAAGTCACA	15.	GCTCAACGAACCCACCATC	16.
ELF5	GCTGATTCCAACTGCTTGAAAAC	17.	CAGTTTTCTTCAGGAGATAGAAGC	18.
EXOSC7	CCAAATGAAGGCTACTTGGAGT	19.	TAGAGGGTGTTAGCGATCTCG	20.
E2F4	ATCGGGCTAATCGAGAAAAAGTC	21.	TGCTGGTCTAGTTCTTGCTCC	22.
IDH3A	AGCCGGTCACCCATCTATGAA	23.	TAGAGACACATGGTCGGACAT	24.
LILRA3	GCTCACTCAGCTCCAACC	25.	TCACCAGCCTTGGATTCG	26.
LYN	TTCTGGTCTCCGAGTCACTCA	27.	GCCGTCCACTTAATAGGGAACT	28.
MEGF8	CGCCTGTCTTCGTCACGTC	29.	CTGCTGAAAGGTGAGCAAGT	30.
MMP7	GTGGAGTGCCAGATGTTGC	31.	ATCGATCCACTGAATATGCG	32.
PRKCH	GTGACTTGATGTTCCACATTCAG	33.	ATTGTCCAGTTTCAGATCTCTATAG	34.
RCVRN	CACGCCGGAAAAGCGAGC	35.	GGATCAGTCGCAGAATTTCC	36.
RPP38	GACTTTGTGGACGAAGTAAGAGC	37.	GCTTTCCAGAGGTTCAGTCTC	38.
STK11	CTGCAAGCAGCAGTGAGG	39.	AACCGGCAGGAAGACTGAG	40.
STYXL1	GACCCCAAGATTCAGAAGG	41.	TCCGGGGAATCTTCTATCC	42.
TCEAL1	TCGTTCTCGCCCGCAATTTAG	43.	GATAAGGACGGCTCCGTTTTG	44.
TMEM140	TCGGCTTCTATAACTTCTGCCT	45.	CTGTTGCACTGGGCTAGGAG	46.
TRAF4	TGCCTATCCGCTGCATCC	47.	TTCATGGGGCAGCGATTAGC	48.
UBAP2L	ATAGCAGCGGCAATACGTGG	49.	GAAGACACATTAGAGGCAGTGAA	50.
WNT7B	GAAGCAGGGCTACTACAACCA	51.	CGGCCTCATTGTTATGCAGGT	52.
ZACN	GAGAGGGGAACAGCGAGAG	53.	CAGTCTCAGGCCAGCTTCTC	54.
Mouse Gene				
Bap1	TAGTCCTCCCAGCAAATGTAAG	55.	GTCTTCCTCCTCCTGCATAG	56.
Bcap29	TTCTGTCTGCCCTTTATTCCTCC	57.	TCTTACTTCTCTCACGGCATCT	58.
Cd22	AAGCTGGATGTCCATTATGCTC	59.	TCTGTAGGAGGTGACGTCTG	60.
Cela1	TCTGGATGCCAGGGTGATTC	61.	TATTCATCCAGGAAATGTAAGCAG	62.
Mclec5a	GAAACTGGGATTTTCACCAAGG	63.	TCCTGAAGATACTTCAGTTTCTC	64.
Dnase1l1	TATGTGTATATCTACAGGTCTGAC	65.	ACCACACTTGGAAGAGTTTTGC	66.
Dpm1	GTAATTTTGATATTGTCTCTGGAAC	67.	CTTCTTTTCGGTATAATCTGAAGC	68.
Ebf1	CTCACCCTATGCCATTGTGC	69.	CGAAAGCACTCTTCTGTTTCAC	70.
Elf5	TGCCTTTGAGCATCAGACAG	71.	TACTGGTCGCAGCAGAATTG	72.
Exosc7	GTGATGACCTTGGCACAGAG	73.	CATTCCAGCAGCAGCACATC	74.
E2f4	ACATCTGAGATTGCAGTGAGTG	75.	TACTACTATCCAGCAGTGCAG	76.
Idh3a	TGGGTGTCCAAGGTCTCTC	77.	CTCCCACTGAATAGGTGCTTTG	78.
Megf8	CTGCCAGTGTTCTAGGAAACTAC	79.	ATGTGAGTAACGGCCACTAGG	80.

Table 6. List of primer sequences used for quantitative real-time RT-PCR.				
Forward primer sequence (5' → 3')		**#**	**Forward primer sequence (5' → 3')**	**#**
Mmp7	TGAGGACGCAGGAGTGAAC	81.	CGTCCTTTGTAAGACTGAAGTC	82.
Prkch	TCCGGCACGATGAAGTTCAAT	83.	TACGCTCACCGTCAGGTAGG	84.
Rcvrn	ACGACGTAGACGGCAATGG	85.	CCGCTTTTCTGGGGTGTTTT	86.
Rpp38	CTTCTGCTCAGGGTTTTCAAG	87.	ATGTCTTCTCTCTCCAAGGTG	88.
Stk11	AGTATGACTGTAGTGCCCTAC	89.	CAGGACCTGTCCAGGCAC	90.
Styxl1	CTGCTTTTCTGCGAGCCAAC	91.	TGTCGTTTTGATCGGACATCC	92.
Tceal1	GTATCCGCCCTCAATTCATAG	93.	CTCCGTTTTGCCTTCCAATGC	94.
Tmem140	CAGCGTTGGTTTTTGTCTCCC	95.	GAGGAGAGCGTAGAACATCAG	96.
Traf4	CCCGGCTTCGACTACAAGTTC	97.	TCAGGGCATTTGAAGACTCCT	98.
Ubap2l	TGCTACAACTTCAGGAAAAGCTC	99.	GTCTGGAGCATCTGTAAATCATC	100.
Wnt7b	CCCGATGCCATCATTGTGATC	101.	GTAGGGAGTCGAGAGGCTG	102.

#, SEQ ID NO.

Cell lines and culture

BCR-ABL+ positive human CML cell lines K562 (ATCC), K562R (kindly provided by Nicholas J. Donato, University of Michigan) and KYO-1 (kindly provided by Brian Druker) were maintained in RPMI 1640 medium containing 10% fetal bovine serum (FBS), 4 mM L-glutamine, 100 units/ml penicillin, and 100 µg/ml streptomycin. 32D/BCR-ABL cells (kindly provided by Tomasz Skorski, Temple University) were maintained in RPMI 1640 with 10% FBS.

RNAi screen

The RNAi Consortium (TRC) lentiviral human shRNA library (Open Biosystems/Thermo Scientific) was obtained through the University of Massachusetts RNAi Core facility. Twenty-two lentivirus pools, each comprising ~5000 shRNA clones, were generated with titers of ~$2x10^7$ cfu/ml, as previously described (*47*). $2x10^6$ K562 cells were transduced at a multiplicity of infection <1 with the lentiviral stocks in 6-well plates, and 2 days later puromycin selected (1 µg ml^{-1}) for 5 days. Cells were then treated with 20 µM IM (LC Laboratories) for 7 days, and washed twice with fresh medium until >99% of control cells (i.e., those expressing a non-silencing shRNA) died off. Surviving cells from all shRNA pools were combined and allowed to recover in IM-free medium with 1 µg/µl puromycin for 4 days. Live cells were sorted out with a Dead Cell Removal kit (Miltenyi Biotec) and harvested, and genomic DNA was prepared for sequencing identification of the integrated shRNA as previously described (Gavin et al., Nature 449, 1073-1077 (2007)).

Cell viability assay

To validate candidates, K562 or KYO-1 cells were stably transduced with a lentivirus carrying an individual shRNA and puromycin selected for 5 days. $2.5x10^3$ IMSG KD K562 cells or $1x10^4$ IMSG KD KYO-1 cells were plated in 96-well plates, and IM (10 µM for K562 cells or 0.1 µM for KYO-1 cells) or vehicle (DMSO) was added for 3 days. MTT reagent (Promega) or Alamar Blue (Invitrogen) was added to each well in 1:10 volume and incubated, and absorbance at 570 nm was recorded using a VICTOR^3 (PerkinElmer) or SpectraMAX M5 (Molecular Devices) plate reader.

For other cell viability assays, IMSG KD K562 cells or K562/*PRKCH* cells were treated for 3 days with a range of IM concentrations as indicated (Fig. 1E and 3B), or 0.1 μM IM, 1.5 nM trametinib or both (Fig. 4, A and B), and analyzed as described above. For Figure 1E and 3B and Figure 12, data were plotted in GraphPad Prism and a dose response curve was fit with nonlinear regression to calculate $IC50^{IM}$. For Figure 1F, IMSG KD K562 cells were treated with 10 μM IM or 500 nM dasatinib (ChemieTeK) and cell viability was analyzed as described above. The curve was fit with linear regression and correlation coefficient was calculated using GraphPad Prism.

Colony formation assay

For Figure 1D, mouse primary bone marrow cells were harvested from CML mice as described below, and subjected to two rounds of infection with a mouse IMSG shRNA lentivirus (listed in table 5). Two days later, $5x10^4$ IMSG KD cells were mixed with cytokine-free methycellulose-based medium (MethoCult M3234; STEMCELL Technologies) and 0.5 μM IM and plated in 35 mm dishes. Colonies were counted under brightfield microscope at day 7. For Fig.4C, primary bone marrow cells were transduced for two rounds with a retrovirus expressing *Prkch*, generated by PCR amplifying mouse *Prkch* cDNA (an MGC clone; Open Biosystems/Thermo Scientific) using forward (5'-ATAGGTTAACGCCACCATGTCGTCCGGCACGATGA-3'; SEQ ID NO:103) and reverse (5'-ATAGGAATTCCTACAGTTGCAATTCCGGTGA-3'; SEQ ID NO:104) primers, and digesting the PCR product with HpaI and EcoRI and cloning it into MSCV-IRES-GFP (Addgene plasmid 20672). Two days after transduction, $5x10^4$ cells were mixed with methylcellulose and 0.5 μM IM, 2 nM trametinib (ChemieTek) or both. For Fig. 5 B and C, primary bone marrow cells were collected from *Prkch* knockdown CML mice (generated using a retrovirus co-expressing BCR-ABL and a *Prkch* shRNA; see below), and 1x105 cells were plated in methylcellulose in the absence (Fig. 5B) or presence of 0.1 μM IM (Fig. 5C). For Fig. 7C, primary bone marrow cells were collected from either NS or *Prkch* knockdown CML mice, BCR-ABL+ murine stem cells (Lin-Sca1+Kit+) were isolated from the mice by fluorescence activated cell sorting (FACS), and IM sensitivity determined as described above for Fig. 5, B and C.

Immunoblot analysis

After 5 days puromycin selection, ~$1x10^6$ IMSG KD K562 cells were plated into 6-well dishes and treated with 10 μM IM for 36 hours. Cells were harvested and lysed with RIPA buffer (10x, 200 mM HEPES pH 6.8, 1400 mM NaCl, 25 mM $MgCl_2$, 25 mM $CaCl_2$, 10% NP40, and 5% sodium deoxycholate) plus phosphatase (Sigma) and protease inhibitors (Roche). Blots were probed with the following primary antibodies, all obtained from Cell Signaling Technology: BCR-ABL PathScan (p-BCR-ABL, p-STAT5, p-CRKL) (#5300S), total BCR-ABL (#2862S), p-ERK1/2 (#4377S), total ERK1/2 (#4695S), t-STAT5 (#9358S), p-AKT (#4060S), t-AKT (#4685S), p-SFK (#2105S), t-LYN (#2796S), t-CRKL (#3182S), p-MARCKS (#8722S), t-MARCKS (#5607S), ARAF (#4432S), BRAF (#9433S), CRAF (#9422S). The PKCη antibody (Santa Cruz Technology; C-15) was diluted in 5% skim milk at 1:150. The β-actin antibody (Sigma; AC-74) diluted in 5% BSA at 1:5000. Blots were developed with Pico/Femato super signal (Sigma) and visualized using autoradiography or a Bio-Rad ChemiDoc MP Imaging System.

RNA preparation and qRT-PCR

Total RNA was isolated from cells using TriPure Isolation Reagent (Roche) followed by treatment with turbo DNase (Ambion) to remove contaminating genomic DNA. Reverse transcription was performed using MMLV reverse transcriptase (NEB) followed by qPCR using Fast SYBR Green Master Mix (Applied Biosystems) using primers listed in table 6. The expression level of each gene was normalized to that of *GAPDH*. Knockdown efficiency was calculated relative to that obtained with a control non-silencing shRNA.

In vitro kinase assay

A plasmid expressing Flag-tagged PKCη was generated by PCR amplifying *PRKCH* from a cDNA clone (Open Biosystems/Thermo Scientific), and cloning the PCR product into expression vector p3xFlag-Myc-CMV-25 (Sigma). The kinase-dead K384R mutant was generated by PCR-based site-directed mutagenesis using PfuTurbo DNA polymerase (Agilent). Plasmids were transfected individually into 293T cells, and proteins were immunopurified from cell lysate using an anti-Flag antibody (Sigma). In vitro phosphorylation reactions were set up in a 20 μl reaction volume as follows: 1 μl ^{32}P-γ-ATP (10 mCi), 1 μl 10 μM ATP, 0.2 mM microcystin, 4 μl 5X kinase buffer [23 mM MOPS, 11.5 mM β-glycerophosphate, 23 mM $MgCl_2$,

4.6 mM EGTA, 1.8 mM EDTA, 0.25 mM DTT (pH 7.0)], 60 nM purified Flag-PKCη diluted in 1X kinase buffer, and 10 μM substrate (GST or GST fused to a peptide corresponding to amino acids 491-505 of CRAF, purified from *E. coli*) diluted in 1X kinase buffer. Reactions were incubated for 30 min at 30°C and stopped using 2X Laemmli Sample Buffer. Incorporation of the radiolabel into the peptide was monitored by autoradiography.

Flow cytometry analysis

Fifteen days after induction of CML-like disease (see below), bone marrow cells were flushed out of femur and tibia bones with RBC lysis buffer (155 mM NH_4Cl, 12 mM $NaHCO_3$, 0.1 mM EDTA), spun down at 1,000 rpm for 10 min, and washed once with PBS. 2-5x10^6 cells from each sample were aliquoted for staining. A cocktail of primary antibodies [APC-conjugated Sca-1 antibody (eBioscience), PE-conjugated c-Kit antibody (eBioscience) and Biotin-conjugated Lineage antibody cocktail (Miltenyi Biotec)] was added to each sample in a total volume of 100 μl, incubated on ice for 30 min, washed once by adding PBS (1 ml) and spin down at 1,000 rpm for 10 min. The secondary antibody (APC-eFluor780-conjugated Straptavidin; eBioscience) was added in a total volume of 100 μl, incubated for 20 min on ice, and then washed once with PBS. FACS analysis was performed immediately using an LSR II flow cytometer (BD Biosciences). The Lin+ population was separated from the Lin- population by magnetic beads (Miltenyi Biotec). GFP+Lin-Sca1+Kit+ and GFP+Lin- cells were then FACS sorted from the Lin- population, and GFP+Lin+Gr1+ cells were FACS sorted from the Lin+ population.

For Lin-Sca1+Kit+ apoptosis staining, 5 μl Annexin-V antibody [eFluor450-conjugated Annexin V (eBioscience)] was added to each sample after the last wash, and incubated for 20 min in the dark at room temperature. Samples were washed once, and 2 μl 7AAD (eBioscience) was added within 4 h before FACS analysis.

For intracellular phosphorylated-ERK1/2 analysis, bone marrow cells isolated from leukemic mice were treated with 5 μM IM or 10 nM trametinib for 3 hours, fixed in 4% paraformaldehyde (Electron Microscopy Sciences) for 10 min at 37°C, washed twice with wash buffer (0.05% BSA in 1x PBS), spun down, and resuspended in 100 μl wash buffer. Ice-cold methanol (900 μl) was added to the cells while gently vortexing to reach a final 90% for permeabilization. Samples were incubated on ice for 30 min, washed twice, and resuspended in 100 μl wash buffer. IgG control

antibody (Cell signaling) was added (at 1:100 dilution) for 10 min at room temperature for blocking, followed by addition of 2 µl conjugated IgG control (Pacific Blue-conjugated IgG^{XP} Rabbit mAb, Cell Signaling) or phospho-ERK antibody (Pacific Blue-conjugated P-p44/42(T202/Y204)^{XP} Rabbit mAb, Cell Signaling). Samples were gently mixed and incubated at room temperature for 1 hour. Thirty minutes after the start of the incubation, a cocktail of primary antibodies for cell surface markers (described above) was added, incubated for a further 30 min, washed once with PBS, and incubated with the secondary antibody for 20 min on ice. Samples were then washed once with wash buffer prior to FACS analysis. Relative phosphorylated ERK1/2 staining was calculated by first subtracting the IgG background staining and then normalizing the absolute fluorescence intensity (median) of the treatment group (Prkch knockdown or IM or trametinib treatment) to that of the control group (NS shRNA or DMSO).

Construction of BCR-ABL/shRNA or BCR-ABL/*Prkch* co-expression plasmids

shRNAs were subcloned from an effective TRC shRNA plasmid into the MluI site downstream of GFP in the retroviral vector MSCV-BCR-ABL-IRES-GFP (*22*) (using forward [5'-ATAGACGCGTTTCTTGGCTTTATATATCTTGTGG-3'; SEQ ID NO:105] and reverse [5'-ATAGACGCGTCAAAGTGGATCTCTGCTGTC-3'; SEQ ID NO:106] primers, where underlining indicates the MluI site) to ensure the shRNA would be expressed in the same transcript as BCR-ABL and GFP. Similarly, mouse *Prkch* cDNA was subcloned into MSCV-BCR-ABL-IRES-GFP as described above to generate an MSCV-BCR-ABL-IRES-mPRKCH-IRES-GFP triple gene expression construct. Virus titer was tested in NIH 3T3 cells. Briefly, $5x10^4$ cells were plated in each well of a 6-well plate, and virus was added at 1:1 dilution with fresh DMEM medium (10% FBS) plus Polybrene (Qiagen), and then cultured for 48 hours. FACS was performed to analyze GFP percentage. Only those viruses showing ≥90% infection were used for in vivo CML induction.

Mouse models of CML

Mice with CML-like disease were generated as previously described (*22*). Briefly, wild-type male C57BL/6 mice 6–8 weeks of age (Jackson Laboratory) were tail-vein injected with 5-fluorouracil (200 mg/kg; Sigma) for 4 days to enrich for slow-cycling hematopoietic stem cells. At day 5, bone marrow cells were harvested

and pre-incubated overnight in the presence of IL-3, IL-6 and SCF (all from PeproTech) to increase infection efficiency. At days 6 and 7, bone marrow cells were infected with a BCR-ABL retrovirus by co-sedimentation method at 3,000 rpm for 90 min at room temperature. Four hours after the second round of retroviral infection, $0.5x10^6$ bone marrow cells were injected into the tail vein of syngeneic recipient mice that had been lethally irradiated (twice at 550 R). Mice were randomly allocated to each group after bone marrow transplantation.

For drug treatment, mice were oral gavaged twice a day with IM (dissolved in filtered ddH_2O) at 100 mg/kg and/or once a day with trametinib (dissolved in 0.5% hydroxypropylmethycellulose and 0.2% Tween-80 in filtered ddH_2O) at 2 mg/kg.

White Blood Count

Peripheral blood (~25 µl) was collected from mouse tail veins into Microtainer tubes (BD Biosciences), and analyzed using a Hemavet 950 FS (Drew Scientific, Inc) cell counter within 3 hours after blood collection.

Acquisition and storage of CML patient samples

After informed consent in accordance with Institutional Review Board (IRB)-approved protocols, bone marrow aspirate or peripheral blood samples were collected from CML patients. For samples provided by the Druker lab and Emory University, mononuclear cells were isolated by Ficoll gradient and, depending on the number of viable cells available, cells were stored as pellets or guanidinium thiocynate (GTC) lysates (resuspended in Qiagen RLT lysis buffer + beta-mercaptoethanol) at -80°C, or resuspended in fetal bovine serum (FBS) + 10% DMSO, frozen slowly overnight, and then transferred to liquid nitrogen for long-term storage. For samples provided by the University of Massachusetts Medical School, white blood cells were isolated by red cell lysis, and cells were resuspended in FBS + 10% DMSO, frozen slowly overnight, and then transferred to liquid nitrogen for long-term storage. All samples were provided in a deidentified manner. Samples from normal donors were purchased from a commercial vendor (AllCells or Lonza).

Analysis of human CML patient samples

To analyze gene expression in IM-sensitive and IM-resistant CML patient samples (Fig. 3, C and D), RNA was obtained in the form of purified RNA or extracted independently from GTC lysate or Trizol stock, and qRT-PCR was performed as described above.

To culture primary cells derived from CML patients and normal individuals for functional experiments (Figs. 3E, 4D and 7F-G and Figs. 17A-B and 23B), frozen patient cells were first warmed for 10 min at 37°C. 1 ml of pre-warmed thawing medium (Iscove's Modified Dulbecco's Media [IMDM] with 5% FBS, 0.1 mg/ml DNase, and 400 U/ml heparin) was added slowly, followed by 10 ml of wash medium (IMDM with 5% FBS, 0.1mg/ml DNase). After passing through a 70 μm filter, cells were spun at 300 g for 10 min. Cell pellets were then resuspended in an adequate amount of culture medium (IMDM with 20% BIT [STEMCELL Technologies], 20 ng/ml IL-3, 20 ng/ml IL-6, 20 ng/ml FLT3, 100 ng/ml granulocyte colonystimulating factor (G-CSF), and 100 ng/ml SCF [PeproTech]) and incubated overnight at 37°C. Cells were then either directly used, or further enriched for the CD34+ population using CD34 MicroBead Kit UltraPure (Miltenyi Biotec).

For *PRKCH* knockdown, a volume of *PRKCH* shRNA-GFP lentivirus equal to the volume of cells was used to infect cells at 2,000 g for 90 min at room temperature. After culturing for an additional 16-24 hours, cells were pelleted at 300 g for 10 min and resuspended in culture medium with 1% of initial cytokines, a more physiologically relevant concentration. Cells were then treated with DMSO, 5 μM IM, 5 nM trametinib, or both drugs for 4 days. The cell viability of the target population was then calculated by multiplying the percentage of target population, which was obtained by FACS analysis, and the total number of live cells, which was determined by trypan blue staining.

To analyze *PRKCH* expression in human CML stem cells (CD34+CD38-) and progenitor cells (CD34+CD38+) (Fig. 6B), freshly thawed CML cells or CD34+-enriched CML cells were directly stained for CD34 and CD38 cell surface markers. The target population was isolated by FACS and total RNA was extracted by Trizol for qRT-PCR analysis as described above. For bioinformatic analysis (Fig. 6C), CEL files were downloaded from Gene Expression Omnibus (GEO accession GSE43754), and *PRKCH* expression analysis was performed using the R program 'RMA' in the BioConductor 'oligo' package (*66*) with full probeset annotation.

Chromatin immunoprecipitation (ChIP)

K562 cells (1x107) were crosslinked with 1% formaldehyde for 12 min at room temperature, followed by addition of 0.125 mM glycine for 10 min. Cells were washed twice and lysed in ChIP lysis buffer (50 mM HEPES pH 8.0, 150 mM NaCl,

1 mM EDTA, 0.1%Na-deoxycholate, 1% TritonX-100, 0.1%SDS, plus protease inhibitor) for 15 min on ice. The lysate was sonicated for 12 rounds (30 seconds on, 1 minute 30 seconds off, power output 6.0) using Sonicator 3000 (Qsonica), and clarified by centrifugation. 50 µl 50% protein-G agarose bead slurry was used to pre-clear 5 mg of chromatin for over 4 hours at 4°C. For ChIP experiments, 500 µg pre-cleared chromatin were incubated overnight with either 5 µg anti-ELF5 antibody ((N-20) X, Santa Cruz) or IgG, followed by addition of 50 µl 50% protein-G agarose bead slurry and incubation for 4 hours at 4°C. Beads were pelleted by centrifugation and washed twice with ChIP lysis buffer, once with high salt lysis buffer (ChIP lysis buffer adjusted to 1M NaCl), thrice with LiCl wash buffer (50 mM HEPES pH 8.0, 250 mM LiCl, 1 mM EDTA, 0.5% deoxycholate, 0.5% NP40, plus protease inhibitor), and once with Tris-EDTA buffer. After the last wash, the supernatant was removed and 400 µl elution buffer (1% SDS, 0.1% NaHCO3) was added and incubated for 15 min at 65°C with occasional vortexing. Beads were pelleted, and the supernatant was transferred to a new tube and reverse-crosslinked overnight at 65°C. RNase A (2 µl of 10 mg/ml) was added to each ChIP sample and incubated for 1 hour at 37°C, followed by addition of 5 µl Protease K (20 mg/ml, Promega) and incubation for 2 hours at 55°C. DNA was phenol:chloroform extracted and isopropanol precipitated, and subjected to qPCR with the following primers: TSS-for (5'-AGGAGGAGAAGCAAGAGGAG-'3'; SEQ ID NO:107) and TSS-rev (5'-CCGACCGTCCCTTCCAAG-3'; SEQ ID NO:108), 500-for (5'-GACCTTTCCTGCTCTATGTG-3'; SEQ ID NO:109) and 500-rev (5'-CTGCAGAGGCTAATTACACAG-3'; SEQ ID NO:110), and 1000-for (5'-CATAGCAGCGTAGGCTAAAA G-3'; SEQ ID NO:111) and 1000-rev (5'-CGGAAGAAATTGCCTCTTCTAG-3'; SEQ ID NO:112). Fold enrichment was calculated by setting the IgG control to a value of 1.

Luciferase reporter assays

A 2 kb genomic DNA region upstream of the PRKCH transcription start site was PCR amplified from a BAC clone (RP11-1069E8) using forward and reverse primers (5'-ATAGGCTAGCGTTCTGAACAGGGCCTTAGAG-3'; SEQ ID NO:113 and 5'-ATAGAAGCTTGATGCGGACCCTCAAATAGC-3'; SEQ ID NO:114, respectively), digested with NheI and HindIII, and ligated into the firefly luciferase reporter vector PGL4.14[luc2/Hygro] (Promega). 2 µg of this reporter and 40 ng of

pRL-TK Renilla luciferase control reporter vector (Promega) were co-transfected into ELF5 knockdown or overexpression K562 cells by electroporation. After 48 hours of culturing, cells were lysed and centrifuged. Supernatants were incubated with luciferase substrate (Promega) and the luciferase activity was recorded by VICTOR3 (PerkinElmer) plate reader.

Statistics

All quantitative data were collected from experiments performed in at least triplicate, and expressed as mean +/- standard deviation. Animal experiments were expressed as mean +/- standard error of the mean. Statistical analyses were performed using R, a system for statistical computation and graphics (Ihaka and Gentleman, J Comput Graph Stat 5, 299-314 (1996)). Relative cell viability data (Fig. 1, B and C, 3E, 4D, 7F, 7G, 9, 10A, 17B and 23B) and cell death data (Fig. 22A) were first arcsine transformed to homogenize the variance. Colony number (Fig. 1D and Fig. 11B and 20) and cell number (Fig. 7D) data were first log transformed. Levene's test was performed to test for homogeneity of variance. When the assumption of homogeneity of variances was met, ANOVA was performed followed by predetermined contrasts within the ANOVA framework. When the assumption was violated, a non-parametric counterpart of ANOVA (Kruskal–Wallis test for completely randomized design or Friedman rank sum test for randomized complete block design) was performed. In some instances, *P* values were adjusted to counteract the problem of multiple comparisons (Benjamini and Hochberg, J. Roy. Statist Soc Ser B 57, 289-300 (1995)). Significant differences were considered when $P<0.05$; $*P\leq0.05$ and $**P\leq0.01$. Statistical tests and exact *P* values are provided in table 4.

Statistical analysis for drug synergy was performed using R (Ihaka and Gentleman, J Comput Graph Stat 5, 299-314 (1996)) to assess whether the combined effects from IM and trametinib were additive (responses were equal to the sum of the single-drug effects), synergistic (greater than the sum of the single-drug effects) or antagonistic (less than the sum of the single-drug effects). Two-way analysis of variance (ANOVA) was used to test for the main effects of IM and trametinib and their interaction on cell viability and apoptosis. Benjamini and Hochberg (BH)-adjusted *P* value was calculated to counteract the problem of multiple comparisons (Benjamini and Hochberg, J. Roy. Statist Soc Ser B 57, 289-300 (1995)). The difference between observed effects and the expected additive effects for the cell lines

exposed to both drugs were compared as previously described (Slinker, J Mol Cell Cardiol 30, 723-731 (1998)). The difference was estimated as the interaction coefficient in ANOVA. For cell viability, if there was a significant positive difference (interaction coefficient > 0 and BH-adjusted *P* value < 0.05), then the impact from the combined drugs was classified as antagonism; if there was a significant negative difference (interaction coefficient < 0 and BH-adjusted *P* value < 0.05), then the impact from the combined drugs was classified as synergistic; if there was no significant difference, then the impact from the combined drugs was classified as additive. For apoptosis, if there was a significant positive difference, then the impact from the combined drugs was classified as synergism; if there was a significant negative difference, then the impact from the combined drugs was classified as antagonism.

Example 1. A large-scale shRNA screen identifies IM-sensitizing genes

To identify IM-sensitizing genes (IMSGs), IM-sensitive human CML K562 cells (*18*) were stably transduced with pools of a genome-wide human short hairpin RNA (shRNA) library (*19*) followed by IM treatment (Fig. 1A). Surviving cells from all pools were combined and shRNAs, corresponding to 89 genes, were identified by sequence analysis. Validation experiments with individual shRNAs corresponding to those isolated from the primary screen, as well as second, unrelated shRNAs targeting the same genes, confirmed that knockdown of 25 genes conferred >2-fold increased K562 cell survival in the presence of IM relative to a control non-silencing (NS) shRNA (Fig. 1B and Fig. 9 and 10A). The extent of IM resistance after IMSG knockdown was roughly similar to that of the well-studied experimentally-derived IM-resistant cell line K562R and an IM-resistant patient-derived cell line, SUPB15 (Fig. 10B). Quantitative real-time RT-PCR (qRT-PCR) confirmed in all cases that expression of the target gene was decreased in the corresponding K562 knockdown (KD) cell line (Figs. 10C and D).

To confirm that these results were generalizable, the validated candidates were analyzed in KYO-1 cells, another IM-sensitive human CML cell line (*20*). Figure 1C shows that 21 of the 25 shRNA candidates validated in KYO-1 cells. Finally, whether knockdown of the validated candidates would also confer IM resistance was tested in BCR-ABL+ mouse primary bone marrow cells. Toward this end, CML-like disease was induced in C57BL/6 mice using a BCR-ABL-expressing retrovirus (*21, 22*).

Primary bone marrow cells were harvested, infected with a mouse candidate IMSG shRNA, and tested for their ability to form colonies in methylcellulose containing IM. Knockdown of 19 candidate IMSGs (Fig. 11A) rendered BCR-ABL+ primary bone marrow cells IM resistant (Fig. 1D). Equivalent results were obtained using a second, unrelated shRNA for each IMSG (Fig. 11B and C).

To quantify IM resistance, we determined the IC50 for imatinib ($IC50^{IM}$) of IMSG KD K562 cells. Knockdown of 11 IMSGs increased the $IC50^{IM}$ greater than five-fold (Fig. 1E and Fig. 12), and we therefore focused on these IMSGs in our subsequent experiments. The IC50IMs of these 11 IMSG KD K562 cell lines were similar to those of IM-resistant cell lines derived from CML patients (Quentmeier et al., J Hematol Oncol 4, 6 (2011)). These 11 IMSGs are involved in diverse biological processes including transcriptional regulation, signal transduction, protein metabolism and DNA/RNA metabolism (table 1).

Next, whether knockdown of IMSGs would cause resistance to the second-generation tyrosine kinase inhibitor, dasatinib (*23*) was tested. As a control, K562R cells were analyzed in parallel, which are resistant to IM but sensitive to dasatinib due to over-expression of the Src family kinase (SFK) LYN (*24*). All of the IMSG shRNAs that conferred IM resistance also caused resistance to dasatinib (Fig. 1F).

Table 1. List of 11 IMSGs obtained from the genome-wide RNAi screen. All candidates were validated with a second, unrelated shRNA. Knockdown conferred IM resistance in BCR-ABL-transformed primary bone marrow cells and increased $IC50^{IM}$ greater than 5-fold in K562 cells.

Biological process	**Gene symbol**	**Gene name**
Cell signaling	*CLEC5A*	C-type lectin domain family 5, member A
	STK11	Serine/threonine kinase 11
	WNT7B	Wingless-type MMTV integration site family, member 7B
DNA/RNA metabolism	*DNASE1L1*	Deoxyribonuclease I-like 1
	EXOSC7	Exosome component 7
	RPP38	Ribonuclease P/MRP 38kDa subunit
Protein metabolism	*BAP1*	BRCA1 associated protein-1 (ubiquitin carboxy-terminal hydrolase)
Transcriptional regulation	*ELF5*	E74-like factor 5 (ets domain transcription factor)
Immunity	*CD22*	CD22 molecule
Unknown	*MEGF8*	Multiple EGF-like-domains 8
	TMEM140	Transmembrane protein 140

Example 2. Knockdown of IMSGs in BCR-ABL+ cells results in sustained RAF/MEK/ERK signaling after IM treatment

Next, a series of experiments was performed to identify the regulatory pathway(s) through which IMSGs promote IM sensitivity. IMSG KD K562 cell lines were cultured in the presence or absence of IM followed by immunoblotting for characteristic markers of relevant cell signaling pathways. The results, shown in Figure 2, indicated that knockdown of IMSGs had no effect on total BCR-ABL levels. Moreover, in all IMSG KD K562 cell lines, IM inhibited BCR-ABL protein kinase activity, as evidenced by decreased BCR-ABL autophosphorylation and decreased phosphorylation of the BCR-ABL substrate CRKL (*25*). We also monitored the effect of IMSG knockdown on SFK activity, whose elevation, as mentioned above, is responsible for IM resistance in K562R cells. None of the IMSG KD K562 cell lines had elevated SFK activity or expression, consistent with their resistance to dasatinib.

The effect of IMSG knockdown was next analyzed on known downstream signaling pathways of BCR-ABL. All IMSG KD K562 cell lines had normal levels of phosphorylated STAT5 and AKT, indicating that JAK/STAT and PI3K/AKT signaling pathways were not affected by IMSG knockdown. In contrast, most of the IMSG KD K562 cell lines had increased RAF/MEK/ERK kinase pathway activity, as evidenced by increased phosphorylation of ERK1/2. As expected, after IM treatment of control K562 cells, there was a substantial decrease in phosphorylated-ERK1/2 levels. However, all of the IMSG KD K562 cell lines had, to varying extents, sustained levels of phosphorylation of ERK1/2 following IM treatment. Thus, in IMSG KD K562 cell lines there is an alternative pathway that activates RAF/MEK/ERK signaling after inhibition of BCR-ABL.

Previous studies have reported that the protein kinase C (PKC) pathway can stimulate RAF/MEK/ERK signaling (*26-28*). Therefore PKC pathway activity was analyzed in IMSG KD K562 cells by monitoring phosphorylation of a universal PKC substrate, MARCKS (*29*). Levels of MARCKS phosphorylation were elevated in all IMSG KD K562 cell lines, indicating elevated PKC activity.

Example 3. *PRKCH* is upregulated in BCR-ABL-independent IM-resistant CML cell lines and patient samples

Next, the PKC family member(s) responsible for the increased PKC activity were identified. The qRT-PCR results, shown in Figure 3A, showed that *PRKCH*,

which encodes PKCη, was upregulated in nearly all IMSG KD K562 cell lines. Similar results were obtained with a second shRNA targeting each IMSG (Fig. 13A). Immunoblot analysis confirmed that PKCη protein levels were also increased in the IMSG KD K562 cell lines (Fig. 13B).

As a first step toward understanding the basis by which IMSGs regulate PRKCH expression, one of the IMSGs, ELF5, a known transcriptional repressor (Chakrabarti et al., Nat Cell Biol 14, 1212-1222 (2012); Escamilla-Hernandez et al., BMC Mol Biol 11, 68 (2010)), was further analyzed. A chromatin immunoprecipitation assay was used; the results showed that ELF5 was directly bound at the transcription start site of PRKCH (Fig. 14A), consistent with the results of a study analyzing ELF5 occupancy genome-wide (Kalyuga et al., PLoS Biol 10, e1001461 (2012)). Moreover, we found that expression of a PRKCH promoter-luciferase reporter construct was increased by ELF5 knockdown and, conversely, decreased by ectopic expression of ELF5 (Fig. 14B and C). Thus, ELF5 is a direct transcriptional repressor of PRKCH, explaining why decreased ELF5 levels result in increased PRKCH expression.

To verify that increased PKCη expression is responsible for the IM resistance, we derived K562 cell lines that over-expressed *PRKCH* (K562/*PRKCH* cells) to varying degrees. In several K562/*PRKCH* cell lines, PKCη levels were comparable to those found in IMSG KD K562 cells (Fig. 15A). The elevated *PRKCH* expression resulted in a 10–20-fold increase in IM resistance (Fig. 3B). Conversely, knockdown of *PRKCH* abrogated the IM resistance of representative IMSG KD K562 cell lines (Fig. 15B).

To determine the clinical relevance of these results, *PRKCH* mRNA levels were analyzed in IM-resistant CML patient samples harboring wild-type BCR-ABL. As a control, *PRKCH* mRNA levels were also analyzed in IM-resistant CML patient samples that contained a known IM-resistance mutation in BCR-ABL (table 2). The results shown in Figure 3C show that PRKCH mRNA levels were significantly ($P<0.01$) higher in IM-resistant CML patient samples containing wild-type BCR-ABL compared to those with mutant BCR-ABL. In addition, the average expression levels of three IMSGs (*CLEC5A*, *ELF5*, and *WNT7B*) were significantly ($P<0.01$, <0.05, <0.05, respectively) lower in IM-resistant CML patient samples containing wild-type BCR-ABL compared to those with mutant BCR-ABL (Fig. 3D). Moreover, in all 11

IM-resistant CML patient samples containing wild-type BCR-ABL at least one IMSG was down-regulated >2-fold, and in 9/11 samples at least one IMSG was down-regulated >5-fold, relative to the average expression in IM-resistant mutant BCR-ABL samples (table 3). Finally, the results in Figure 3E show that knockdown of *PRKCH* increased IM sensitivity of leukemic cells from BCR-ABL-independent IM-resistant CML patients.

[1]WT, BCR-ABL wild-type; Mut, BCR-ABL kinase domain mutant
[2]AP, accelerated phase; BC, blast crisis; CP, chronic phase; Ly BP, lymphoid blast crisis phase; My BP, myeloid blast crisis phase.
OHSU= Druker lab, OHSU Knight Cancer Institute; WCI= Hematology Bank, Winship Cancer Institute; UMMS = Department of Pathology, UMMS
BM = Bone marrow; PB = Peripheral blood

Table 2. List of CML patient samples used

Sample ID[1]	Source	BCR-ABL mutation	CML phase[2]	Origin	IM resistant/ sensitive	Basis of IM resistance	Relevant figure
WT-1	OHSU	--	CP	BM	Resistant	Cytogenic relapse or suboptimal primary response to IM	Fig. 3C and 3D
WT-2	OHSU	--	CP	BM	Resistant	Cytogenic relapse or suboptimal primary response to IM	Fig. 3C and 3D
WT-3	OHSU	--	CP	BM	Resistant	Cytogenic relapse or suboptimal primary response to IM	Fig. 3C and 3D
WT-4	OHSU	--	CP	BM	Resistant	Cytogenic relapse or suboptimal primary response to IM	Fig. 3C and 3D
WT-5	WCI	--	My BP	BM	Resistant	Loss of hematological response	Fig. 3C and 3D
WT-6	WCI	--	CP	BM	Resistant	Loss of cytogenic response	Fig. 3C and 3D
WT-7	WCI	--	My BP	BM	Resistant	Lack of major cytgenic response	Fig. 3C and 3D
WT-8	WCI	--	CP	BM	Resistant	Lack of major molecular response	Fig. 3C and 3D
WT-9	WCI	--	CP	BM	Resistant	Lack of major cytgenic response	Fig. 3C and 3D
WT-10	WCI	--	CP	PB	Resistant	Loss of complete cytogenic response	Fig. 3C and 3D
WT-11	WCI	--	CP	PB	Resistant	Loss of hematological response	Fig. 3C and 3D
Mut-1	OHSU	G250E	CP	BM	Resistant	Cytogenic relapse or suboptimal primary response to IM	Fig. 3C and 3D
Mut-2	OHSU	M244V	AP	BM	Resistant	Cytogenic relapse or suboptimal primary response to IM	Fig. 3C and 3D
Mut-3	OHSU	Y253F	CP	PB Leuka-pheresis	Resistant	Cytogenic relapse or suboptimal primary response to IM	Fig. 3C and 3D
Mut-4	OHSU	T315I	BC	Leuka-pheresis	Resistant	Cytogenic relapse or suboptimal primary response to IM	Fig. 3C and 3D
Mut-5	OHSU	T315I T315I, E255R	AP	PB	Resistant	Cytogenic relapse or suboptimal primary response to IM	Fig. 3C and 3D
Mut-6	WCI	E255R	My BP	BM	Resistant	Transformation to blast phase on IM	Fig. 3C and 3D
Mut-7	WCI	F317L	Ly BP	BM	Resistant	Transformation to blast phase on IM	Fig. 3C and 3D
Mut-8	WCI	T315I	CP	BM	Resistant	Lack of hematological response	Fig. 3C and 3D
Mut-9	WCI	T315I	CP	BM	Resistant	Loss of complete histological response	Fig. 3C and 3D
Mut-10	WCI	T315I	CP	BM	Resistant	No complete histological response	Fig. 3C and 3D
Mut-11	WCI	F317L	CP	PB	Resistant	Lack of major cytogenic response	Fig. 3C and 3D
CML(R)1	UMMS	--	CP	PB	Resistant	Failure to achieve major molecular response	Fig. 3E and 4D and 17A-B
						Loss of major molecular response/complete molecular response and complete cytogenic response	Fig. 3E and 4D and 17A-B
CML(R)2	UMMS	--	CP	PB	Resistant		

Table 2. List of CML patient samples used

Sample ID[1]	Source	BCR-ABL mutation	CML phase[2]	Origin	IM resistant/ sensitive	Basis of IM resistance	Relevant figure
CML(R)3	OHSU	--	CP	BM	Resistant	Cytogenic relapse or suboptimal primary response to IM	Fig. 3E and 4D and 17A-B
CML(R)4	OHSU	--	CP	BM	Resistant	Cytogenic relapse or suboptimal primary response to IM	Fig. 3E and 4D and 17A-B
CML(R)5	OHSU	--	CP	BM	Resistant	Cytogenic relapse or suboptimal primary response to IM	Fig. 3E and 4D and 17A-B
CML(R)6	OHSU	--	BC	PB	Resistant	Cytogenic relapse or suboptimal primary response to IM	Fig. 4D and 17A-B
WT-1	WCI	--	CP	PB	Sensitive	N/A	Fig. 3C
WT-2	WCI	--	CP	PB	Sensitive	N/A	Fig. 3C
WT-3	WCI	--	CP	PB	Sensitive	N/A	Fig. 3C
WT-4	WCI	--	CP	BM	Sensitive	N/A	Fig. 3C
WT-5	UMMS	--	CP	BM	Sensitive	N/A	Fig. 3C
WT-6	UMMS	--	CP	BM	Sensitive	N/A	Fig. 3C
WT-7	UMMS	--	CP	BM	Sensitive	N/A	Fig. 3C
WT-8	UMMS	--	CP	PB	Sensitive	N/A	Fig. 3C
WT-9	UMMS	--	CP	PB	Sensitive	N/A	Fig. 3C
WT-10	UMMS	--	CP	PB	Sensitive	N/A	Fig. 3C
WT-11	UMMS	--	CP	PB	Sensitive	N/A	Fig. 3C
CML(S)1	UMMS	--	CP	PB	Sensitive	N/A	Fig. 4D, 6B, 7F, 7G and 17A-B
CML(S)2	UMMS	--	CP	PB	Sensitive	N/A	Fig. 4D, 6B, 7F, 7G and 17A-B
CML(S)3	OHSU	--	CP	BM	Sensitive	N/A	Fig. 4D, 6B, 7F, 7G and 17A-B
CML(S)4	OHSU	--	CP	BM	Sensitive	N/A	Fig. 6B
CML(S)5	OHSU	--	CP	BM	Sensitive	N/A	Fig. 6B

Table 3. Relative expression level of IMSGs in IM-resistant BCR-ABL-wt CML patient samples. Relative expression was calculated by determining the average expression of a given gene in all 11 mutant BCR-ABL patient samples, and dividing by the expression of the gene in the individual wild-type BCR-ABL sample. Thus, the value represents the fold down-regulation in wild-type BCR-ABL samples.

Table 3. Relative expression of IMSGs in IM-resistant BCR-ABL-wt CML patient samples.													
Sample ID	Relative expression												
	BAP1	*CD22*	*CLEC5A*	*DNASE1L1*	*ELF3*	*EXOSC7*	*MEGF8*	*RPP38*	*STK11*	*TMEM140*	*WNT7B*	*PRKCH*
WT-1	0.498	3.723	13.781	1.231	9.882	1.299	3.806	0.541	0.607	3.559	15.608	0.204
WT-2	1.294	5.749	2.379	1.198	8.263	3.765	9.764	1.872	2.876	7.013	10.095	0.688
WT-3	1.086	0.651	12.468	1.058	1.963	3.295	0.915	0.784	1.710	1.780	1.552	0.176
WT-4	0.723	1.042	1.828	1.401	1.208	3.210	1.713	7.357	.0842	0.478	1.191	0.838
WT-5	0.437	0.976	2.717	1.268	0.953	.0332	1.431	0.437	3.192	0.503	4.125	0.116
WT-6	1.222	0.655	2.400	0.918	0.790	1.807	0.696	2.904	2.692	0.404	1.341	0.287
WT-7	7.936	16.193	22.845	2.368	13.862	0.195	5.888	5.464	1.770	3.420	96.887	2.075
WT-8	5.844	3.436	3.760	2.744	13.486	2.027	3.035	1.708	5.362	3.521	10.836	1.735
WT-10	0.574	0.569	7.508	0.852	1.954	2.260	1.537	0.102	0.795	0.438	2.595	2.107
WT-11	3.389	2.881	12.961	1.870	5.556	0.682	15.311	7.422	1.651	8.578	31.855	0.565
WT-12	1.509	2.863	2.445	1.921	5.634	1.999	3.179	0.611	2.273	1.422	1.549	0.208

Example 4. PKCη increases RAF/MEK/ERK signaling through phosphorylation and activation of CRAF

The next experiments were performed to understand in greater detail how PKCη increased RAF/MEK/ERK signaling. Figure 3F shows that even a relatively modest knockdown of *PRKCH* in IM-sensitive K562 cells decreased both phosphorylated MEK and ERK1/2 (see also Fig. 10A) and increased IM sensitivity (Fig. 15B). Conversely, K562/*PRKCH* cells had increased levels of both phosphorylated MEK and ERK1/2 (Fig. 3F). Most importantly, K562/*PRKCH* cells maintained high levels of phosphorylated MEK and ERK1/2 after IM treatment (Fig. 3F).

The finding that PKCη affected both phosphorylated-MEK and -ERK1/2 levels indicated that PKCη functioned upstream of MEK by, for example, stimulating RAF activity. There are three known RAF kinases: ARAF, BRAF and CRAF (*30*). In K562/*PRKCH* cells, knockdown of CRAF, but not ARAF or BRAF, resulted in decreased phosphorylated-ERK1/2 levels (Fig. 3F and Fig. 15B). Most importantly, in IM-treated K562/*PRKCH* cells, knockdown of CRAF, but not ARAF or BRAF, resulted in loss of sustained phosphorylated-ERK1/2 levels.

To determine whether CRAF was a direct substrate of PKCη, a glutathione-S-transferase (GST) fusion-protein containing a CRAF peptide bearing a potential PKC phosphorylation site at S497/S499 (*31, 32*) was derived. The *in vitro* kinase assay showed (see Fig. 3H) that wild-type PKCη, but not a kinase-dead mutant (K384R) (*33*), could phosphorylate the CRAF S497/S499 site. These results are consistent with several previous findings including phosphorylation of CRAF by PKC isoforms (*31, 32, 34-36*), and reduced activity of a CRAF S497A/S499A mutant (*32, 34*).

Example 5. Combined treatment with IM and a MEK inhibitor synergistically kill BCR-ABL-independent IM-resistant CML cells

The results presented above show that BCR-ABL-independent IM resistance can result from increased *PRKCH* expression, leading to sustained RAF/MEK/ERK signaling after IM treatment. An implication of this conclusion is that simultaneous inhibition of BCR-ABL and RAF/MEK/ERK signaling might efficiently kill BCR-ABL-independent IM-resistant CML cells. To investigate this possibility, the effect of combining IM

treatment with the FDA-approved MEK inhibitor trametinib (also called GSK1120212) was analyzed. Treatment with both IM and trametinib had a substantially greater effect than either drug alone in killing K562/*PRKCH* cells (Fig. 4A), representative IMSG KD K562 cell lines (Fig. 4B), and BCR-ABL+ mouse primary bone marrow cells over-expressing *Prkch* (Fig. 4C). In most instances, the effect of combined drug treatment was synergistic (table 4). The modest effect of trametinib alone on K562 cell lines likely reflects stimulation of RAF/MEK/ERK signaling by BCR-ABL. Finally, treatment with both IM and trametinib had a significantly ($P<0.01$) greater effect than either drug alone in killing primary leukemic cells from BCR-ABL-independent IM-resistant CML patients (Fig. 4D and Fig. 17A), Moreover, these leukemic cells were killed more effectively by combined treatment with IM and trametinib than by IM and a JAK-STAT or PI3K inhibitor, and neither of these latter two drug combinations were significantly more effective than IM alone (Fig. 17B).

Table 4. Actual P values for all comparisons in this study.

Figure 1B

Statistical test: One-way ANOVA (P value=1.0406E-06) followed by predetermined contrasts within the ANOVA framework with Benjamini-Hochberg correction.

Sample	P value (shRNA vs NS)	BH-adjusted P value (shRNA vs NS)
BAP1	1.07513E-06	5.59068E-06
BCAP29	0.00040146	0.000497046
CD22	3.00752E-05	8.36825E-05
CELA1	2.68843E-08	2.32997E-07
CLEC5A	7.71503E-10	1.00295E-08
DNASE1L1	0.000726651	0.000787205
DPM1	9.38085E-06	4.06503E-05
EBF1	7.19634E-05	0.000133646
ELF5	0.000235868	0.000360739
EXOSC7	3.21856E-05	8.36825E-05
E2F4	0.000317805	0.000434891
IDH3A	0.000552982	0.000653525
LILRA3	6.15163E-05	0.000123033
MEGF8	0.00011352	0.000184469
MMP7	1.8066E-05	6.71023E-05
RCVRN	0.000260338	0.000376044
RPP38	4.7514E-05	0.000102947
STK11	2.38392E-11	6.19818E-10
STYXL1	0.002841565	0.002955228

Table 4. Actual P values for all comparisons in this study.

TCEAL1	2.34123E-05	7.60901E-05
TMEM140	0.004475609	0.004475609
TRAF4	0.000616875	0.000697337
UBAP2L	0.000377057	0.000490174
WNT7B	4.09493E-05	9.67892E-05
ZACN	8.87069E-05	0.000153759

Figure 1C

Statistical test: One-way ANOVA (P value=6.23277E-38) followed by predetermined contrasts within the ANOVA framework with Benjamini-Hochberg correction

Sample	P value (shRNA vs NS)	BH-adjusted P value (shRNA vs NS)
BAP1	8.98213E-33	1.12277E-31
BCAP29	2.17058E-22	9.04407E-22
CD22	1.29641E-10	1.80057E-10
CELA1	1.86785E-09	2.33481E-09
CLEC5A	4.92614E-25	3.07884E-24
DNASE1L1	1.07278E-11	1.57761E-11
DPM1	2.13891E-18	5.94141E-18
EBF1	8.31631E-07	8.66282E-07
ELF5	2.24623E-17	5.10507E-17
EXOSC7	1.48547E-34	3.71366E-33
E2F4	2.55704E-15	4.91739E-15
IDH3A	1.11839E-24	5.59197E-24
LILRA3	1.43058E-21	5.1092E-21
MEGF8	3.72116E-12	5.81431E-12
MMP7	1.42847E-25	1.19039E-24
RCVRN	4.84833E-07	5.26993E-07
RPP38	2.01321E-17	5.03303E-17
STK11	2.26331E-10	2.97804E-10
STYXL1	1.03672E-07	1.17809E-07
TCEAL1	3.00559E-13	5.36713E-13
TMEM140	2.36532E-20	7.39161E-20
TRAF4	0.008468345	0.008468345
UBAP2L	4.54415E-17	9.46698E-17
WNT7B	1.88709E-12	3.14516E-12
ZACN	1.86812E-08	2.22395E-08

Table 4. Actual P values for all comparisons in this study.

Figure 1D

Statistical test: One-way ANOVA (P value=8.581e-15) followed by predetermined contrasts within the ANOVA framework with Benjamini-Hochberg correction

Sample	**P value (shRNA vs NS)**	**BH-adjusted P value (shRNA vs NS)**
Bap1	0.000105724	0.000121582
Bcap29	5.20E-05	6.29E-05
Cd22	4.04E-11	1.55E-10
Cela1	0.014187481	0.01553867
Clec5a	2.69E-09	6.86E-09
Dnase1l1	1.74E-11	1.00E-10
Dpm1	2.26E-09	6.49E-09
Ebf1	5.32E-07	1.02E-06
Elf5	8.98E-13	1.03E-11
Exosc7	3.83E-12	2.94E-11
E2f4	9.80E-11	3.22E-10
Idh3a	3.12E-11	1.44E-10
Megf8	7.52E-06	1.24E-05
Mmp7	0.357567304	0.357567304
Rcvrn	5.24E-07	1.02E-06
Rpp38	2.06E-05	2.76E-05
Stk11	2.16E-05	2.76E-05
Styxl1	0.180762343	0.188978814
Tceal1	2.13E-07	4.91E-07
Tmem140	7.51E-13	1.03E-11
Traf4	1.10E-05	1.68E-05
Ubap2l	7.65E-07	1.35E-06
Wnt7b	1.20E-05	1.73E-05

Figure 1F

Statistical test: Correlation analysis (performed in GraphPad Prism 6). Pearson's correlation coefficient was calculated to reach a two-tailed P value with 95% confidence interval.

P value
0.0117

Example 6. IM and a MEK inhibitor prolong survival in mouse models of BCR-ABL-independent IM-resistant CML

Based upon the cell culture results, the ability of this drug combination to prolong survival was analyzed in mouse models of BCR-ABL-independent IM-resistant CML. Briefly, mouse primary bone marrow cells were transduced with a retrovirus co-

expressing BCR-ABL and either *Prkch* (Fig. 18A) or an shRNA targeting one of two representative IMSGs, *Clec5A* or *Elf5* (Fig. 18B), followed by transplantation into lethally irradiated syngeneic mice. Combined treatment with IM and trametinib was substantially more effective than either drug alone at suppressing leukemic progression, as evidenced by a reduced white blood cell count (Fig. 4, E and F), and prolonging survival (Fig. 4, F and G). In addition to prolonged survival, the general appearance and behavior of mice treated with IM and trametinib was normal, suggesting minimal drug toxicity.

Example 7. *PRKCH* modulates proliferation of BCR-ABL+ cells, disease progression, and IM sensitivity

The finding that knockdown of *PRKCH* in K562 cells reduced levels of phosphorylated-ERK1/2 (Fig. 3F) raised the possibility that *PRKCH* might modulate the proliferation and survival of BCR-ABL+ cells and thus affect disease progression. To investigate this possibility, mouse primary bone marrow cells were transduced with a retrovirus co-expressing BCR-ABL and a *Prkch* shRNA (Fig. 5A). *Prkch* knockdown led decreased levels of phosphorylated-ERK1/2, similar to the results in K562 cells. Figure 5B shows that knockdown of *Prkch* (Fig. 19A) reduced the ability of untreated BCR-ABL+ mouse primary bone marrow cells to form colonies in methylcellulose (see also Fig. Fig. 19B). Moreover, the colony formation assay in Figure 5C shows that knockdown of Prkch markedly increased the IM sensitivity of BCR-ABL+ mouse primary bone marrow cells.

Next, the *Prkch* KD bone marrow cells were transplanted into syngeneic mice to induce CML-like disease and analyzed the effect of *Prkch* knockdown on leukemic progression. In untreated mice, *Prkch* knockdown resulted in a lower white blood cell count (Fig. 5D), reduced spleen size (Fig. 5E), decreased infiltration of the lung and spleen by leukemic cells (Fig. 5F), and increased survival (Fig. 5G). Thus, in the absence of IM treatment, PRKCH promotes disease progression, although this effect may be relatively minor. More importantly, knockdown of Prkch markedly increased survival of IM-treated mice with CML-like disease (Fig. 5G).

Example 8. IM-resistant murine and human CML stem cells contain high levels of *PRKCH*

To investigate the possibility that *PRKCH* might contribute to the intrinsic resistance of CML stem cells to IM, a CML-like disease was induced in mice, and BCR-ABL+ murine stem cells (Lin-Sca1+Kit+), progenitor cells (Lin-) and mature cells (Lin+Gr1+) were isolated by fluorescence activated cell sorting (FACS) (Hamilton et al., Blood 119, 1501-1510 (2012); Neering et al., Blood 110, 2578-2585 (2007)). The qRT-PCR results, shown in Figure 6A, demonstrated that IM-resistant murine CML stem cells (Hamilton et al., Blood 119, 1501-1510 (2012); Zhang et al., Cancer Cell 17, 427-442 (2010); Zhang et al., Nat Genet 44, 861-871 (2012)) and see below) had substantially higher expression of *Prkch* compared to murine CML progenitor and mature cells, both of which are IM sensitive ((Hamilton et al., Blood 119, 1501-1510 (2012); Li et al., Cancer Cell 21, 266-281 (2012)) and Fig. 20).

The next experiments asked whether *PRKCH* expression levels were also high in human CML stem cells. CML stem cells (CD34+CD38-) and CML progenitor cells (CD34+CD38+) (Corbin et al., J Clin Invest 121, 396-409 (2011); Jiang et al., Leukemia 21, 926-935 (2007); Lobo et al., Annu Rev Cell Dev Biol 23, 675-699 (2007)) were isolated from newly diagnosed CML patients. The qRT-PCR results in Figure 6B show that IM-resistant human CML stem cells (Graham et al., Blood 99, 319-325 (2002); Corbin et al., J Clin Invest 121, 396-409 (2011); Bhatia et al., Blood 101, 4701-4707 (2003); Chomel et al., Blood 118, 3657-3660 (2011); Pellicano et al., Stem Cells 32, 1373-1379 (2014)) and see below) had substantially higher expression of *PRKCH* compared to human CML progenitor cells, which are IM sensitive (Corbin et al., J Clin Invest 121, 396-409 (2011); Jiang et al., Leukemia 21, 926-935 (2007)). Analysis of a published expression profiling study comparing highly enriched human CML stem and progenitor cell populations (Gerber et al., Oncotarget 4, 715-728 (2013)) revealed similar differences in *PRKCH* expression levels (Fig. 6C). Microarray analysis indicates that PRKCH expression is much higher in hematopoietic stem cells than in mature myeloid cells (Konuma et al., Exp Hematol 39, 697-709 e695 (2011); Bagger et al., Nucleic Acids Res 41, D1034-1039 (2013)), suggesting that high PRKCH expression may be a marker of stemness.

Example 9. High *Prkch* expression contributes to the IM resistance of CML stem cells

Several experiments were performed to determine whether the high *Prkch* levels in murine CML stem cells contributes to their IM resistance. First the contribution of *Prkch*, and as a comparison BCR-ABL, to RAF/MEK/ERK signaling was assessed in murine CML stem cells. *Prkch* KD bone marrow cells were isolated from leukemic mice, permeabilized and incubated with an antibody against phosphorylated-ERK1/2 or IgG isotype antibody as a negative control, and then analyzed by FACS to determine the phosphorylated-ERK1/2 levels in CML progenitor and stem cells. Figure 7A shows that knockdown of *Prkch* reduced levels of phosphorylated ERK1/2 in both CML progenitor and stem cells (see also Fig. 21A).

To evaluate the role of BCR-ABL, bone marrow cells were isolated from leukemic mice and treated with either IM or trametinib, and phosphorylated ERK1/2 was monitored as described above. Figure 7B shows, as expected, that trametinib reduced phosphorylated ERK1/2 in both CML progenitor and stem cells (see also Fig. 21B). In contrast, IM reduced levels of phosphorylated ERK1/2 in IM-sensitive CML progenitor cells but not in IM-resistant CML stem cells. Collectively, these results indicate that in CML stem cells PKCη has a more prominent role than BCR-ABL in promoting RAF/MEK/ERK signaling.

Next, a series of experiments was performed to determine whether *Prkch* affects survival of CML stem cells after IM treatment. In the first experiment, mouse primary bone marrow cells were transduced with a retrovirus co-expressing BCR-ABL and either *Prkch* or a control non-silencing (NS) shRNA, followed by transplantation into lethally irradiated syngeneic mice. BCR-ABL+ murine stem cells (Lin-Sca1+Kit+) were isolated from the mice and IM sensitivity determined in a colony formation assay. The results in Figure 7C show that *Prkch* knockdown markedly increased the IM sensitivity of CML stem cells. In the second experiment, mice with CML-like disease were treated with either vehicle or IM in parallel for two weeks, and then sacrificed at the same time followed by quantification of CML stem cells by FACS analysis. Figure 7D shows, as expected, that IM treatment had little effect on the number of CML stem cells expressing a control NS shRNA, confirming that murine CML stem cells are IM-resistant. In

contrast, IM treatment markedly reduced the number of *Prkch* KD CML stem cells. Annexin V staining revealed that IM treatment induced a higher level of apoptosis in *Prkch* KD compared to control CML stem cells (Fig. 22A and B). Finally, combined treatment with IM and trametinib synergistically killed murine CML stem cells (Fig. 7E), which was due, at least in part, to the induction of apoptosis (Fig. 22C and D). By contrast, treatment with IM and trametinib had negligible effect on normal murine hematopoietic stem cells (Fig. 23A).

Knockdown of PRKCH also increased the IM sensitivity of IM-resistant human CML stem cells (Fig. 7F). Moreover, treatment with both IM and trametinib had a substantially greater effect than either drug alone in killing human CML stem cells (Fig. 7G), and a negligible effect on normal human hematopoietic CD34+ cells and hematopoietic stem cells (CD34+CD38-) (Fig. 23B). Collectively, these results indicate that PRKCH is expressed at relatively high levels in both mouse and human CML stem cells and this contributes to their IM resistance.

REFERENCES AND NOTES

1. S. Faderl, M. Talpaz, Z. Estrov, S. O'Brien, R. Kurzrock, H. M. Kantarjian, The biology of chronic myeloid leukemia. N Engl J Med 341, 164-172 (1999).

2. M. W. Deininger, J. M. Goldman, J. V. Melo, The molecular biology of chronic myeloid leukemia. Blood 96, 3343-3356 (2000).

3. R. Kurzrock, H. M. Kantarjian, B. J. Druker, M. Talpaz, Philadelphia chromosome-positive leukemias: from basic mechanisms to molecular therapeutics. Ann Intern Med 138, 819-830 (2003).

4. J. Colicelli, ABL tyrosine kinases: evolution of function, regulation, and specificity. Sci Signal 3, re6 (2010).

5. L. S. Steelman, S. C. Pohnert, J. G. Shelton, R. A. Franklin, F. E. Bertrand, J. A. McCubrey, JAK/STAT, Raf/MEK/ERK, PI3K/Akt and BCR-ABL in cell cycle progression and leukemogenesis. Leukemia 18, 189-218 (2004).

6. X. An, A. K. Tiwari, Y. Sun, P. R. Ding, C. R. Ashby, Jr., Z. S. Chen, BCR-ABL tyrosine kinase inhibitors in the treatment of Philadelphia chromosome positive chronic myeloid leukemia: a review. Leuk Res 34, 1255-1268 (2010).

7. N. von Bubnoff, C. Peschel, J. Duyster, Resistance of Philadelphia-chromosome positive leukemia towards the kinase inhibitor imatinib (STI571, Glivec): a targeted oncoprotein strikes back. Leukemia 17, 829-838 (2003).

8. A. Quintas-Cardama, H. M. Kantarjian, J. E. Cortes, Mechanisms of primary and secondary resistance to imatinib in chronic myeloid leukemia. Cancer Control 16, 122-131 (2009).

9. E. Jabbour, H. Kantarjian, D. Jones, M. Talpaz, N. Bekele, S. O'Brien, X. Zhou, R. Luthra, G. Garcia-Manero, F. Giles, M. B. Rios, S. Verstovsek, J. Cortes, Frequency and clinical significance of BCR-ABL mutations in patients with chronic myeloid leukemia treated with imatinib mesylate. Leukemia 20, 1767-1773 (2006).

10. N. P. Shah, J. M. Nicoll, B. Nagar, M. E. Gorre, R. L. Paquette, J. Kuriyan, C. L. Sawyers, Multiple BCR-ABL kinase domain mutations confer polyclonal resistance to the tyrosine kinase inhibitor imatinib (STI571) in chronic phase and blast crisis chronic myeloid leukemia. Cancer cell 2, 117-125 (2002).

11. E. Weisberg, P. W. Manley, S. W. Cowan-Jacob, A. Hochhaus, J. D. Griffin, Second generation inhibitors of BCR-ABL for the treatment of imatinib-resistant chronic myeloid leukaemia. Nature reviews. Cancer 7, 345-356 (2007).

12. N. J. Donato, J. Y. Wu, J. Stapley, H. Lin, R. Arlinghaus, B. B. Aggarwal, S. Shishodia, M. Albitar, K. Hayes, H. Kantarjian, M. Talpaz, Imatinib mesylate resistance through BCR-ABL independence in chronic myelogenous leukemia. Cancer research 64, 672-677 (2004).

13. J. S. Khorashad, M. Anand, D. Marin, S. Saunders, T. Al-Jabary, A. Iqbal, S. Margerison, J. V. Melo, J. M. Goldman, J. F. Apperley, J. Kaeda, The presence of a BCR-ABL mutant allele in CML does not always explain clinical resistance to imatinib. Leukemia 20, 658-663 (2006).

14. M. Dean, T. Fojo, S. Bates, Tumour stem cells and drug resistance. Nature reviews. Cancer 5, 275-284 (2005).

15. S. M. Graham, H. G. Jorgensen, E. Allan, C. Pearson, M. J. Alcorn, L. Richmond, T. L. Holyoake, Primitive, quiescent, Philadelphia-positive stem cells from patients with chronic myeloid leukemia are insensitive to STI571 in vitro. Blood 99, 319-325 (2002).

16. A. S. Corbin, A. Agarwal, M. Loriaux, J. Cortes, M. W. Deininger, B. J. Druker, Human chronic myeloid leukemia stem cells are insensitive to imatinib despite inhibition of BCR-ABL activity. The Journal of clinical investigation 121, 396-409 (2011).

17. A. Hamilton, G. V. Helgason, M. Schemionek, B. Zhang, S. Myssina, E. K. Allan, F. E. Nicolini, C. Muller-Tidow, R. Bhatia, V. G. Brunton, S. Koschmieder, T. L. Holyoake, Chronic myeloid leukemia stem cells are not dependent on Bcr-Abl kinase activity for their survival. Blood 119, 1501-1510 (2012).

18. L. C. Andersson, K. Nilsson, C. G. Gahmberg, K562--a human erythroleukemic cell line. International journal of cancer. Journal international du cancer 23, 143-147 (1979).

19. J. M. Silva, M. Z. Li, K. Chang, W. Ge, M. C. Golding, R. J. Rickles, D. Siolas, G. Hu, P. J. Paddison, M. R. Schlabach, N. Sheth, J. Bradshaw, J. Burchard, A. Kulkarni, G. Cavet, R. Sachidanandam, W. R. McCombie, M. A. Cleary, S. J. Elledge, G. J. Hannon, Second-generation shRNA libraries covering the mouse and human genomes. Nat Genet 37, 1281-1288 (2005).

20. T. Ohkubo, T. Kamamoto, K. Kita, A. Hiraoka, Y. Yoshida, H. Uchino, A novel Ph1 chromosome positive cell line established from a patient with chronic myelogenous leukemia in blastic crisis. Leukemia research 9, 921-926 (1985).

21. G. Q. Daley, R. A. Van Etten, D. Baltimore, Induction of chronic myelogenous leukemia in mice by the P210bcr/abl gene of the Philadelphia chromosome. Science 247, 824-830 (1990).

22. S. Li, R. L. Ilaria, Jr., R. P. Million, G. Q. Daley, R. A. Van Etten, The P190, P210, and P230 forms of the BCR/ABL oncogene induce a similar chronic myeloid leukemia-like syndrome in mice but have different lymphoid leukemogenic activity. The Journal of experimental medicine 189, 1399-1412 (1999).

23. N. P. Shah, C. Tran, F. Y. Lee, P. Chen, D. Norris, C. L. Sawyers, Overriding imatinib resistance with a novel ABL kinase inhibitor. Science 305, 399-401 (2004).

24. N. J. Donato, J. Y. Wu, J. Stapley, G. Gallick, H. Lin, R. Arlinghaus, M. Talpaz, BCR-ABL independence and LYN kinase overexpression in chronic myelogenous leukemia cells selected for resistance to STI571. Blood 101, 690-698 (2003).

25. J. ten Hoeve, R. B. Arlinghaus, J. Q. Guo, N. Heisterkamp, J. Groffen, Tyrosine phosphorylation of CRKL in Philadelphia+ leukemia. Blood 84, 1731-1736 (1994).

26. T. Takahashi, H. Ueno, M. Shibuya, VEGF activates protein kinase C-dependent, but Ras-independent Raf-MEK-MAP kinase pathway for DNA synthesis in primary endothelial cells. Oncogene 18, 2221-2230 (1999).

27. Y. Ueda, S. Hirai, S. Osada, A. Suzuki, K. Mizuno, S. Ohno, Protein kinase C activates the MEK-ERK pathway in a manner independent of Ras and dependent on Raf. The Journal of biological chemistry 271, 23512-23519 (1996).

28. R. M. Uht, S. Amos, P. M. Martin, A. E. Riggan, I. M. Hussaini, The protein kinase C-eta isoform induces proliferation in glioblastoma cell lines through an ERK/Elk-1 pathway. Oncogene 26, 2885-2893 (2007).

29. A. Aderem, The MARCKS brothers: a family of protein kinase C substrates. Cell 71, 713-716 (1992).

30. C. Wellbrock, M. Karasarides, R. Marais, The RAF proteins take centre stage. Nature reviews. Molecular cell biology 5, 875-885 (2004).

31. M. P. Carroll, W. S. May, Protein kinase C-mediated serine phosphorylation directly activates Raf-1 in murine hematopoietic cells. The Journal of biological chemistry 269, 1249-1256 (1994).

32. W. Kolch, G. Heidecker, G. Kochs, R. Hummel, H. Vahidi, H. Mischak, G. Finkenzeller, D. Marme, U. R. Rapp, Protein kinase C alpha activates RAF-1 by direct phosphorylation. Nature 364, 249-252 (1993).

33. T. Suzuki, B. C. Elias, A. Seth, L. Shen, J. R. Turner, F. Giorgianni, D. Desiderio, R. Guntaka, R. Rao, PKC eta regulates occludin phosphorylation and epithelial tight junction integrity. Proceedings of the National Academy of Sciences of the United States of America 106, 61-66 (2009).

34. H. Cai, U. Smola, V. Wixler, I. Eisenmann-Tappe, M. T. Diaz-Meco, J. Moscat, U. Rapp, G. M. Cooper, Role of diacylglycerol-regulated protein kinase C isotypes in growth factor activation of the Raf-1 protein kinase. Molecular and cellular biology 17, 732-741 (1997).

35. D. C. Schonwasser, R. M. Marais, C. J. Marshall, P. J. Parker, Activation of the mitogen-activated protein kinase/extracellular signal-regulated kinase pathway by

conventional, novel, and atypical protein kinase C isotypes. Molecular and cellular biology 18, 790-798 (1998).

36. O. Sozeri, K. Vollmer, M. Liyanage, D. Frith, G. Kour, G. E. Mark, 3rd, S. Stabel, Activation of the c-Raf protein kinase by protein kinase C phosphorylation. Oncogene 7, 2259-2262 (1992).

37. J. M. Gerber, J. L. Gucwa, D. Esopi, M. Gurel, M. C. Haffner, M. Vala, W. G. Nelson, R. J. Jones, S. Yegnasubramanian, Genome-wide comparison of the transcriptomes of highly enriched normal and chronic myeloid leukemia stem and progenitor cell populations. Oncotarget 4, 715-728 (2013).

38. L. M. Packer, S. Rana, R. Hayward, T. O'Hare, C. A. Eide, A. Rebocho, S. Heidorn, M. S. Zabriskie, I. Niculescu-Duvaz, B. J. Druker, C. Springer, R. Marais, Nilotinib and MEK inhibitors induce synthetic lethality through paradoxical activation of RAF in drug-resistant chronic myeloid leukemia. Cancer cell 20, 715-727 (2011).

39. J. Hentschel, I. Rubio, M. Eberhart, C. Hipler, J. Schiefner, K. Schubert, I. F. Loncarevic, U. Wittig, A. Baniahmad, F. von Eggeling, BCR-ABL- and Ras-independent activation of Raf as a novel mechanism of Imatinib resistance in CML. Int J Oncol 39, 585-591 (2011).

40. T. Nambu, N. Araki, A. Nakagawa, A. Kuniyasu, T. Kawaguchi, A. Hamada, H. Saito, Contribution of BCR-ABL-independent activation of ERK1/2 to acquired imatinib resistance in K562 chronic myeloid leukemia cells. Cancer Sci 101, 137-142 (2010).

41. R. Chakrabarti, J. Hwang, M. Andres Blanco, Y. Wei, M. Lukacisin, R. A. Romano, K. Smalley, S. Liu, Q. Yang, T. Ibrahim, L. Mercatali, D. Amadori, B. G. Haffty, S. Sinha, Y. Kang, Elf5 inhibits the epithelial-mesenchymal transition in mammary gland development and breast cancer metastasis by transcriptionally repressing Snail2. Nature cell biology 14, 1212-1222 (2012).

42. R. Escamilla-Hernandez, R. Chakrabarti, R. A. Romano, K. Smalley, Q. Zhu, W. Lai, M. S. Halfon, M. J. Buck, S. Sinha, Genome-wide search identifies Ccnd2 as a direct transcriptional target of Elf5 in mouse mammary gland. BMC molecular biology 11, 68 (2010).

43. M. Kalyuga, D. Gallego-Ortega, H. J. Lee, D. L. Roden, M. J. Cowley, C. E. Caldon, A. Stone, S. L. Allerdice, F. Valdes-Mora, R. Launchbury, A. L. Statham, N.

Armstrong, M. C. Alles, A. Young, A. Egger, W. Au, C. L. Piggin, C. J. Evans, A. Ledger, T. Brummer, S. R. Oakes, W. Kaplan, J. M. Gee, R. I. Nicholson, R. L. Sutherland, A. Swarbrick, M. J. Naylor, S. J. Clark, J. S. Carroll, C. J. Ormandy, ELF5 suppresses estrogen sensitivity and underpins the acquisition of antiestrogen resistance in luminal breast cancer. PLoS biology 10, e1001461 (2012).

44. J. Mullenders, R. Bernards, Loss-of-function genetic screens as a tool to improve the diagnosis and treatment of cancer. Oncogene 28, 4409-4420 (2009).

45. D. Bruennert, A. Czibere, I. Bruns, R. Kronenwett, N. Gattermann, R. Haas, F. Neumann, Early in vivo changes of the transcriptome in Philadelphia chromosome-positive CD34+ cells from patients with chronic myelogenous leukaemia following imatinib therapy. Leukemia 23, 983-985 (2009).

46. J. P. Radich, H. Dai, M. Mao, V. Oehler, J. Schelter, B. Druker, C. Sawyers, N. Shah, W. Stock, C. L. Willman, S. Friend, P. S. Linsley, Gene expression changes associated with progression and response in chronic myeloid leukemia. Proceedings of the National Academy of Sciences of the United States of America 103, 2794-2799 (2006).

47. C. Gazin, N. Wajapeyee, S. Gobeil, C. M. Virbasius, M. R. Green, An elaborate pathway required for Ras-mediated epigenetic silencing. Nature 449, 1073-1077 (2007).

48. B. S. Carvalho, R. A. Irizarry, A framework for oligonucleotide microarray preprocessing. Bioinformatics 26, 2363-2367 (2010).

49. R. Ihaka, R. Gentleman, R: A language for data analysis and graphics. J. Comput. Graph Stat. 5, 299-314 (1996).

50. Y. Benjamini, Y. Hochberg, Controlling the false discovery rate: a practical and powerful approach to multiple testing. J. Roy. Statist. Soc. Ser. B 57, 289-300 (1995).

51. B. K. Slinker, The statistics of synergism. J Mol Cell Cardiol 30, 723-731 (1998).

OTHER EMBODIMENTS

It is to be understood that while the invention has been described in conjunction with the detailed description thereof, the foregoing description is intended to illustrate and not limit the scope of the invention, which is defined by the scope of the appended

claims. Other aspects, advantages, and modifications are within the scope of the following claims.

WHAT IS CLAIMED IS:

1. A method for treating chronic myeloid leukemia (CML) in a mammalian subject, the method comprising administering a combination of a BCR-ABL inhibitor and a MEK inhibitor.

2. The method of claim 1, wherein the CML is BCR-ABL independent IM-resistant CML, e.g., wherein the BCR-ABL is wild-type or lacks a mutation that confers IM-resistance.

3. The method of claim 1, wherein the BCR-ABL inhibitor is imatinib, Nilotinib (AMN107); Dasatinib (BMS-345825); Bosutinib (SKI-606); Ponatinib (AP24534); Bafetinib (INNO-406); thiazol or a thiazol derivatives, e.g., 1,3,4 thiadiazole derivatives.

4. The method of claim 3, wherein the BCR-ABL inhibitor is imatinib.

5. The method of claim 1, wherein the MEK inhibitor is Trametinib (GSK1120212), Selumetinib, MEK162, PD-325901, cobimetinib (XL518; [3,4-Difluoro-2-(2-fluoro-4-iodoanilino)phenyl]{3-hydroxy-3-[(2S)-piperidin-2-yl]azetidin-1-yl} methanone), CL-1040, or PD035901.

6. The method of claim 5, wherein the MEK inhibitor is trametinib.

7. The method of claim 1, wherein the subject is human.

8. Use of a BCR-ABL inhibitor and a MEK inhibitor in the treatment of chronic myeloid leukemia (CML) in a mammalian subject.

9. The use of claim 8, wherein the CML is BCR-ABL inhibitor imatinib mesylate (IM)-resistant CML.

10. The use of claim 8, wherein the BCR-ABL inhibitor is imatinib, Nilotinib (AMN107); Dasatinib (BMS-345825); Bosutinib (SKI-606); Ponatinib (AP24534);

Bafetinib (INNO-406); thiazol or a thiazol derivatives, e.g., 1,3,4 thiadiazole derivatives.

11. The use of claim 10, wherein the BCR-ABL inhibitor is imatinib.

12. The use of claim 8, wherein the MEK inhibitor is Trametinib (GSK1120212), Selumetinib, MEK162, PD-325901, cobimetinib (XL518; [3,4-Difluoro-2-(2-fluoro-4-iodoanilino)phenyl]{3-hydroxy-3-[(2S)-piperidin-2-yl]azetidin-1-yl} methanone), CL-1040, or PD035901.

13. The use of claim 12, wherein the MEK inhibitor is trametinib..

14. A method of selecting a subject with chronic myeloid leukemia (CML) for treatment with a BCR-ABL inhibitor and a MEK inhibitor, the method comprising:
detecting a level of PRKCH mRNA or PKCeta protein in a sample comprising leukemic cells, e.g., leukemic stem cells, from the subject;
comparing the level of PRKCH mRNA or PKCeta protein in the sample to a reference level;
selecting a subject who has a level of PRKCH mRNA or PKCeta protein above the reference level for treatment with a BCR-ABL inhibitor and a MEK inhibitor; and
optionally administering the treatment to the selected subject.

15. The method of claim 14, wherein the CML is BCR-ABL inhibitor imatinib mesylate (IM)-resistant CML.

16. The method of claim 14, wherein the BCR-ABL inhibitor is imatinib, Nilotinib (AMN107); Dasatinib (BMS-345825); Bosutinib (SKI-606); Ponatinib (AP24534); Bafetinib (INNO-406); thiazol or a thiazol derivatives, e.g., 1,3,4 thiadiazole derivatives.

17. The method of claim 16, wherein the BCR-ABL inhibitor is imatinib.

18. The method of claim 14, wherein the MEK inhibitor is Trametinib (GSK1120212), Selumetinib, MEK162, PD-325901, cobimetinib (XL518; [3,4-Difluoro-2-(2-fluoro-

4-iodoanilino)phenyl]{3-hydroxy-3-[(2S)-piperidin-2-yl]azetidin-1-yl} methanone), CL-1040, or PD035901.

19. The method of claim 18, wherein the MEK inhibitor is trametinib..

20. The method of claim 14, wherein the level of PRKCH mRNA is determined using RNA in situ hybridization, Southern or Northern analyses, polymerase chain reaction analyses and probe arrays.

21. The method of claim 14, wherein the level of PKCeta protein is determined using an immunoassay.

Figures 1A-F

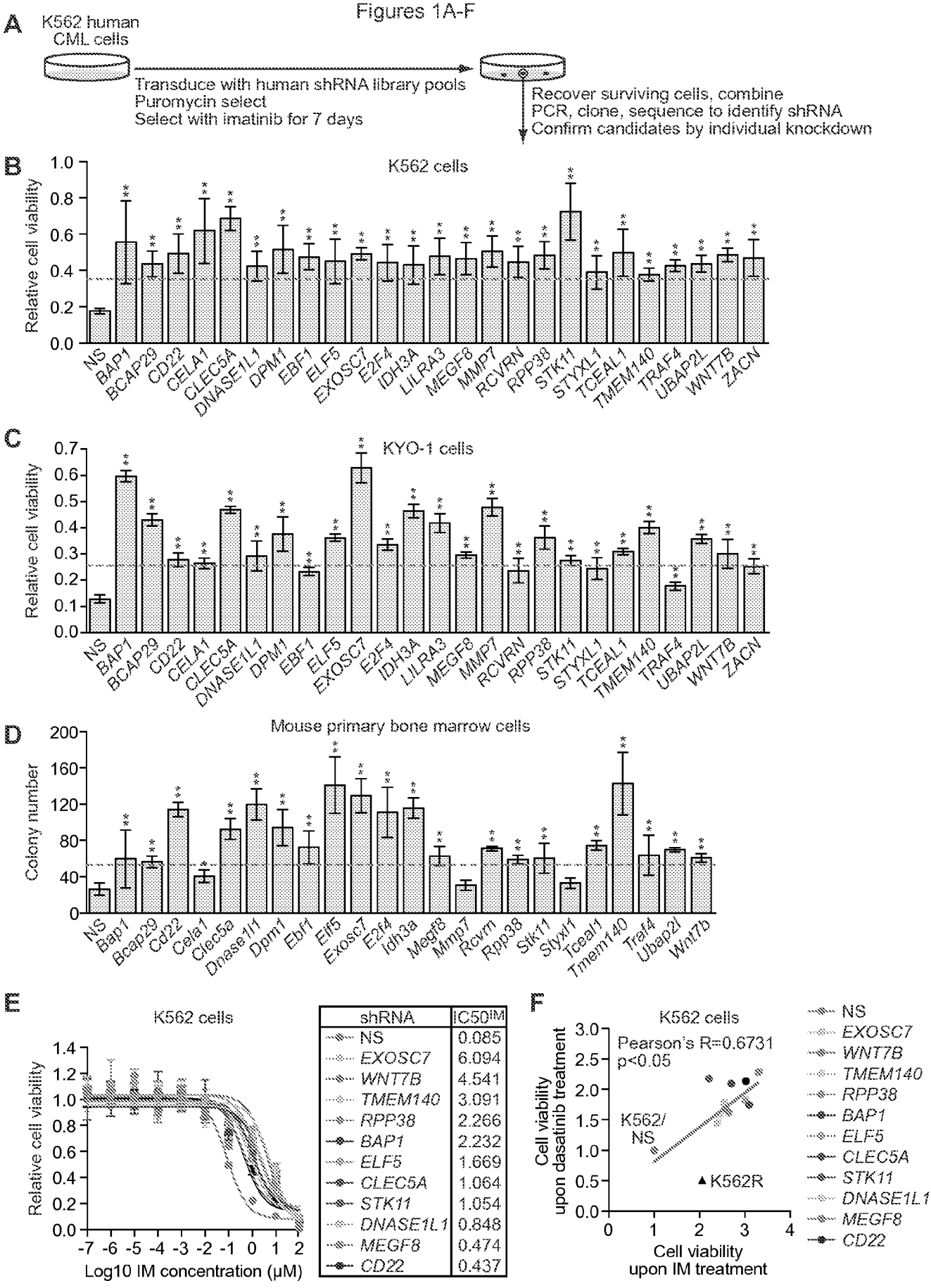
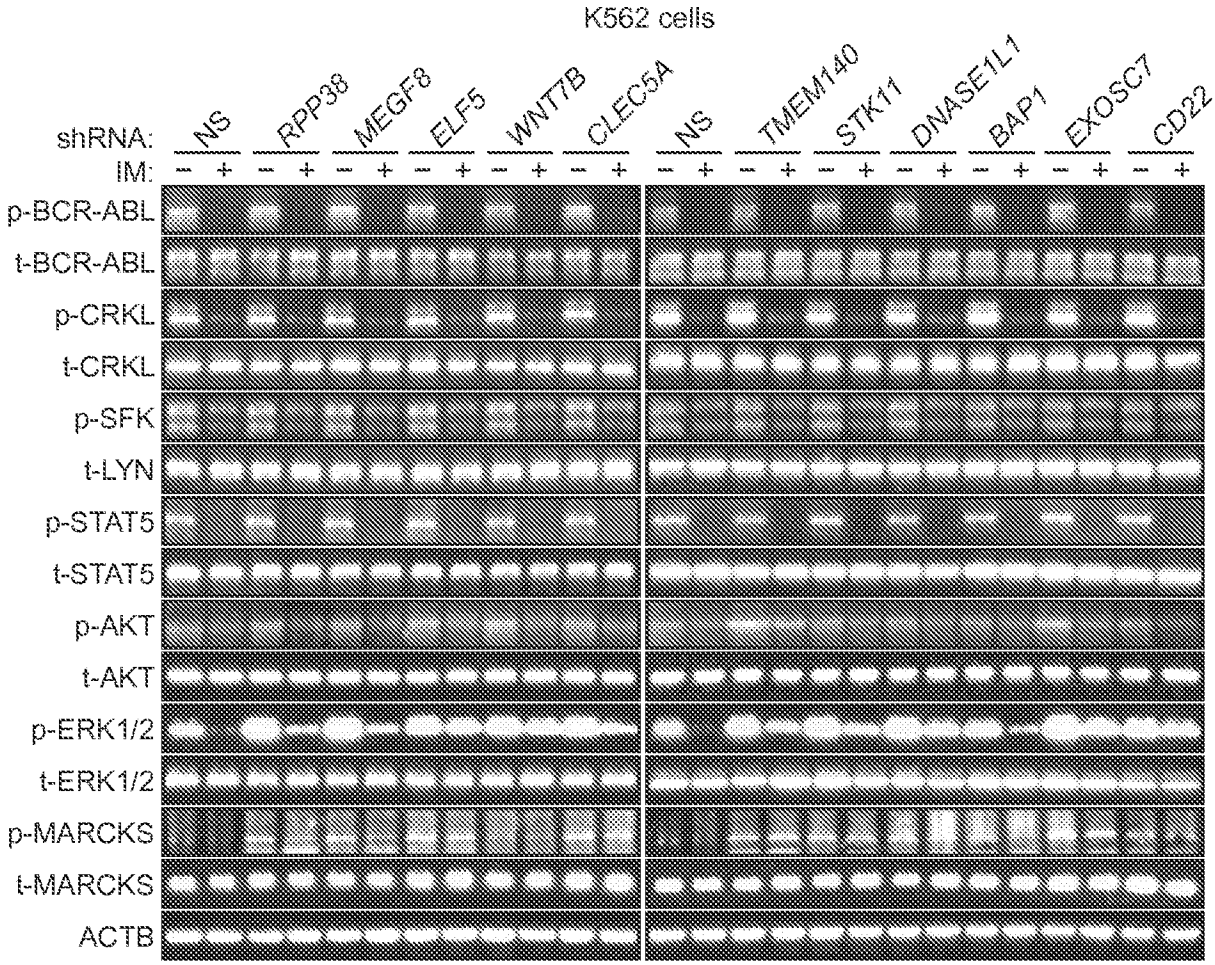
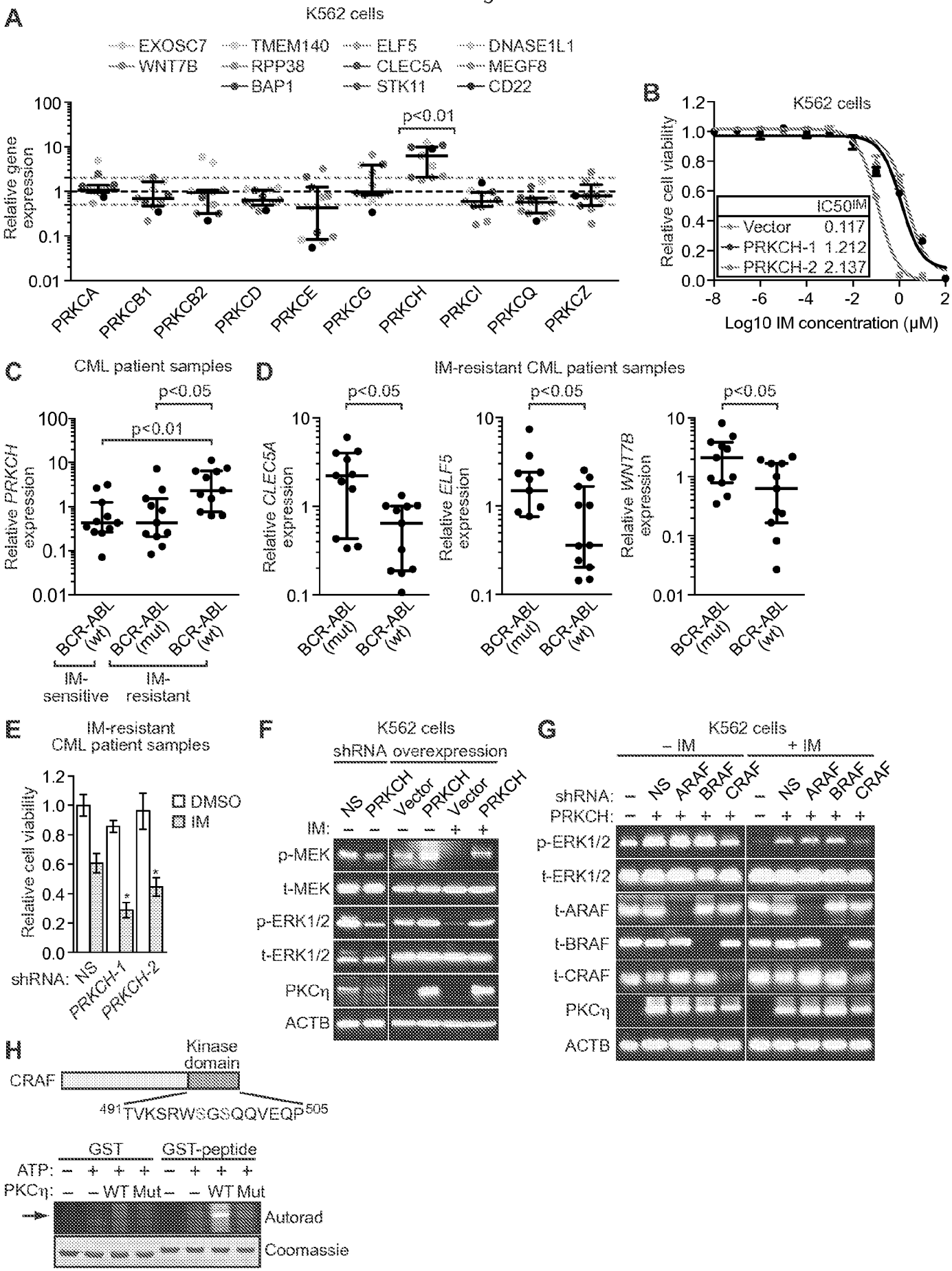

A
K562 human CML cells
Transduce with human shRNA library pools
Puromycin select
Select with imatinib for 7 days
Recover surviving cells, combine
PCR, clone, sequence to identify shRNA
Confirm candidates by individual knockdown
B
K562 cells
Relative cell viability
NS
BAP1
BCAP29
CD22
CELA1
CLEC5A
DNASE1L1
DPM1
EBF1
ELF5
EXOSC7
E2F4
IDH3A
LILRA3
MEGF8
MMP7
RCVRN
RPP38
STK11
STYXL1
TCEAL1
TMEM140
TRAF4
UBAP2L
WNT7B
ZACN
C
KYO-1 cells
Relative cell viability
D
Mouse primary bone marrow cells
Colony number
E
K562 cells
Relative cell viability
Log10 IM concentration (μM)
shRNA | IC50IM
NS 0.085
EXOSC7 6.094
WNT7B 4.541
TMEM140 3.091
RPP38 2.266
BAP1 2.232
ELF5 1.669
CLEC5A 1.064
STK11 1.054
DNASE1L1 0.848
MEGF8 0.474
CD22 0.437
F
K562 cells
Pearson's R=0.6731
p<0.05
K562/ NS
K562R
Cell viability upon dasatinib treatment
Cell viability upon IM treatment
NS
EXOSC7
WNT7B
TMEM140
RPP38
BAP1
ELF5
CLEC5A
STK11
DNASE1L1
MEGF8
CD22

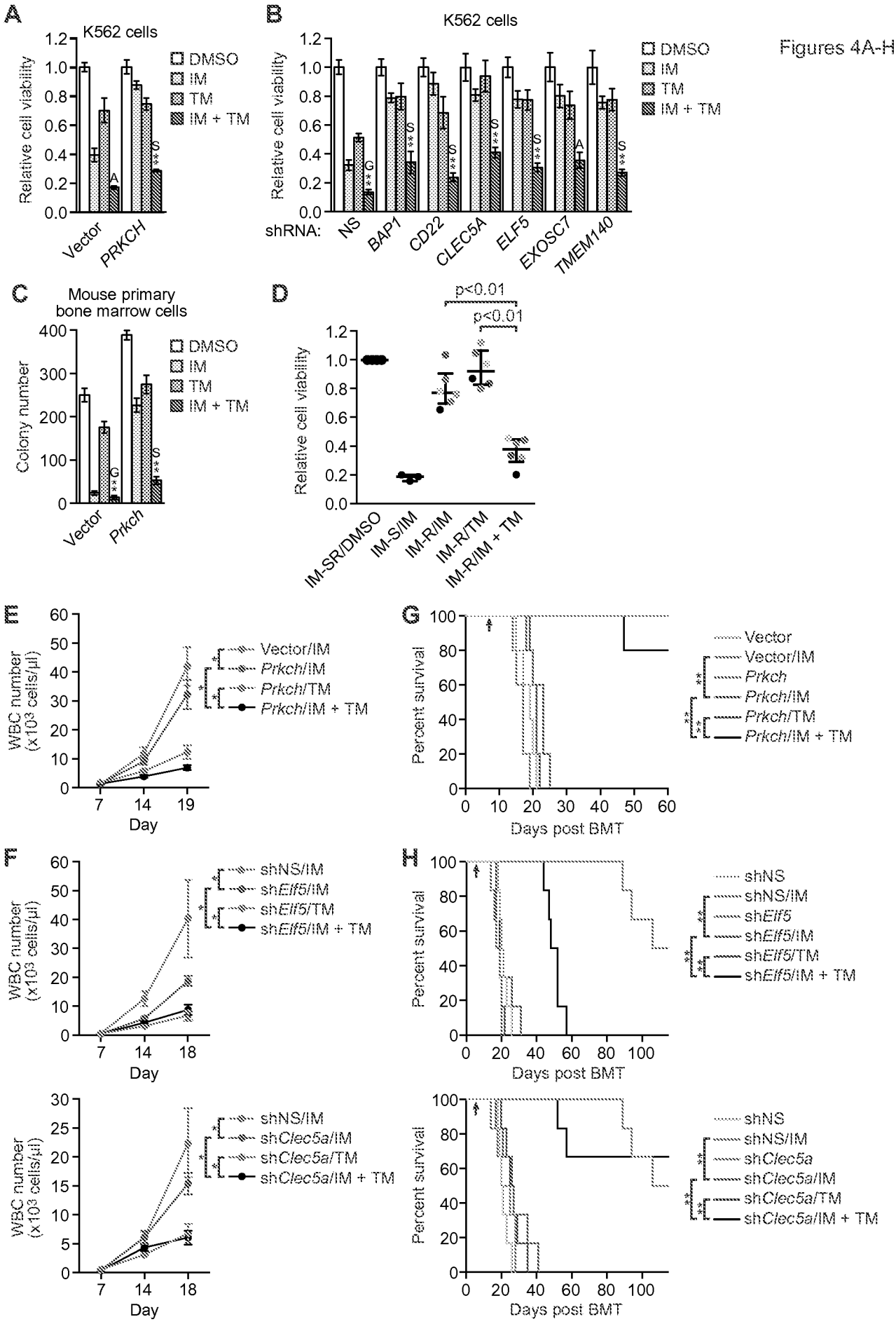
Figure 2


K562 cells
shRNA:
NS
RPP38
MEGF8
ELF5
WNT7B
CLEC5A
NS
TMEM140
STK11
DNASE1L1
BAP1
EXOSC7
CD22
IM:
− + − + − + − + − + − + − + − + − + − + − + − + − +
p-BCR-ABL
t-BCR-ABL
p-CRKL
t-CRKL
p-SFK
t-LYN
p-STAT5
t-STAT5
p-AKT
t-AKT
p-ERK1/2
t-ERK1/2
p-MARCKS
t-MARCKS
ACTB

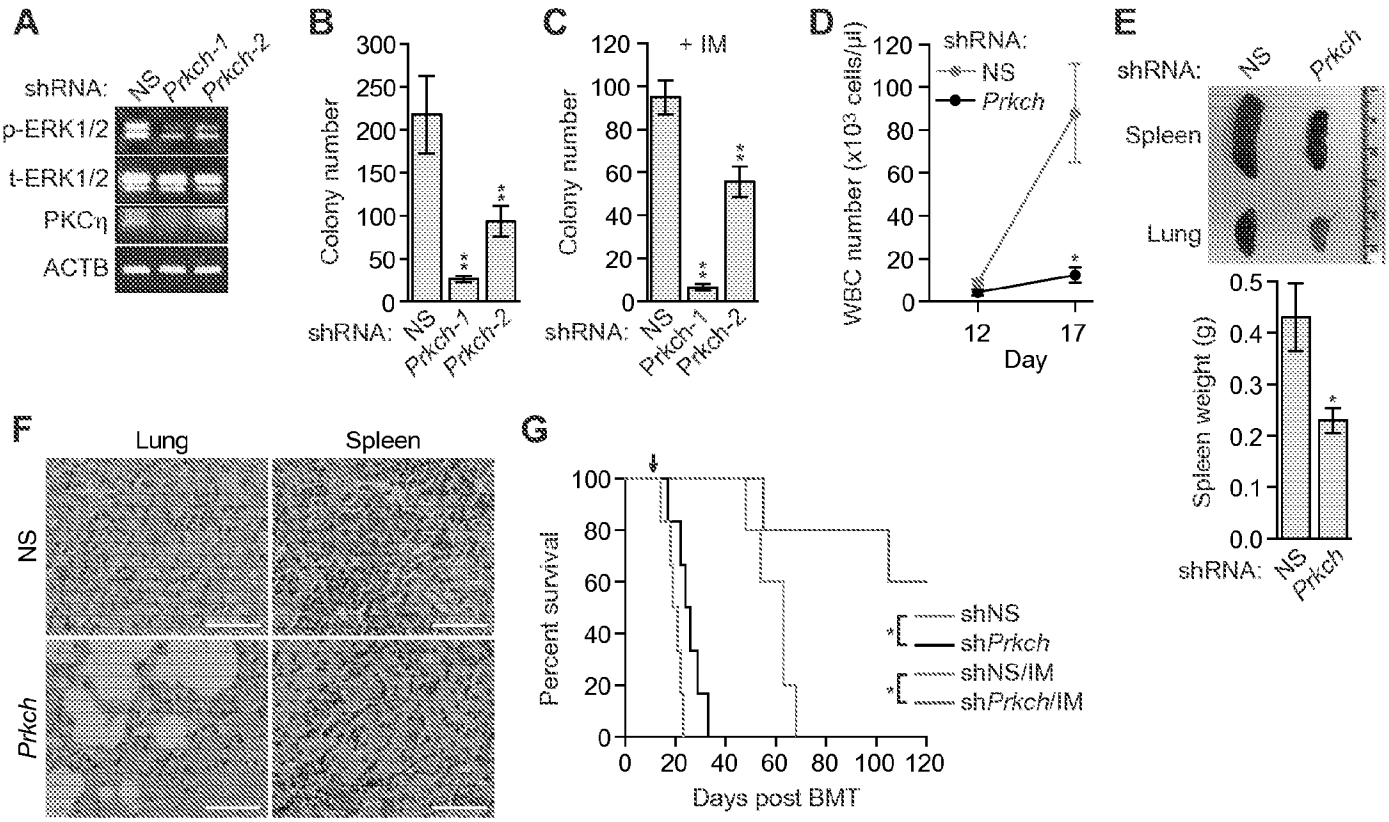
Figures 3A-H


A
K562 cells
EXOSC7
TMEM140
ELF5
DNASE1L1
WNT7B
RPP38
CLEC5A
MEGF8
BAP1
STK11
CD22
p<0.01
Relative gene expression
PRKCA
PRKCB1
PRKCB2
PRKCD
PRKCE
PRKCG
PRKCH
PRKCI
PRKCQ
PRKCZ
B
K562 cells
Relative cell viability
IC50IM
Vector 0.117
PRKCH-1 1.212
PRKCH-2 2.137
Log10 IM concentration (μM)
C
CML patient samples
p<0.05
p<0.01
Relative PRKCH expression
BCR-ABL (wt)
BCR-ABL (mut)
BCR-ABL (wt)
IM-sensitive
IM-resistant
D
IM-resistant CML patient samples
p<0.05
Relative CLEC5A expression
Relative ELF5 expression
Relative WNT7B expression
BCR-ABL (mut)
BCR-ABL (wt)
E
IM-resistant CML patient samples
Relative cell viability
DMSO
IM
shRNA: NS
PRKCH-1
PRKCH-2
F
K562 cells
shRNA overexpression
NS
PRKCH
Vector
PRKCH
Vector
PRKCH
IM:
p-MEK
t-MEK
p-ERK1/2
t-ERK1/2
PKCη
ACTB
G
K562 cells
– IM
+ IM
shRNA:
NS
ARAF
BRAF
CRAF
PRKCH:
p-ERK1/2
t-ERK1/2
t-ARAF
t-BRAF
t-CRAF
PKCη
ACTB
H
Kinase domain
CRAF
491TVKSRWSGSQQVEQP505
GST
GST-peptide
ATP:
PKCη:
WT
Mut
Autorad
Coomassie

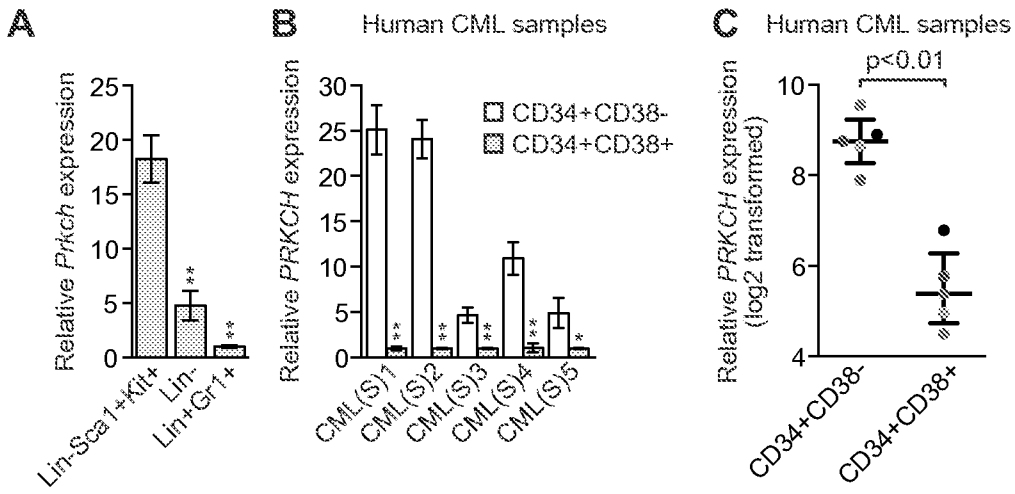
Figures 4A-H


A
K562 cells
Relative cell viability
DMSO
IM
TM
IM + TM
Vector
PRKCH
B
K562 cells
shRNA:
NS
BAP1
CD22
CLEC5A
ELF5
EXOSC7
TMEM140
C
Mouse primary bone marrow cells
Colony number
Vector
Prkch
D
p<0.01
p<0.01
IM-SR/DMSO
IM-S/IM
IM-R/IM
IM-R/TM
IM-R/IM + TM
E
WBC number (x10³ cells/μl)
Day
Vector/IM
Prkch/IM
Prkch/TM
Prkch/IM + TM
G
Percent survival
Days post BMT
Vector
Vector/IM
Prkch
Prkch/IM
Prkch/TM
Prkch/IM + TM
F
shNS/IM
shElf5/IM
shElf5/TM
shElf5/IM + TM
H
shNS
shNS/IM
shElf5
shElf5/IM
shElf5/TM
shElf5/IM + TM
shNS/IM
shClec5a/IM
shClec5a/TM
shClec5a/IM + TM
shNS
shNS/IM
shClec5a
shClec5a/IM
shClec5a/TM
shClec5a/IM + TM

Figures 5A-G


A
shRNA: NS Prkch-1 Prkch-2
p-ERK1/2
t-ERK1/2
PKCη
ACTB
B
Colony number
shRNA: NS Prkch-1 Prkch-2
C
+ IM
Colony number
shRNA: NS Prkch-1 Prkch-2
D
shRNA:
NS
Prkch
WBC number (x10³ cells/μl)
Day
E
shRNA: NS Prkch
Spleen
Lung
Spleen weight (g)
shRNA: NS Prkch
F
Lung
Spleen
NS
Prkch
G
Percent survival
Days post BMT
shNS
shPrkch
shNS/IM
shPrkch/IM

Figures 6A-C


A
Relative Prkch expression
25
20
15
10
5
0
**
**
Lin-Sca1+Kit+
Lin-
Lin+Gr1+
B
Human CML samples
Relative PRKCH expression
30
25
20
15
10
5
0
CD34+CD38-
CD34+CD38+
**
**
**
**
*
CML(S)1
CML(S)2
CML(S)3
CML(S)4
CML(S)5
C
Human CML samples
p<0.01
Relative PRKCH expression
(log2 transformed)
10
8
6
4
CD34+CD38-
CD34+CD38+

Figures 7A-G

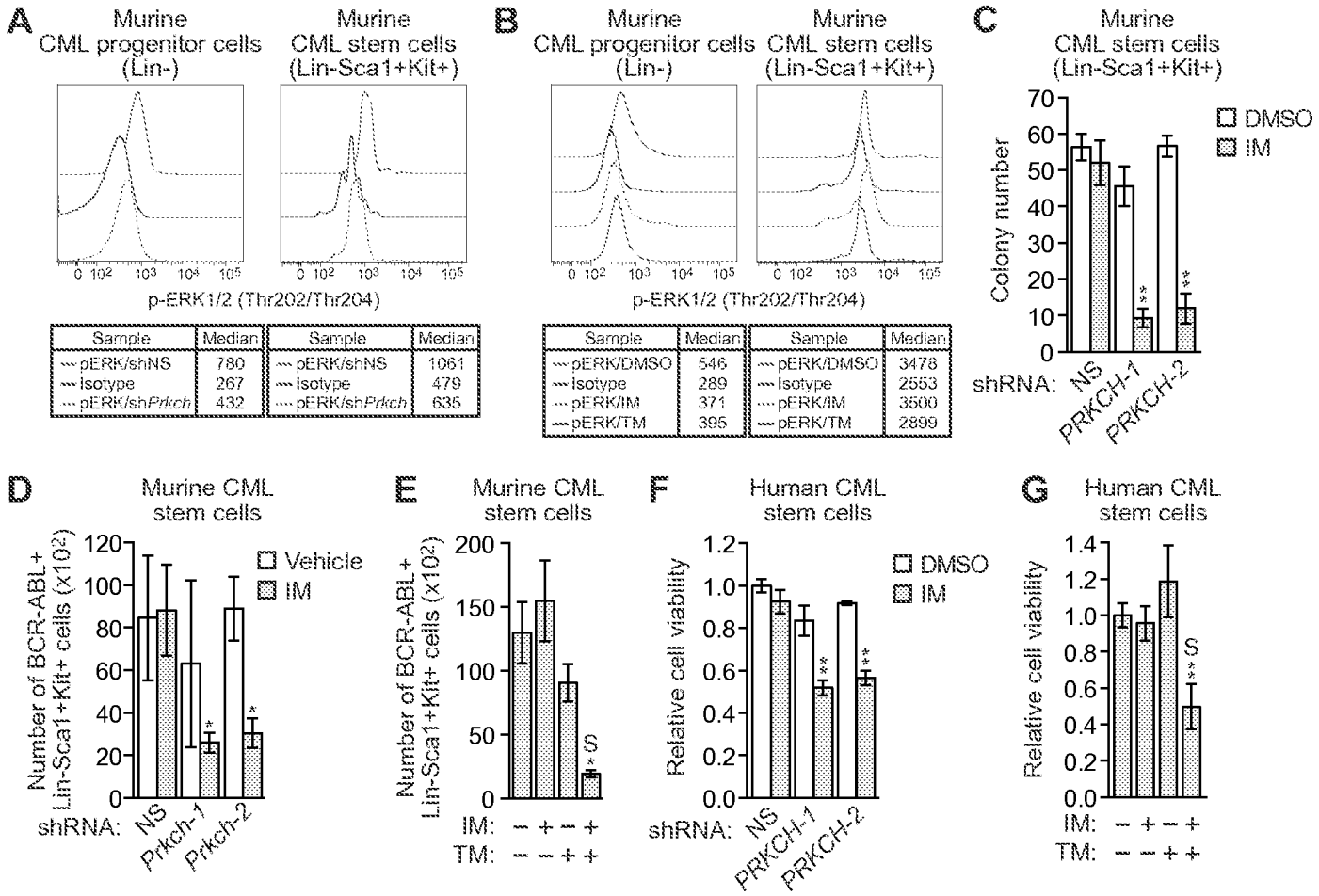

A
Murine CML progenitor cells (Lin-)
Murine CML stem cells (Lin-Sca1+Kit+)
p-ERK1/2 (Thr202/Thr204)
Sample | Median | Sample | Median
pERK/shNS 780 | pERK/shNS 1061
Isotype 267 | Isotype 479
pERK/shPrkch 432 | pERK/shPrkch 635
B
Murine CML progenitor cells (Lin-)
Murine CML stem cells (Lin-Sca1+Kit+)
p-ERK1/2 (Thr202/Thr204)
Sample | Median | Sample | Median
pERK/DMSO 546 | pERK/DMSO 3478
Isotype 289 | Isotype 2553
pERK/IM 371 | pERK/IM 3500
pERK/TM 395 | pERK/TM 2899
C
Murine CML stem cells (Lin-Sca1+Kit+)
Colony number
DMSO
IM
shRNA: NS PRKCH-1 PRKCH-2
D
Murine CML stem cells
Number of BCR-ABL+ Lin-Sca1+Kit+ cells (x10²)
Vehicle
IM
shRNA: NS Prkch-1 Prkch-2
E
Murine CML stem cells
Number of BCR-ABL+ Lin-Sca1+Kit+ cells (x10²)
IM:
TM:
F
Human CML stem cells
Relative cell viability
DMSO
IM
shRNA: NS PRKCH-1 PRKCH-2
G
Human CML stem cells
Relative cell viability
IM:
TM:

Figure 8

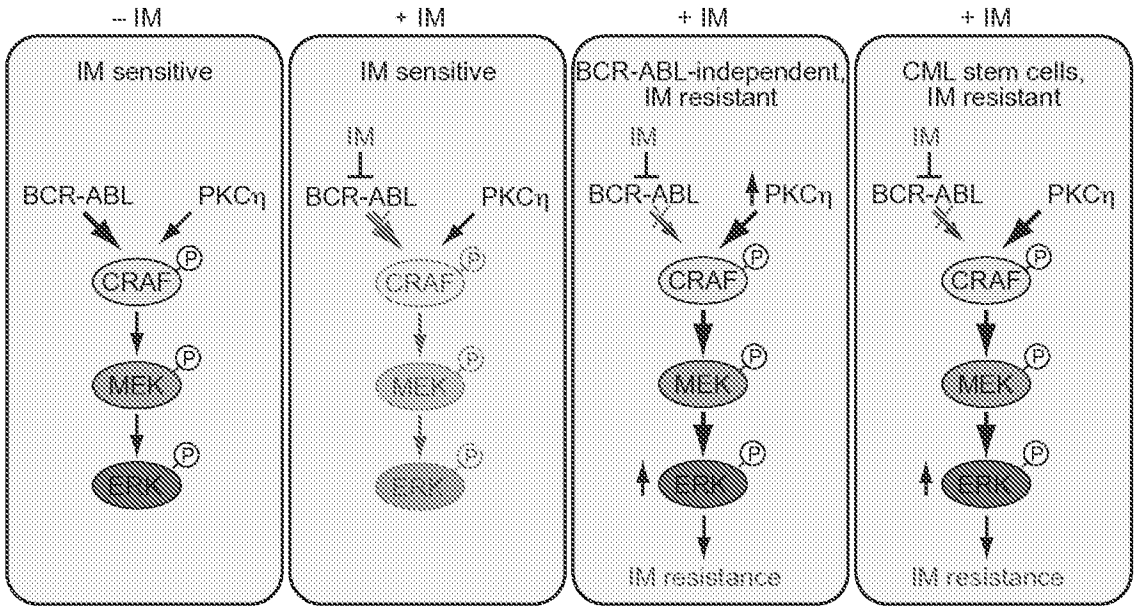
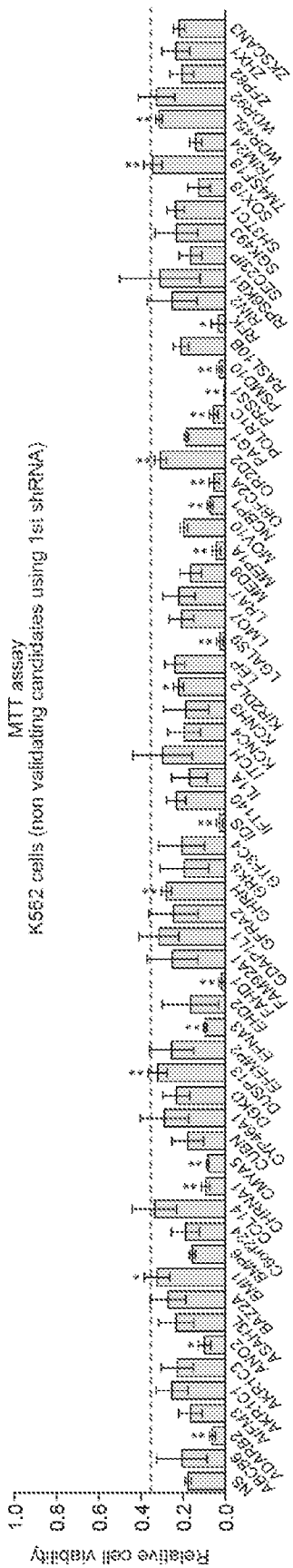
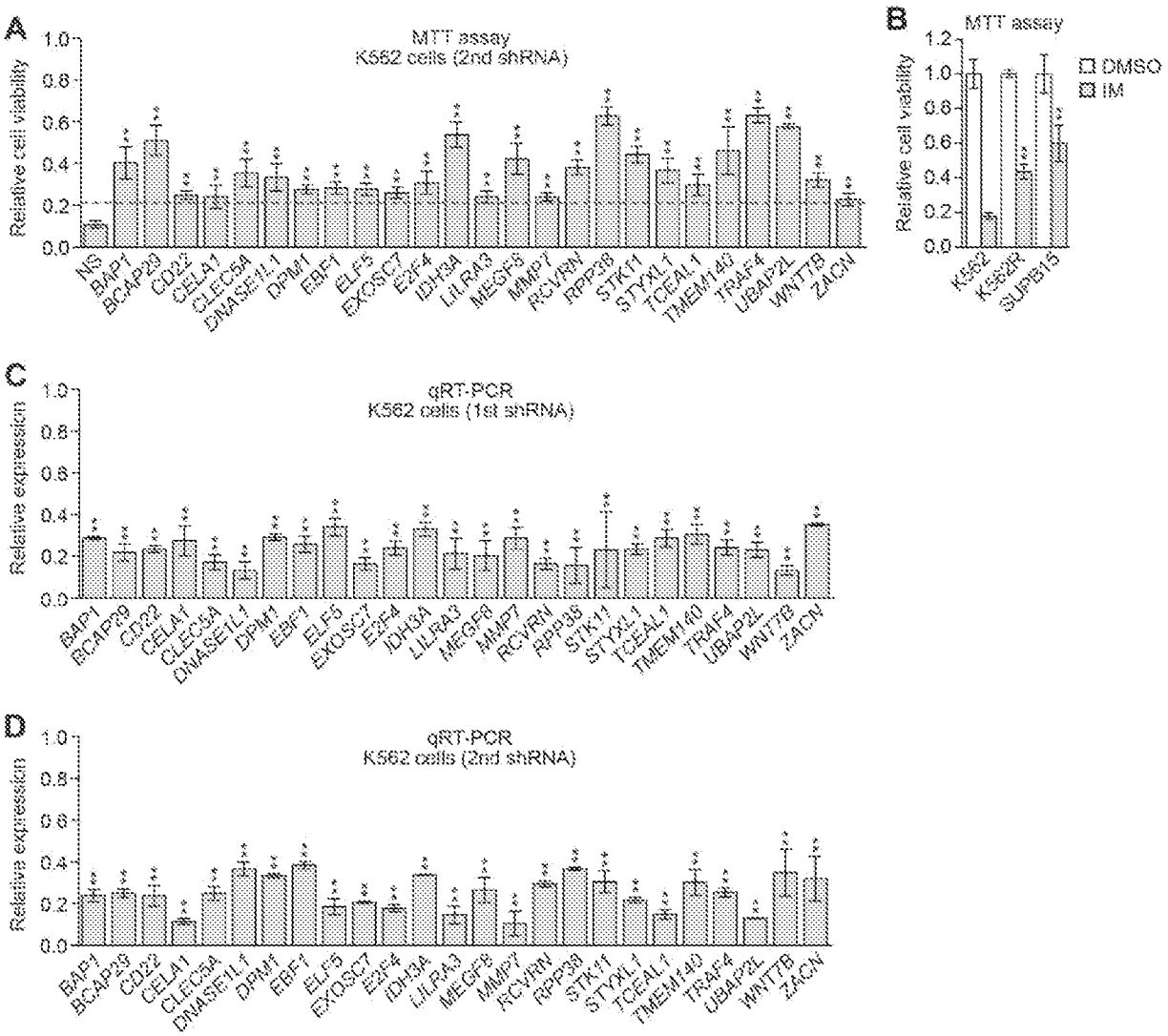
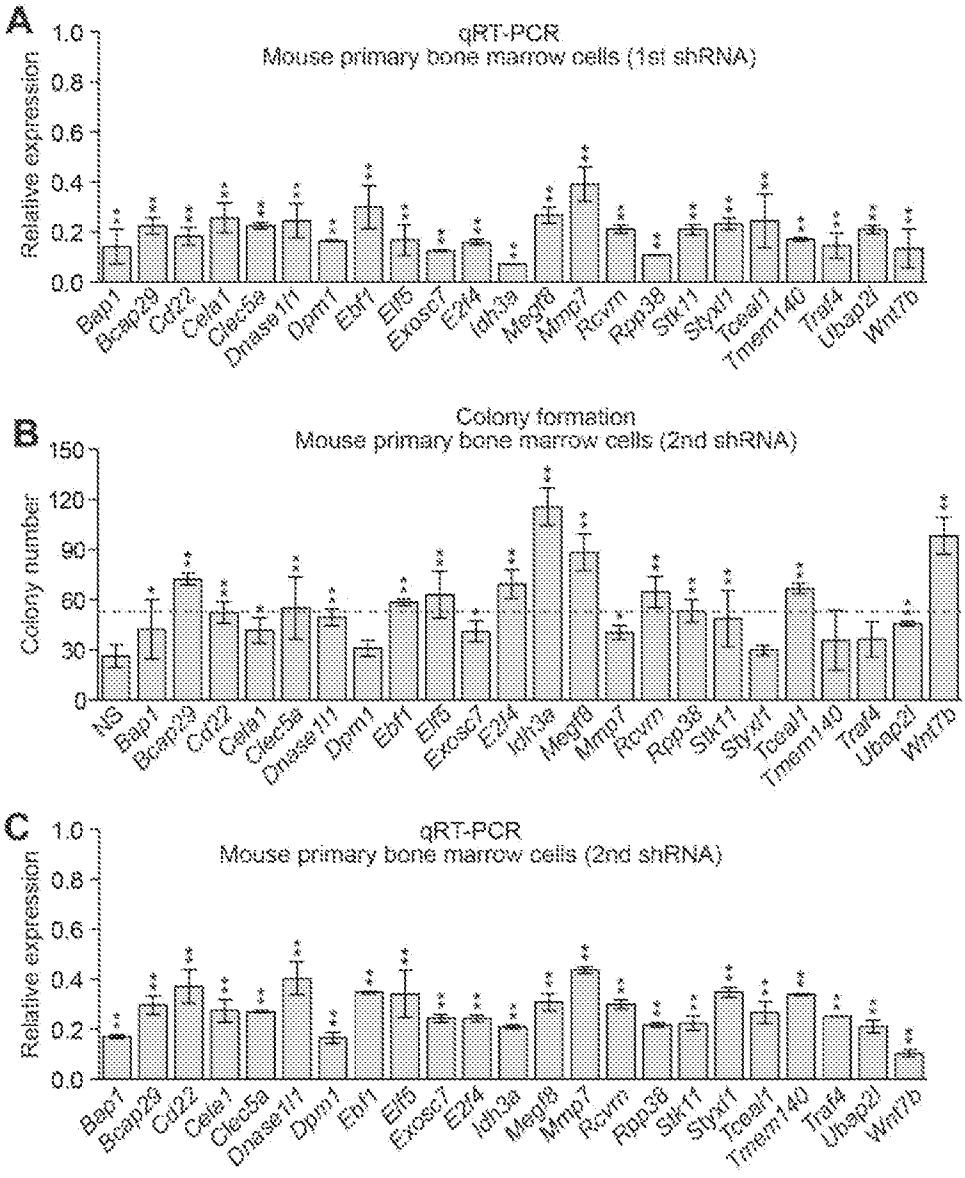

– IM
IM sensitive
BCR-ABL
PKCη
CRAF
MEK
ERK
+ IM
IM sensitive
IM
BCR-ABL
PKCη
CRAF
MEK
ERK
+ IM
BCR-ABL-independent, IM resistant
IM
BCR-ABL
PKCη
CRAF
MEK
ERK
IM resistance
+ IM
CML stem cells, IM resistant
IM
BCR-ABL
PKCη
CRAF
MEK
ERK
IM resistance

FIGURE 9


MTT assay
K562 cells (non validating candidates using 1si shRNA)
Relative cell viability
1.0
0.8
0.6
0.4
0.2
0.0
NS
ADCY8
ADRB2
AFAP1
AKAP13
AKT1S1
ANO2
ATP13A2
BAI1
BMP6
C20orf24
CCR1
CHRNA1
CMYA5
CUBN
CYP4A11
DGKD
DUSP13
EFCAB2
EPHA3
FHOD1
FKBP1A
GPR124
GPR182
GRIA2
GRIK3
GTF2IRD1
IGSF4
IFT140
ITGA1
ITGB4
KCNH8
KIF20A
LEF1
LGALS9
LMO1
LPAL1
MED8
MEF2A
MOV10
NCSP1
OSBPL2A
PAG1
PDLIM1
PSS1
PSMD10
RAB11B
RHOB
RPS6KB1
SEC24B
SGK493
SHISA2
SOX13
TMEM132A
TNIK
WDR82
ZFP82
ZNRF1
ZASCAN3



Figures 10A-D



Figures 11A-C

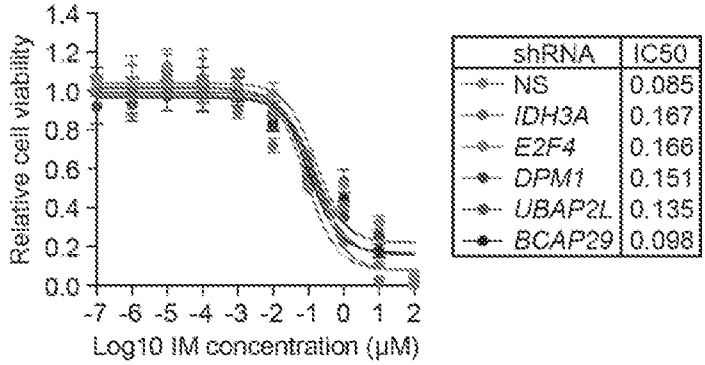
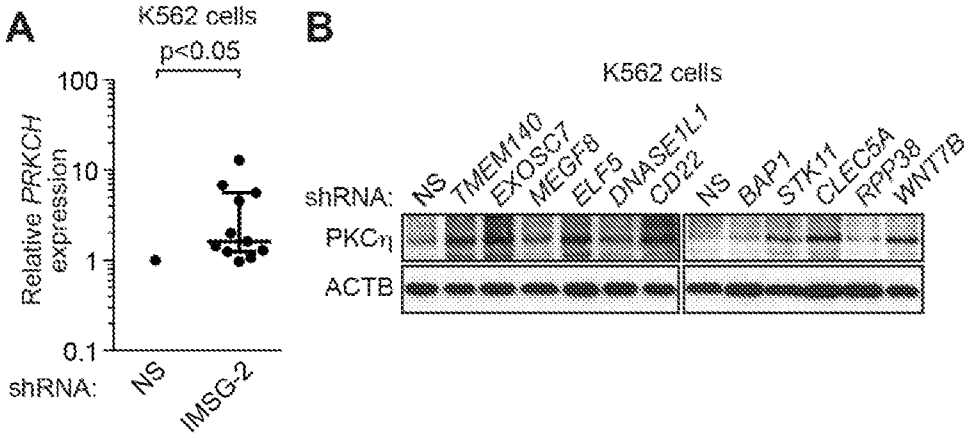
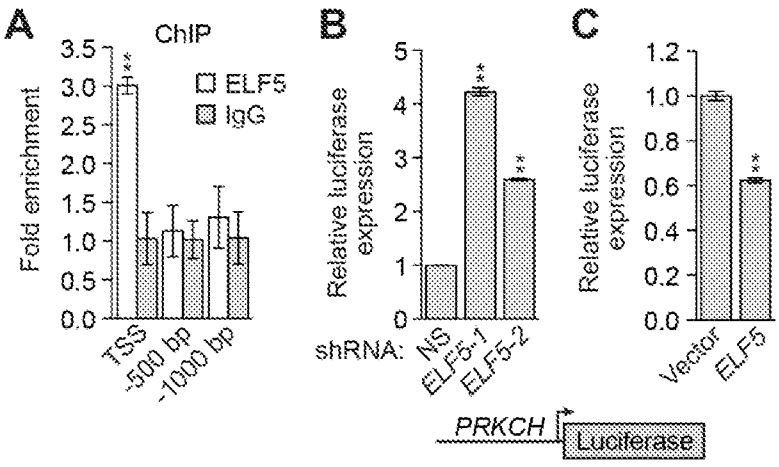


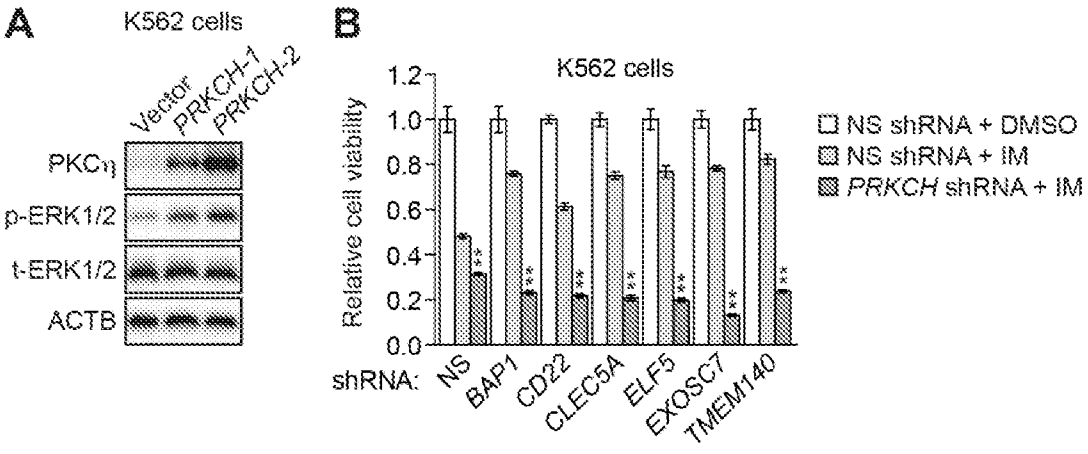
Figure 12



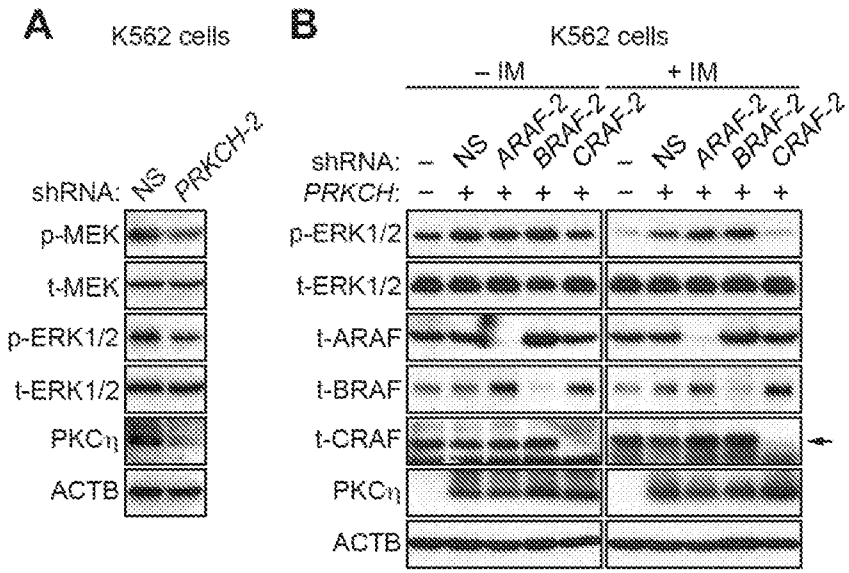
Figures 13A-B



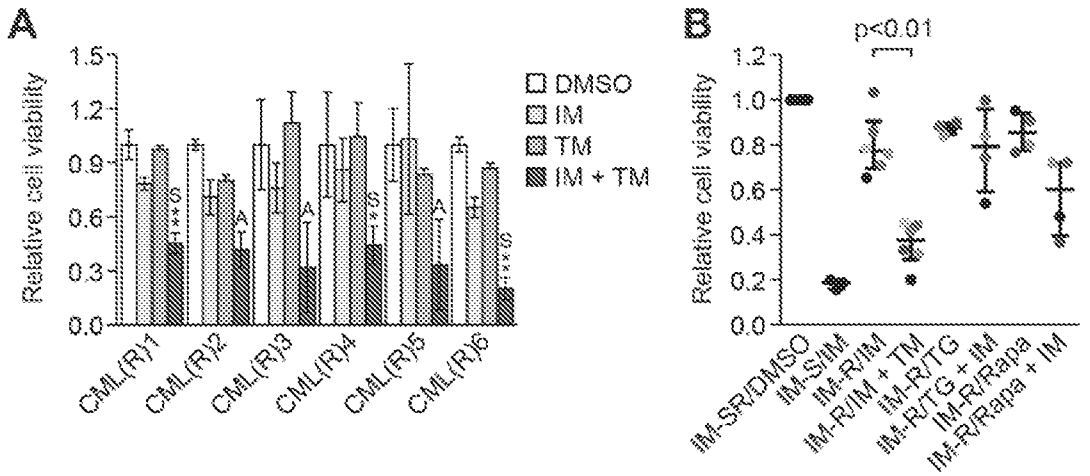
Figures 14A-C



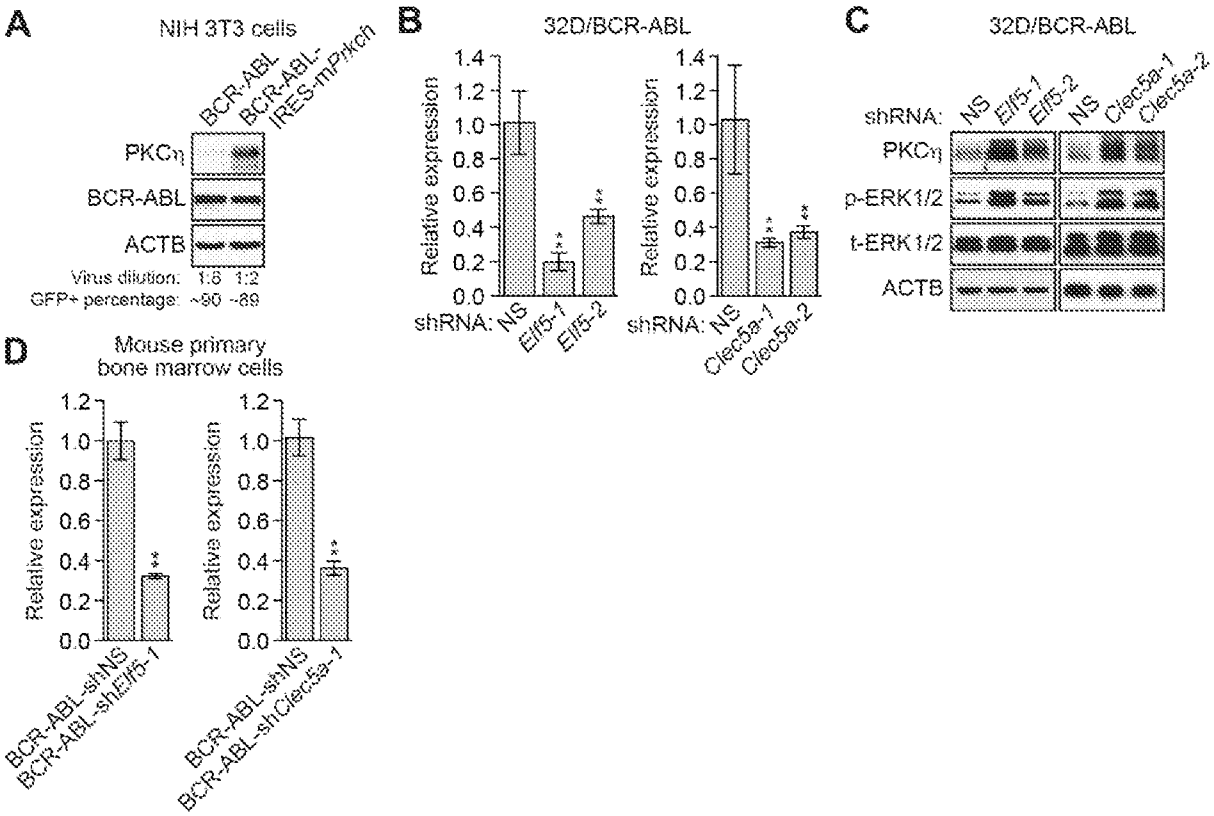
Figures 15A-B



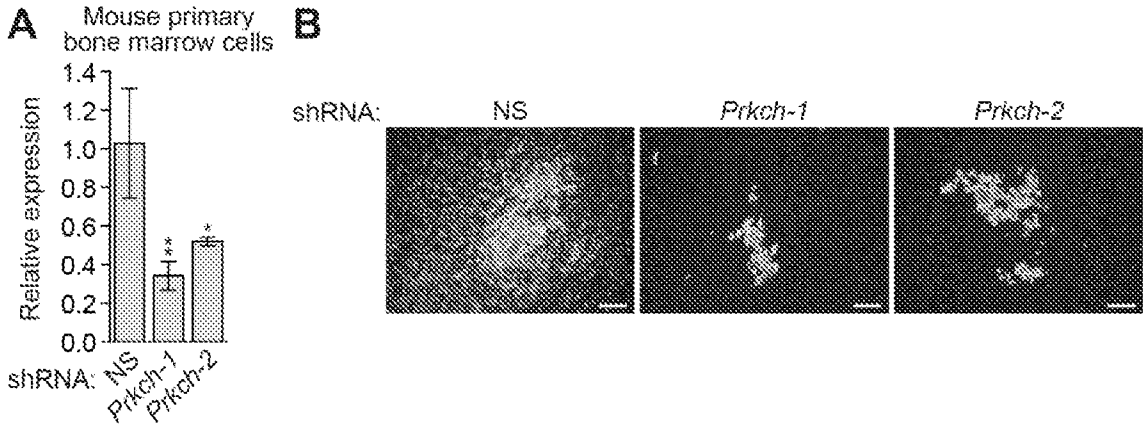
Figures 16A-B



Figures 17A-B



Figures 18A-D



Figures 19A-B

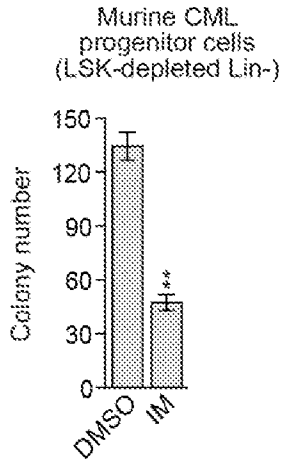
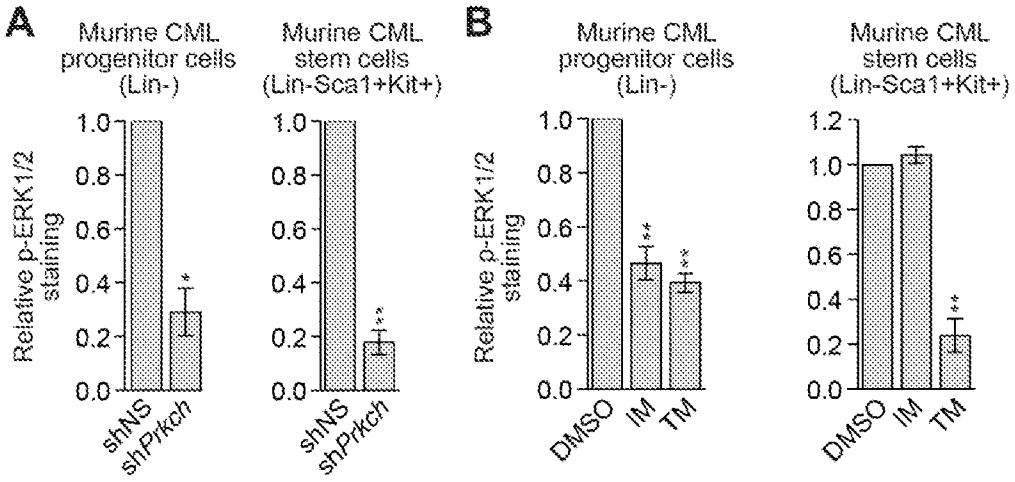
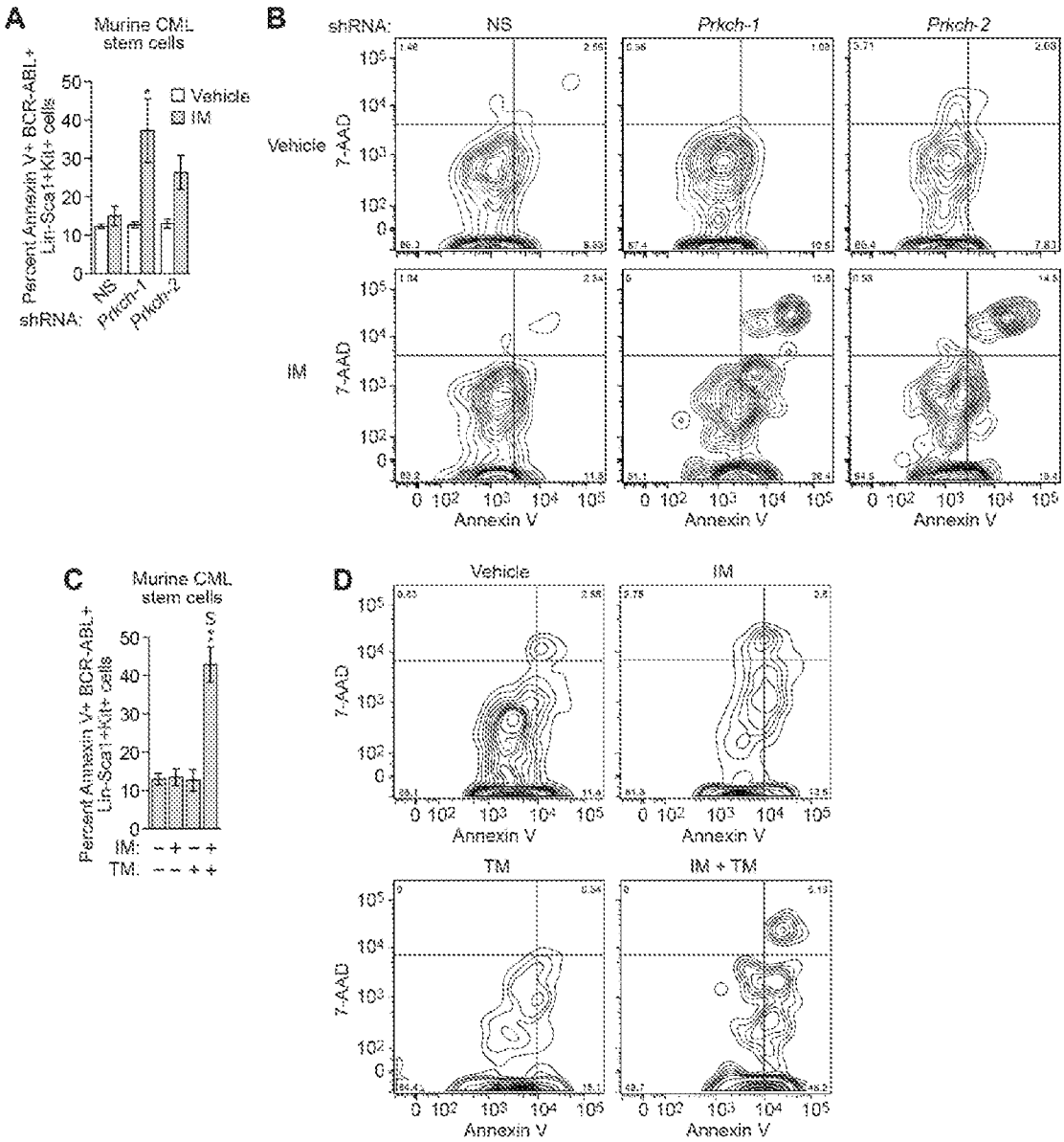


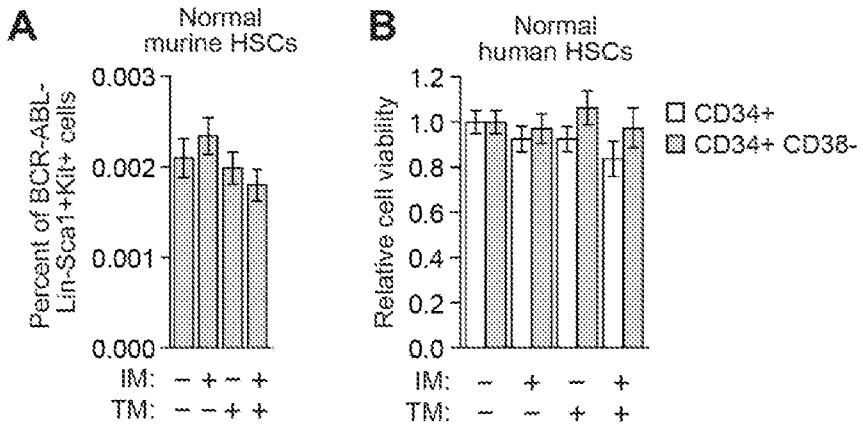
Figure 20



Figures 21A-B



Figures 22A-D



Figures 23A-B